Generation of transgenic mice for the investigation of ceramide metabolism

INAUGURAL DISSERTATION

zur
Erlangung des Doktorgrades
Dr. rer. nat.

der Fakultät
für Biologie

an der
Universität Duisburg-Essen

vorgelegt von
Martin Knüwer
aus Heiden

Oktober 2013

Die der vorliegenden Arbeit zugrunde liegenden Experimente wurden am Institut für Molekularbiologie des Universitätsklinikum Essen durchgeführt.

1. Gutachter: Prof. Dr. Erich Gulbins

2. Gutachter: Prof. Dr. Shirley Knauer

Vorsitzender des Prüfungsausschusses: Prof. Dr. Andrea Vortkamp

Tag der Disputation: 28.01.2014

Table of contents

ABBREVIATIONS

A	Ampere
AC	Acid Ceramidase (protein)
AP	Alkaline Phosphatase
APS	Ammoniumpersulphate
Asah1	Gene symbol of Acid Ceramidase (Mouse)
ASAH1	Gene symbol of Acid Ceramidase (Human)
ASM	Acid Sphingomyelinase (protein)
bp	Base pair
BSA	Bovine Serum Albumin
°C	Celsius Scale
CAG promoter	CMV early Enhancer/Chicken β-actin promoter
cDNA	Complementary deoxyribonucleic acid
CRD	Ceramide Rich Domain
ddH_2O	Double distilled H_2O
DMSO	Dimethyl sulfoxide
DMEM	Dulbecco's modified Eagle's Medium
DNA	Deoxyribonucleic acid
dNTP	Deoxynucleotide triphosphate
DTA	Diphteria Toxin-A
E. coli	*Escherichia coli*
EDTA	Ethylendiamintetra acetic acid
ES cells	Embryonic stem cells
FBS	Fetal Bovine Serum
FELASA	Federation of European Laboratory Animal Science Associations
floxed	Flanked by loxP sites
g	Gram
GL261	Mouse glioma cell line
h	Hour
H_2O	Water
HEPES	N-2-Hydroxyethylpiperazine-N'-2-ethanesulfonic acid
kDa	Kilodalton
kb	Kilobase
KO	Knockout
LIF	Leukaemia Inhibitory Factor
loxP	Locus of crossover in phage P1
LB	Luria Bertani
m	Milli (10^{-3})
µ	Micro (10^{-6})
M	Molar
MEF	Mouse Embryonic Fibroblast
MS	Mass spectrometry

mg	Milligram
ml	Milliliter
mM	Millimolar
mRNA	Messenger ribonucleic acid
nm	Nanometer
PAGE	Polyacrylamide gel electrophoresis
PBS	Phosphate Buffered Saline
PCR	Polymerase Chain Reaction
rpm	Revolutions per minute
RT	Room Temperature
SD	Standard Deviation
SDS	Sodium Dodecyl Sulphate
Smpd1	Gene symbol of acid sphingomyelinase (mouse)
SMPD1	Gene symbol of acid sphingomyelinase (human)
SPH	Sphingosine
TAE	Tris-actetate-EDTA buffer
TBS	Tris-buffered saline
TBS-T	Tris-buffered saline-Tween
TE	Tris-EDTA buffer
Tris	Tris(hydroxymethyl)aminomethane
Tween 20	Polyoxyethylene sorbitan monolaurate
UV	Ultraviolet
V	Voltage
v/v	Volume/volume
µl	Microliter
ZTL	"Zentrales Tierlaboratorium", Central Animal Facility

1. INTRODUCTION

1.1 Genetic engineering

Genomic sequencing efforts have mapped the entire code of the human and murine genome (Venter *et al.* 2001; Waterston *et al.* 2002). Data comparison allows for the identification of homology regions and conserved domains. But what is the benefit of the knowledge about the technical design of a musical instrument when you do not know how to play it? In the case of the human and murine genome, we still need to gather information on gene regulation and gene function. To analyze the function of a gene, the corresponding protein must be analyzed by biochemical methods. Naturally occurring genetic mutations in organisms were the first opportunity to identify a disrupted protein and ascertain its genetic cause. Using the "clinical picture"/phenotype as a starting point, functionality was ascribed to the gene and its protein. In order to accelerate the acquisition of knowledge, scientists started to deliberately expose flies and worms to mutagens (Auerbach 1947; Auerbach and Robson 1947; Muller 1955). Still, changes in the genetic code were induced at random. Genetic engineering is the term used for technologies that are able to specifically alter the genetic makeup of an organism. DNA is either inserted or removed from the genome. Genetic engineering started with the genetic modification of a plasmid that was transformed into an *E. coli* bacterium (Cohen *et al.* 1973). Soon, mice were the targets of genetic engineering (Jaenisch and Mintz 1974). Due to their similarity to humans with regard to genetics, physiology, biochemistry and disease they are the ideal experimental animal. In addition, mice are small and easy to breed. Of capital importance however is the feasibility to efficiently induce specific genetic modifications. Gain of function/overexpression models and gene disruption/"knockout" models are powerful tools for the scientist. The impact on cells, tissues and the organism can be investigated. Furthermore, genetically altered mice allow evaluating the therapeutic value of a gene and its protein in a pathophysiological context.

1.1.1 Transgenic mice

The transgene technology comprises the transfer of a foreign DNA strand into the genome of an organism (Gordon and Ruddle 1981). Classically, an artificially constructed expression cassette is inserted into the host genome to produce a particular protein. Molecular cloning

techniques allow for the exogenous assembly of genetic elements. By DNA manipulation promoter-, coding- and terminator- sequences can be arranged in a bacterial plasmid. In the mouse model, the DNA construct is injected into the pronucleus of a fertilized ovum. The embryo is then transferred into the uterus of a surrogate mother (Gordon *et al.* 1980). Expression cassettes randomly integrate into the murine genome. The offspring of the foster mother can then be analyzed for the presence of the expression cassette. Heritage of the genetic modification follows the Mendelian distribution pattern (Gordon and Ruddle 1981). Accordingly, the genetic modification is present in all cells of the organism. Transcription of the transgene is subjected to the epigenetic regulations of the integration site (Allen *et al.* 1988). Further determinants of expression levels are the deployed promoter and the total number of transgene integrants. Consequentially, the protein synthesis of a trangene is unpredictable – this is the major drawback of transgene engineering.

1.1.2 Gene targeted mice

Gene targeting is a technique that allows to change the DNA sequence of a specific endogenous gene by homologous recombination with a targeting/replacement vector (Doetschman *et al.* 1987; Thomas and Capecchi 1987). The targeting vector is comprised of DNA sequences identical to the gene of interest with modifications that were introduced via standard recombinant DNA technology. By electroporation, the targeting vector is introduced into pluripotent embryonic stem (ES-) cells. The two DNA entities, genomic DNA and targeting vector DNA, interact, recombine and exchange DNA sequences. By this method, genes can be disrupted to “knockout” an allele and generate “null mutants”. Alternatively, DNA material can be introduced, a so-called “knock-in”, to modify gene expression. Next, the ES cells are selected and screened, often by Polymerase Chain Reactions (PCRs) and/or Southern blots, for the desired modifications at the defined gene locus. “Positive” ES cell clones are injected into blastocysts. The blastocysts are reimplanted into pseudopregnant females. In the case that the modified ES cells contribute to the germline of chimeric offspring, the targeted allele becomes inherent part of the genome effective from the next generation.

The conventional knockout strategy affects every cell of an organism at any time. As a consequence, genetic modifications may be lethal at an early embryonic stage (Farese *et al.* 1995; Fassler and Meyer 1995; Accili *et al.* 1996). Furthermore, the function of an enzyme

can never be analyzed in a single cell type, tissue or at a defined time point of development or disease. In order to have temporal and spatial control of the genetic knockout approach, the conditional knockout technology was developed (Gu *et al.* 1994; Rajewsky *et al.* 1996). The main requirement for this adaption is a system that is able to disrupt a gene in an inducible way. This is accomplished by site-specific recombinases, Cre- and FLP-recombinase, which recognize specific recombination sites and rearrange the DNA in-between (Orban *et al.* 1992; Vooijs *et al.* 1998). A recombination site is a 34 bp DNA sequence. An asymmetric 8 bp center is flanked by 13 bp palindromes (see figure 1.1 A) (Hoess *et al.* 1982). The asymmetric center of the recombination sites confers directionality and determines whether two recombination sites are in the same or opposite orientation. Cre- and FLP recombinase recognize loxP- (locus of cross-over in bacteriophage P1) or FRT (FLP recombination target) sites, respectively. Two recombination sites are cloned into non-coding DNA of the targeting vector and frame a DNA sequence that is essential for the function of the targeted gene. Just like in the conventional knockout approach, the modifications are transferred into the murine genome by homologous recombination within ES cells. Following germline transmission of the "floxed" (flanked by loxP sites) allele, flox-mice are bred with mice transgenic for the Cre-recombinase. The cells of the offspring will hold a disrupted targeted allele under the "condition" that the Cre-recombinase is expressed. In the case that the recombination sites were arranged with the same orientation, the recombinase disrupts the gene via excision of the floxed segment (see figure 1.1 B). Opposite orientation causes gene disruption by inversion of the floxed element (Hoess *et al.* 1986). The promoter of the Cre-transgene determines the spatial and temporal expression profile of Cre-recombinase and thus the profile of gene disruption. Inducible promoters allow for selective gene knockout (Metzger and Chambon 2001).

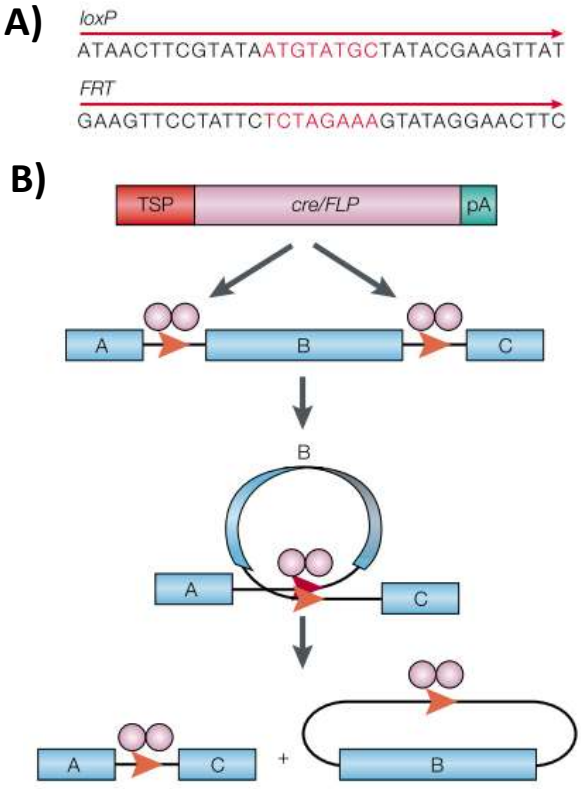

Figure 1.1: Cre-loxP and FLP-FRT recombination system. A) Palindromic sequences (black) of the loxP and FRT recombination sites with asymmetric core (red). B) A tissue specific promoter (TSP) drives the expression of Cre or FLP recombinase. The enzymes recognize their respective recombination sites and excise the flanked DNA segment "B". Adapted by permission from Macmillan Publishers Ltd: [Nature Reviews Genetics] (Lewandoski 2001), copyright (2001).

1.2 Eukaryotic cell membranes

In 1972 Singer and Nicholson proposed the "fluid mosaic model" of lipid membranes (Singer and Nicolson 1972). In this model, they describe the lipid membrane of the cell as a homogenous liquid phase that allows for free lateral movements of proteins. The matrix of the membrane consists of polar lipids with hydrophobic and hydrophilic portions. They form a bilayer structure with hydrophobic tails pointing towards the inside and hydrophilic heads contacting the water interface (see figure 1.2 A). Major lipid constituents of eukaryotic membranes are glycerophospholipids, sphingolipids and sterols (Bretscher and Raff 1975).

Soon there were the first doubts with regard to the random organization of proteins and lipids in membranes substantiated by experimental evidence showing heterogeneous lipid distributions and constrictions of lateral protein movements (Hui and Parsons 1975; Jain and White 1977; Wunderlich *et al.* 1978; de Laat *et al.* 1979). Lipid species are asymmetrically

distributed among the cytosolic and extracellular leaflet (Bretscher 1972; Gordesky and Marinetti 1973). Sphingomyelin for instance, the most prevalent sphingolipid, localizes almost exclusively to the anti-cytosolic leaflet of membranes (Emmelot and Van Hoeven 1975). Furthermore, the "fluid mosaic model" fell short with regard to the effects of lipid interactions and was refined by Simons and Ikonen in 1997 (Simons and Ikonen 1997). Lipid interactions prompt the accumulation of certain lipids in distinct domains and/or cell compartments. The updated model stresses that domains and their connectivity properties modulate the diffusional movement of proteins (see figure 1.2 B). Domain formation facilitates lipid-mediated protein-protein interactions. This is achieved by limiting the lateral movement of proteins and stabilization of protein complexes within the lipid domain (Bagatolli *et al.* 2010).

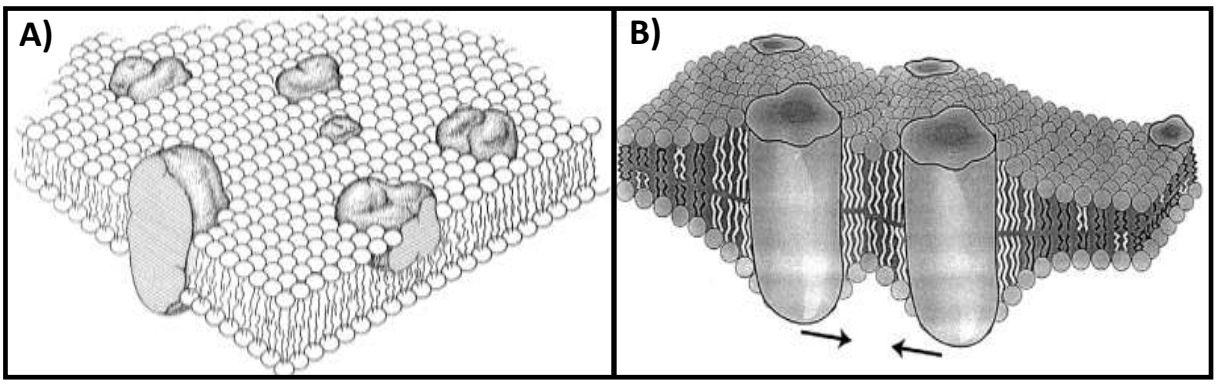

Figure 1.2: Models of the eukaryotic cell membrane. A) The fluid mosaic model as proposed by Singer and Nicolson 1972. Embedded in a homogenous matrix of phospholipids, proteins freely move in the lipid bilayer. B) Lateral membrane structures – lipid domains. According to the model of Simmons and Ikonen 1997, lipid interactions result in lateral segregation and domain formation of certain lipid species. Domain formation confines the diffusional movement of proteins. Figure 1.2 A) from (Singer and Nicolson 1972). Reprinted with permission from AAAS. Figure 1.2 B) reprinted from (Bagatolli et al. 2010), copyright (2010), with permission from Elsevier.

1.2.1 Biophysical properties of ceramide

Ceramide is a sphingolipid composed of sphingosine linked to a fatty acid chain by an amid ester bond with a hydrogen atom as a head group. Ceramide is the basic unit of all complex sphingolipids (Reichel 1940). More than 200 structurally distinct ceramide species exist in mammals differing in their acyl chains, hydroxylations and desaturations (Hannun and Obeid

2011). They are amphiphiles, but with a hydrophobic, non-polar character (Veiga *et al.* 1999). Therefore, ceramides are virtually insoluble in water and exclusively found in membranes. Their interbilayer movement is marginal, restricting ceramides to the compartments of generation. *In vitro* data show that spontaneous intrabilayer "flip-flop" of ceramide occurs at low rate (Bai and Pagano 1997; Contreras *et al.* 2005) and may be restricted by domain formation (Marchesini and Hannun 2004). Ceramides can form pores in mitochondria and permeabilize the membrane (Ruiz-Arguello *et al.* 1996; Siskind and Colombini 2000). Moreover, ceramide directly interacts and modulates the activity of cathepsin D (Heinrich *et al.* 1999), phospholipase A2 (Huwiler *et al.* 1998), kinase suppressor of Ras (Zhang *et al.* 1997), ceramide-activated protein serine–threonine phosphatases (CAPP) (Kowluru and Metz 1997), protein kinase C isoforms (Huwiler *et al.* 1998), potassium channel Kv1.3 (Gulbins *et al.* 1997) and calcium release-activated calcium (CRAC) channels (Lepple-Wienhues *et al.* 1999). In the membrane, ceramides feature a high capacity for intermolecular hydrogen bonding. They act as both, hydrogen bond acceptors and donors for other lipid species and spontaneously self-associate (Shah *et al.* 1995; Simons and Ikonen 1997; Brown and London 1998; Holopainen *et al.* 1998; Kolesnick *et al.* 2000). Hydrophobic van der Waals forces of saturated acyl chains strengthen the interaction of ceramide species (Artetxe *et al.* 2013). The net result of this tight interaction is a lateral segregation from other lipid species and domain formation (Holopainen *et al.* 1998; Kolesnick *et al.* 2000). Microdomains of ceramide fuse and give rise to macrodomains (Grassmé *et al.* 2001).

1.2.2 Ceramide rich domains (CRDs) and transmembrane signaling

The first demonstration of ceramide-rich domain (CRD) formation *in vitro* by Huang et al. in 1996 involved the addition of ceramide to a phasphatidylcholine bilayer. NMR spectroscopy revealed lateral separation of ceramide into domains (Huang *et al.* 1996). Computer models predicted that domain structure may affect the reaction yields of signal transduction pathways (Melo *et al.* 1992; Thompson *et al.* 1995). In living cells, fluorescent immunostainings showed the aggregation of ceramide in distinct lipid domains after stimulation with CD95 and first insights to the physiological function of CRDs were elucidated (Grassmé *et al.* 2001). The following paradigmatic scheme was deduced describing how transmembrane signaling via CRDs may succeed:

An extracellular stimulus induces the generation of ceramide. The net gain in ceramide levels leads to ceramide self-association, lateral segregation from other lipid species, and CRD formation. CRDs reorganize membrane proteins through trapping, stabilization and clustering of receptors. High receptor density facilitates the formation of protein di- and oligomers. Recruitment of intracellular proteins and complex formation activates second messengers and downstream cytoplasmic signaling cascades. In CD95 signaling for instance, ceramide is produced via the activation of acid sphingomyelinase. After an initial activation via the CD95 receptors, the enzyme is relocated to the outer leaflet and induces the formation of CRDs. The activated CD95 receptors become immobilized within the CRDs. Clustering of receptors provides for a feed forward mechanism that amplifies and focuses the signal transduction response (see figure 1.3). Finally, the death-induced signaling complex (DISC) is formed to elicit apoptosis (Grassmé *et al.* 2003a).

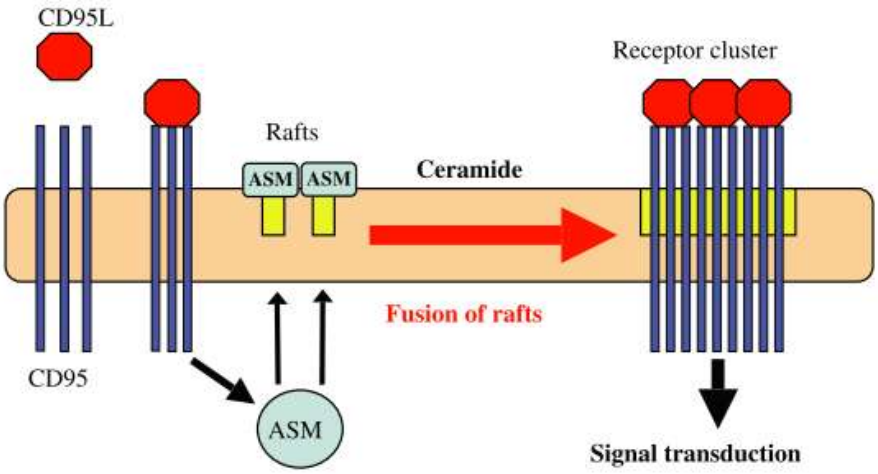

Figure 1.3: Ceramide-rich domains (CRDs) and transmembrane signaling. Initially, activation of the CD95 receptor by its ligand results in the relocalistion of acid sphingomyelinase (ASM) from the lysosome to the outer leaflet of the membrane. ASM hydrolyzes its substrate sphingomyelin and produces ceramide. The net gain in ceramide levels results in the formation of CRDs. CD95 clusters within the CRDs and become spatially organized. The signal transduction response is enhanced and intracellular complex formation induces apoptosis. Figure reprinted from (Grassmé et al. 2007), copyright (2007), with permission from Elsevier.

The initiating stimuli of CRD formation include for instance CD95 ligand (Grassmé *et al.* 2001), TNF-α (Zhang *et al.* 2006), endostatin (Jin *et al.* 2008), CD40 ligand (Grassmé *et al.* 2002), Rituximab (CD20) (Bezombes *et al.* 2004), TRAIL (Dumitru and Gulbins 2006), UV-C

(Charruyer *et al.* 2005), ionizing radiation (IR) (Bionda *et al.* 2007)*, Pseudomonas aeruginosa (Grassmé et al. 2003b)*, *Rhinovirus* (Grassmé *et al.* 2005), cisplatin (Lacour *et al.* 2004), reactive oxygen species (ROS) (Scheel-Toellner *et al.* 2004), and endotoxin (LPS) (Cuschieri *et al.* 2007). Cellular outcomes of CRD transmembrane signaling include apoptosis (Grassmé *et al.* 2001; Lacour *et al.* 2004; Scheel-Toellner *et al.* 2004; Szabo *et al.* 2004; Charruyer *et al.* 2005; Zhang *et al.* 2006; Bionda *et al.* 2007; Cuschieri *et al.* 2007; Jin *et al.* 2008), growth arrest (Bezombes *et al.* 2004), internalization of pathogens (Grassmé *et al.* 2003b; Grassmé *et al.* 2005), release of reactive oxygen species (ROS) (Zhang *et al.* 2008), and induction of inflammation (Teichgraber *et al.* 2008). Deregulated ceramide metabolism and membrane organization has been implied to be involved in many disease pathologies including vascular disorders (Garcia-Barros *et al.* 2003), metabolic disorders (Lang *et al.* 2007), cancer (Goldkorn *et al.* 2013), infections (Grassmé *et al.* 2003b), lung diseases (Teichgraber *et al.* 2008), liver diseases (Seino *et al.* 1997) and diseases of the central nervous system (He *et al.* 2010). Furthermore, disease treatment may be affected by the target cell`s ability to form CRDs (Lacour *et al.* 2004). Consequentially, it is of capital importance to analyze the enzymes involved in the modulation of ceramide levels.

1.3 Ceramide generation

Ceramide can be generated via the de novo- (Mandon *et al.* 1992; Merrill and Wang 1992) and the salvage- pathway (Hoekstra and Kok 1992) (see figure 1.4). Both can be differentially activated, depending on stimulus and cell type (Kitatani *et al.* 2008).

a) The **de novo pathway** is the entry point of sphingolipid metabolism and resides in the endoplasmic reticulum (ER). First, the substrates serine and palmitate are converted by serine palmitoyl transferase (SPT) to produce dihydrosphingosine (Williams *et al.* 1984). Ceramide is synthesized by activity of dihydro-ceramide synthase (CerS) attaching a fatty acid chain to dihydrosphingosine.
b) In the **salvage-pathway**, the acid sphyingomyelinase catalyzes the breakdown of sphingomyelin to produce ceramide in the lysosome. Ceramide is hydrolysed by the acid ceramidase that generates sphingosine. Sphingosine can leave the lysosome and is recycled by ceramide synthase producing ceramide. The neutral sphingomyelinase consumes sphingomyelin in cytoplasmic domains.

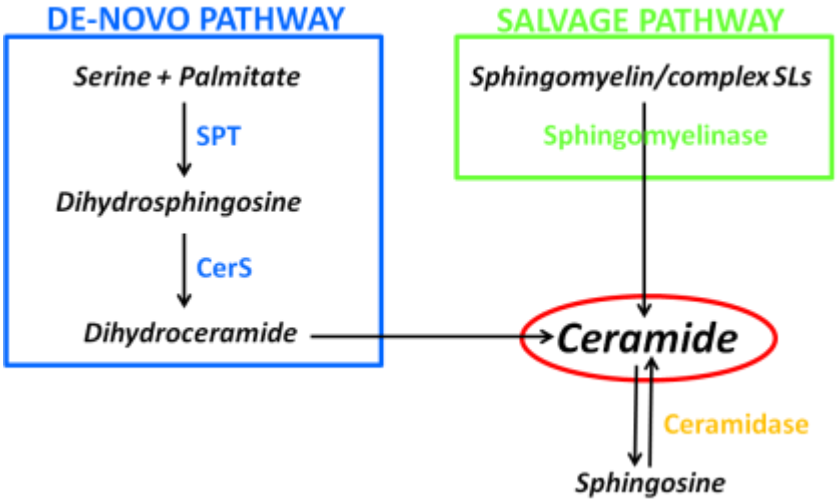

Figure 1.4: Metabolic pathways of ceramide generation. In the de novo pathway, the substrates serine and palmitate are conversed by serine palmitoyl transferase (SPT) to produce dihydrosphingosine. Ceramide is synthesized by activity of dihydro-ceramide synthase (CerS) attaching a fatty acid chain to dihydrosphingosine. In the salvage-pathway, sphyingomyelinases catalyze the breakdown of sphingomyelin and complex sphingolipids (SLs) in the lysosome. Ceramide is further hydrolyzed by ceramidases. Sphingosine is then recycled by ceramide synthase.

1.4 N-acylsphingosine amidohydrolase 1 (AC)

Humans carry 5 genes that encode for ceramide degrading enzymes. According to their pH optima of activity, acid ceramidase (AC), neutral ceramidase (NC), alkaline ceramidase 1 (ACER1), alkaline ceramidase 2 (ACER2), and alkaline ceramidase 3 (ACER3) catalyze hydrolysis of ceramides to generate sphingosine (SPH) and free fatty acid. Acid ceramidase (N-acylsphingosine amidohydrolase 1, AC) was first identified 5 decades ago in rat brain homogenates (Gatt 1963) and purified in 1995 from urine (Bernardo *et al.* 1995). AC catalyzes the deamidation of ceramide to sphingosine with highest rates at a pH of 4.5. Apart from this "forward" hydrolysis mode at a pH of 4.0 – 5.0, the enzyme can work in "reverse" mode at a pH of 5.5 – 6.5 and synthesize ceramide (He *et al.* 2003). Further factors that affect AC activity and mode are the lipid composition (Okino *et al.* 2003) and zinc concentrations (He *et al.* 2003). Exemplarily, phosphatidylserine activates the "reverse mode" while sphingomyelin and zinc promote the "forward mode" (He *et al.* 2003; Okino *et al.* 2003). The activity of AC further depends on the presence of the co-factors saposin C (sapC) and saposin D (sapD) (Azuma *et al.* 1994; Klein *et al.* 1994; Linke *et al.* 2001). Finally, the acyl chain length and saturations of the ceramide substrate affect the metabolic rate *in*

vitro. In these experiments, AC prefers saturated lipids with medium acyl chain length (≥ C6 and ≤ C16) (Momoi *et al.* 1982).

1.4.1 Structural features of AC

The human AC gene (gene symbol: *ASAH1*) is located on the short arm of chromosome 8 (Li *et al.* 1999). The gene contains 14 exons with an open reading frame of 1185 bp that encode for 395 amino acids (Koch *et al.* 1996). The 2.6 kb full length mRNA transcript holds a 110-bp 3-prime untranslated sequence and a 18 bp poly(A) tail. AC mRNA expression is high in kidney and brain and marginal in skeletal muscle and testis as was shown in the mouse (Li *et al.* 1998) and illustrated in the human Expressed Sequence Tag (EST) profile (TiGER database, Johns Hopkins University, MD, USA). In the endoplasmatic reticulum (ER), the spliced mRNA is translated and the AC prepolypeptide synthesized. The prepolypeptide acquires N-linked glycosylations in the ER, which increase its molecular weight and are essential for full enzyme activity (Ferlinz *et al.* 2001). Subsequently, the AC precursor is shuttled through the Golgi network. Only the fraction of AC protein that is mannose-6-phosphorylated by N-acetyl glucosamine phosphotransferase (NAGPT) is addressed to the endo-lysosomal compartment. The non-phosphorylated fraction is released through the secretory pathway (Ferlinz *et al.* 2001). In late endosomes the 53 kDa precursor is processed and yields two subunits (Koch *et al.* 1996). An autocatalytic self-cleavage mechanism activates AC (Shtraizent *et al.* 2008). The α-subunit of 13 kDa and the β-subunit of 40 kDa form the mature heterodimeric AC protein by disulfide bonding (Bernardo *et al.* 1995). The presence of both subunits is essential for AC activity (Li *et al.* 1999; Park and Schuchman 2006). The positively charged AC binds to the negatively charged surface of Bis(monoacylglycero)phosphate (BMP) at the inner membrane of lysosomes. This adhesion positions AC to the interface of the inner membrane and allows for the degradation of its lipid substrate (Gallala and Sandhoff 2011). Furthermore, BMP facilitates the binding of the co-factor saposin D to AC, permitting enhanced AC activity (Azuma *et al.* 1994). AC fulfills housekeeping function by regulating ceramide levels in lysosomes (Sugita *et al.* 1972). A secreted form of AC has also been reported (Romiti *et al.* 2000).

1.4.2 Genotype/phenotype relations

Mutations in the *ASAH1* gene result in a rare disease, named Farber lipogranulomatosis (Farber *et al.* 1957; Sugita *et al.* 1972; Bar *et al.* 2001). The functionality of AC is limited by point mutations or minor deletions of the DNA sequence that result in exon skipping, abnormal splicing or enhanced proteolysis of the mature protein (Park and Schuchman 2006). The reduction of ceramide conversion by AC results in the accumulation of lipids in lysosomes. The clinical picture most prevalently presents with abnormalities in the joints, throat, liver, and central nervous system (Zhang *et al.* 2000; Devi *et al.* 2006). Tissues display infiltration of lipid-laden macrophages (Bar *et al.* 2001). A genetic knockout of both *Asah1* alleles in the mouse genome, deleting exon 3 to 5, was reported to be lethal at the four-cell stage (Li *et al.* 2002; Eliyahu *et al.* 2007). Mortality of early embryos was ascribed to increased ceramide levels (Perez *et al.* 2005; Eliyahu *et al.* 2007). Therefore, AC expression during early embryogenesis is essential to overcome ceramide induced cell death. In a knock-in mouse model, a single nucleotide within a conserved gene region of *Asah1* was exchanged (Alayoubi *et al.* 2013). Consequential conversion of proline 362 to an arginine peptide was reported to reduce AC activity to 10% of the wild type enzyme in Farber patients (Moser *et al.* 1989). Presumably the saposin D binding site of AC is mutated (Alayoubi *et al.* 2013). Knock-in mice were retarded in their growth and viable up to 13 weeks. Increase in cellular ceramide levels seems to promote the release of MCP-1 which is a chemo-attractant for macrophages (Alayoubi *et al.* 2013). Some human cancers display elevated levels of AC expression (Seelan *et al.* 2000; Elojeimy *et al.* 2007). Elevated AC expression in cancer cells confers resistance to chemotherapy and ionizing radiation *in vitro* (Saad *et al.* 2007; Mahdy *et al.* 2009). The consequences of elevated AC expression in an organism are not ascertained at present.

Table 1.1: Summary – Acid ceramidase (AC)

	Human	**Mouse**
Gene Symbol	*ASAH1*	*Asah1*
Cytogenetic location	8p22-p21.3	8 A4
Transcript	mRNA: 2618 bp	mRNA: 2251 bp
	cDNA = 80% identical (Li *et al.* 1998)	
Protein	395 amino acids (1-21 = signaling peptide; 22-142 = α-subunit; 143-395 = β-subunit)	394 amino acids (1-18 = signal peptide; 19-141 = α-subunit, 142 -394 = β-subunit)
	amino acids = 90% identical (Li *et al.* 1998)	
Catalytic activity	N-acylsphingosine + H_2O = carboxylate + sphingosine	
Genetic disorder	Farber disease	

1.5 Acid lysosomal sphingomyelin phosphodiesterase 1 (ASM)

Sphingomyelinases catalyze the conversion of sphingomyelin to ceramide and phosphorylcholine by hydrolization of the phosphodiester bond. At least three different sphingomyelinases exist. They differ in their pH values of maximum enzyme activity and nomenclature distinguishes the three enzymes with the prefixes acid-, neutral-, or alkaline. The first described sphingomyelinase, acid sphingomyelinase (Acid lysosomal sphingomyelin phosphodiesterase I, ASM) was purified from urine (Quintern *et al.* 1987). ASM fulfills a dual role in the cell (Schissel *et al.* 1998). The glycolysation pattern destines whether the enzyme has a housekeeping function in lysosomes or reorganizes microdomain structures at the cell surface (Newrzella and Stoffel 1996; Schissel *et al.* 1998; Jenkins *et al.* 2011).

1.5.1 Structural features of ASM

The human ASM gene (gene symbol: *SMPD1*), mapped to the short arm of chromosome 11 (11p15.1-p15.4), is 4585 bp long with an open reading frame of 1890 bp (da Veiga Pereira *et al.* 1991; Schuchman *et al.* 1992). Six exons encode for 629 amino acids. Exon 2 encodes about 44% of the 75 kDa acid sphingomyelinase prepolypeptide (Schuchman *et al.* 1992). The glycosylated prepolypeptide is synthesized at the rough endoplasmatic reticulum and is processed to a 72 kDa precursor protein. The majority of the enzyme is modified within the trans-golgi-network by mannose-6-phosphate binding which ensures transport to the lysosomal compartment (Ferlinz *et al.* 1997). In the acidic compartment the enzyme matures to the active 65 KDa lysosomal ASM (L-Smase) form (Jenkins *et al.* 2011). L-Smase is exposed to Zn^{2+} in the acidic compartment and by tight interaction its activity becomes "Zn^{2+}-independent" (Schissel *et al.* 1998). A yet to be identified lysosomal thiol protease inactivates L-SMase and produces a 52 kDa form. This protease is a potent regulator of L-SMase activity and sphingolipid signaling (Jenkins *et al.* 2011). Precursor ASM proteins that do not obtain a mannose-6-phosphate are released into the extracellular milieu via the Golgi secretory pathway. Trafficking of secretory ASM (S-Smase) through the Golgi secretory pathway requires "complexing" of N-glycans in order to prevent digestion by endoglycosidase (Hurwitz *et al.* 1994; Schissel *et al.* 1998). In comparison to L-Smase, S-Smase does not encounter a source of Zn^{2+}. Hence, S-Smase remains "Zn^{2+}- dependent" (Schissel *et al.* 1998). A third form of ASM is stored in secretory lysosomes in the vicinity of the plasma membrane. This signaling pool of ASM can be released in a syntaxin 4 dependent

exocytic pathway (Perrotta *et al.* 2010). Stress stimuli can induce the recruitment of ASM to the outer membrane to form CRDs (Cremesti *et al.* 2001; Grassmé *et al.* 2001; Abdel Shakor *et al.* 2004; Rotolo *et al.* 2005; Bao *et al.* 2010; Avota *et al.* 2011). The translocation of the enzyme to the outer leaflet depends on functional microtubules (Grassmé *et al.* 2003a), functional lipid domains (Lacour *et al.* 2004), and phosphorylation of Ser508 of ASM (Zeidan and Hannun 2007).

1.5.2 Genotype/phenotype relations

Genetic mutations in the ASM gene lead to the autosomal recessive disease of Niemann-Pick. Reduced activity of an abnormal ASM gene product causes the accumulation of sphingomyelin in cells (Niemann 1914; Brady *et al.* 1966). In the Niemann-Pick type A variant, neurodegeneration leads to early death of infants. Type B Niemann-Pick patients suffer from progressive visceral impairments (Schuchman and Miranda 1997). More than 100 mutations are described that alter amino acids of the ASM peptide and reduce its functionality (Schuchman 2007). A knockout of the ASM gene to serve as a murine model of Niemann-Pick disease was established by Hourinouchi et al. (Horinouchi *et al.* 1995). Knockout animals fail to thrive and display lipid loaded foam cells in major organs (Horinouchi *et al.* 1995). The mouse model was utilized to ascertain the stress induced formation of ceramide-rich domains and subsequent reorganization of membrane proteins (Cremesti *et al.* 2001; Grassmé *et al.* 2001; Dumitru and Gulbins 2006). A conditional knockout model of the ASM, allowing for temporal and spatial control of the genetic disruption, does not exist at present.

Table 1.2: Summary – Acid sphingomyelinase (ASM)

	Human	**Mouse**
Gene Symbol	*SMPD1*	*Smpd1*
Cytogenetic location	11p15.1-p15.4	7 E3
Transcript	mRNA: 2482 bp	mRNA: 2430 bp
	cDNA = 81% identical (Newrzella and Stoffel 1992)	
Protein	629 amino acids	627 amino acids
	amino acids = 82% identical (Newrzella and Stoffel 1992)	
Catalytic activity	Sphingomyelin + H_2O = N-acylsphingosine + phosphocholine	
Genetic disorder	Niemann-Pick disease	

1.6 Aim of the study

The current study aims to establish two transgenic mouse models with modified sphingolipid metabolism.

In a “gain of function” model, AC expression cassettes will be introduced into the murine genome. The expression cassette comprises a CAG-promoter that drives the transcription of *Asah1* complementary DNA (cDNA). The genetic components of the expression cassette will be assembled by DNA cloning techniques. After verification of expression cassette functionality, the DNA will be delivered to the murine genome by pronuclear injections into fertilized eggs. Transgenic offspring will be identified by PCRs. Founder lines will be established and their genotype and phenotype will be characterized. Generated CAG-Asah1 mice may allow assessing the biological significance of enhanced ceramide hydrolysis.

Furthermore, a targeting construct to introduce recombination sites into the murine *Smpd1* gene will be generated. In the targeting construct, loxP sites are inserted by DNA cloning techniques and flank exon 2 of genomic *Smpd1* DNA. The cloning procedures will be reexamined by PCRs and restriction enzyme digests. Moreover, the recombination competence of the Cre/loxP system will be confirmed in *E. coli.* Subsequently, we will transfect murine ES cells with our targeting construct. Individual ES cell clones are screened for homologous recombination events and the integration of the targeting construct at the *Smpd1* locus by PCRs. Clones with a recombined *Smpd1* locus will be utilized for the injection into murine blastocysts to obtain chimeras. The offspring of chimeras will be reexamined for the modified *Smpd1* locus. The conditional knockout may allow for temporal and spatial control of *Smpd1* gene disruption. Prevention of ceramide synthesis by ASM can be analyzed in single cell types, tissues or at a defined time point.

2. MATERIALS

2.1 Enzymes and antibodies

AccuPrime™ DNA polymerase	Invitrogen™ (Karlsruhe, Germany)
α-acid ceramidase	ProSci Incorporated (Poway, CA, USA)
α-actin	Santa Cruz Biotechnology, Inc. (Delaware Ave, CA, USA)
Alkaline phosphatase-coupled secondary antibodies	Santa Cruz Biotechnology, Inc. (Delaware Ave, CA, USA)
DNA ligase (supplied with buffer)	T4 DNA ligase; New England BioLabs (Beverly, MA, USA)
DNA polymerase I - large Klenow fragment	New England BioLabs (Beverly, MA, USA)
Proteinase K	Sigma-Aldrich Chemie GmbH (Steinheim, Germany)
Restriction enzymes (supplied with buffer)	New England BioLabs (Beverly, MA, USA)
Standard Taq DNA polymerase	Non commercial, made by Dr. R. Waldschütz

2.2 Molecular markers

DNA ladder 100 bp	Invitrogen™ (Karlsruhe, Germany)
DNA ladder 1 kb	New England BioLabs (Beverly, MA, USA)
Protein ladder	Page Ruler Fermentas

2.3 Kits for molecular biology

QIAquick® Gel Extraction Kit	QIAGEN GmbH (Hilden, Germany)
EndoFree® Plasmid Maxi Kit	QIAGEN GmbH (Hilden, Germany)
Effectene® Transfection Reagent	QIAGEN GmbH (Hilden, Germany)

2.4 Bacterial strains and eukaryotic cell lines

E. coli DH10B (for propagation of plasmid DNA)	*Escherichia coli* strain K-12, substrain DH10B; *Taxonomy ID:* 316385 (NCBI); (Durfee *et al.* 2008); purchased from GIBCO®, Invitrogen™ (Karlsruhe, Germany)
E. coli 294-Cre	Gene Bridges GmbH (Heidelberg, Germany), (Buchholz *et al.* 1996)
E. coli 294-FLP	Gene Bridges GmbH (Heidelberg, Germany), (Buchholz *et al.* 1996)
GL261	Established mouse glioma cell line (Szatmari *et al.* 2006). Kind gift of Prof. Dr. M. Weller (University of Zürich)
R1 mouse embryonic stem cells	Received from Prof. Dr. T. Möröy
Mouse embryonic fibroblasts (MEFs)	Generated by Dr. R. Waldschütz from matings of neomycin and hygro resistant mouse strains

2.5 DNA material

2.5.1 Vectors

Litmus28	New England BioLabs (Beverly, MA, USA)
Litmus28-Smpd1/NeoR/loxP	Generated in this project
Litmus28-Smpd1	Generated in this project
Litmus28-Smpd1/LK/loxP	Generated in this project
pBlueSpec2SK	Constructed by Dr. R. Waldschütz
pBS-loxP	Unknown origin
pBS-Smpd1/LK/loxP	Generated in this project
pBS-Smpd1/loxP	Generated in this project
pBSpec2-DT	Generated in this project
pBSpec2Z	Constructed by Dr. R. Waldschütz
pBSpec2Z-Asah1	Generated in this project
pJK plasmid	From the laboratory of Prof. Dr. Gulbins (made by Jutta Kun)
pK11rev2	Constructed by Dr. R. Waldschütz
pLCAG-DnmtI	From the laboratory of Prof. Dr. T. Möröy
pNeb-bGHpA/SCS/Asah1/hGHpA/FRT/SCS	Generated in this project
pNeb-bGHpA/SCS/CAG/Asah1/hGHpA/FRT/SCS (referred to as “CAG-Asah1”)	Generated in this project
pNeb-bGHpA/SCS/CAG/Asah1/hGHpA/NeoR/SCS (referred to as CAG-Asah1/NeoR)	Generated in this project
pNEB193bGHpA/SCS/L2/SCS	Constructed by Dr. R. Waldschütz
pNEB-bGHpA/SCS/lck/iCre/hGHpA/FRT/SCS	Constructed by Dr. R. Waldschütz
pNEB-bGHpA/SCS/lck/ICre/hGHpA/NeoR/SCS	Constructed by Dr. R. Waldschütz
pKO-DT	From the laboratory of Prof. Dr. T. Möröy
pk18	Unknown origin
pk18-CAG	Generated in this project
pK18-bGHpA/SCS/CAG	Generated in this project
pCMV-Sport6	imaGenes GmbH (Berlin, Germany); Genbank accession: BC003204
pPS-Smpd1	Converted phage (Dr. R. Waldschütz)
pPS-Smpd1/DT	Generated in this project
pPS-Smpd1/KO	Generated in this project

2.5.2 Primers and oligonucleotides

Name	Sequence (5` - 3´)
PB3	CTTCCATTTGTCACGTCCTG

PKLink1	GTTTAAACATAACTTCGTATAGTATACATTATACGAAGTTATGTACACTGCA
PKLink2	GTGTACATAACTTCGTATAATGTATACTATACGAAGTTATGTTTAAACTGCA
Asah1.2	CAATTCCCCTCATTTCCTCTC
Asah1.3	GAAGAAGCCAAGAACACAC
Asah1.4	TCATAGACATCCAAAGACTC
Asah1.6	CTTCTGTGTGGTGTGATTTAG
CAG4	CTCTAGAGCCTCTGCTAACC
DTA1	CTCCATCAACGGTTCAGTGAG
DTA2	CAAACTGCCGTAACCTCTGC
hGHas2	GGGTTAGTGCCCCCGTCCCATC
dSCS2.4	GGCATCTCTGAACATCAGGTG
bpA1	GCTGGTTCTTTCCGCCTCAG
loxPfor	AGAATAACTTCGTATAATGTATGC
loxPSmpd1	CGAAGTTATAAGCTCTAGCAGTACATC
Smpd1.3	GGCTATACAGAGAAACCCTGTC
Smpd1.5	CTTCTCAGTTTAATGACCAGCTG
Smpd1.8	GAAGGTCTGGAAGAGTTGCTC
Smpd1.10	CAAGAAAGGGTCACGAGTCAC
Smpd1.12	GCAAAGTCTTATTCACTGCTCTC
Smpd1.13	GACATCAGTATCTCCCACACAC
Smpd1.14	GTGTCCTCAGCACTCTCTACTG
Smpd1.15	GACAAAGAGTGAGGTGAGTCAG
Smpd1.16	ATCAGTGTAAGGGCCTGTGG
Neo1F	TATTCTGCCTTCCTGATGATAACTG
Ragf	GCTGATGGGAAGTCAAGCGAC
Ragr	GGGAACTGCTGAACTTTCTGTG

2.6 Chemicals

Acetic acid (CH_3COOH)	Sigma-Aldrich Chemie GmbH (Steinheim, Germany)
Acrylamide	Carl Roth GmbH & Co. KG (Karlsruhe, Germany)
Agar	Biozym Scientific GmbH (Oldendorf, Germany)
Agarose	Carl Roth GmbH & Co. KG (Karlsruhe, Germany)
Ammonium persulfate (APS)	Sigma-Aldrich Chemie GmbH (Steinheim, Germany)
Ampicillin	Sigma-Aldrich Chemie GmbH (Steinheim, Germany)
Aprotinin	Serva Electrophoresis GmbH (Heidelberg, Germany)
Bacto-Agar	Beckton, Dickinson and Company (Franklin Lakes, NJ, USA)
Bacto-tryptone	Beckton, Dickinson and Company (Franklin Lakes, NJ, USA)

Bovine serum albumin (BSA)	Carl Roth GmbH & Co. KG (Karlsruhe, Germany)
Bradford reagent	BioRad (München, Germany)
Bromophenol blue	Sigma-Aldrich Chemie GmbH (Steinheim, Germany)
Calcium chloride ($CaCl_2$)	Sigma-Aldrich Chemie GmbH (Steinheim, Germany)
Chemiluminescence detection reagent	CDP-Star®; PerkinElmer (Waltham, MA, USA)
Chloroform ($CHCl_3$)	Ridel-de Haën® (Seelze, Germany)
Deoxycholic acid	Sigma-Aldrich Chemie GmbH (Steinheim, Germany)
Deoxyribonucleotides (dNTP´s)	Bio-Budget Technologies GmbH (Krefeld, Germany) and PEQLAB Biotechnology GmbH (Erlangen, Germany)
DMSO	Sigma-Aldrich Chemie GmbH (Steinheim, Germany)
EDTA	Sigma-Aldrich Chemie GmbH (Steinheim, Germany)
Eosin	Merck KGaA (Darmstadt, Germany)
Ethidium bromide	Sigma-Aldrich Chemie GmbH (Steinheim, Germany)
Ethanol (C_2H_5OH)	Carlo Erba Reagents (Val de Reuil, France)
Evagreen®	Biotium, Inc. (Hayward, CA, USA)
FBS	Gibco/Invitrogen (Karlsruhe, Germany)
Gelatin	Merck KGaA (Darmstadt, Germany)
Geneticin (G418)	Gibco/Invitrogen (Karlsruhe, Germany)
Glycerol	Sigma-Aldrich Chemie GmbH (Steinheim, Germany)
Glycine	Carl Roth GmbH & Co. KG (Karlsruhe, Germany)
Glucose	Sigma-Aldrich Chemie GmbH (Steinheim, Germany)
HEPES	Carl Roth GmbH & Co. KG (Karlsruhe, Germany)
Isopropanol	Sigma-Aldrich Chemie GmbH (Steinheim, Germany)
Kanamycin	Sigma-Aldrich Chemie GmbH (Steinheim, Germany)
Leupeptin	Serva Electrophoresis GmbH (Heidelberg, Germany)
Magnesium chloride ($MgCl_2$)	Sigma-Aldrich Chemie GmbH (Steinheim, Germany)
Magnesium sulfate ($MgSO_4$)	Sigma-Aldrich Chemie GmbH (Steinheim, Germany)
Methanol (CH_3OH)	Carlo Erba Reagents (Val de Reuil, France)
2-Mercaptoethanol	GIBCO®, Invitrogen™ (Karlsruhe, Germany)
Mitomycin C	Sigma-Aldrich Chemie GmbH (Steinheim,

	Germany)
Non-fat dry milk powder	AppliCHem (Darmstadt, Germany)
NP-40	Sigma-Aldrich Chemie GmbH (Steinheim, Germany)
Penicillin/Streptomycin	Gibco/Invitrogen (Karlsruhe, Germany)
Phenol (C_6H_5OH)	Carl Roth GmbH & Co. KG (Karlsruhe, Germany)
Potassium acetate (CH_3CO_2K)	Sigma-Aldrich Chemie GmbH (Steinheim, Germany)
Potassium chloride (KCl)	Sigma-Aldrich Chemie GmbH (Steinheim, Germany)
Potassium dihydrogen phosphate (KH_2PO_4)	Sigma-Aldrich Chemie GmbH (Steinheim, Germany)
Protease inhibitor cocktail tablets (cOmplete Mini EDTA-free)	Roche AG (Basel, Switzerland)
RBM14-12 (synthetic ceramide analog)	(Bedia *et al.* 2007; Bedia *et al.* 2010); provided by Prof. Dr. A. Delgado (Barcelona, Spain)
D(+)-Saccharose	Carl Roth GmbH & Co. KG (Karlsruhe, Germany)
Sodium acetate (CH_3COONa)	Sigma-Aldrich Chemie GmbH (Steinheim, Germany)
Sodium chloride (NaCl)	Carl Roth GmbH & Co. KG (Karlsruhe, Germany)
Sodium dodecyl sulphate (SDS)	Serva Electrophoresis GmbH (Heidelberg, Germany)
Sodium phosphate dibasic (Na_2HPO_4)	Sigma-Aldrich Chemie GmbH (Steinheim, Germany)
Sodium hydroxide (NaOH)	Sigma-Aldrich Chemie GmbH (Steinheim, Germany)
Sodium periodate ($NaIO_4$)	Sigma-Aldrich Chemie GmbH (Steinheim, Germany)
Sodium fluoride (NaF)	Sigma-Aldrich Chemie GmbH (Steinheim, Germany)
Sodium pyrophosphate ($Na_4P_2O_7$)	Sigma-Aldrich Chemie GmbH (Steinheim, Germany)
Tetramethylethylenediamine (TEMED)	Sigma-Aldrich Chemie GmbH (Steinheim, Germany)
Tris	Carl Roth GmbH & Co. KG (Karlsruhe, Germany)
Triton X-100	Sigma-Aldrich Chemie GmbH (Steinheim, Germany)
Tween	Sigma-Aldrich Chemie GmbH (Steinheim, Germany)
Umbelliferone	Sigma-Aldrich Chemie GmbH (Steinheim, Germany)
Xylene cyanol	Sigma-Aldrich Chemie GmbH (Steinheim, Germany)

Yeast extract	Carl Roth GmbH & Co. KG (Karlsruhe, Germany)

2.7 Solutions and buffers

2.7.1 Molecular Biology

DNA and protein buffers

Bacterial lysis buffer	0.2 N NaOH 1% SDS
Neutralization buffer	3 M Potassium acetate pH 5.2
PCR buffer (10x)	200 mM Tris-HCl pH 8.3 500 mM KCl 14 mM $MgCl_2$ 0.1% Gelatin
Resuspension buffer	50 mM Glucose 10 mM EDTA 25 mM Tris-HCl pH 8.0
Sucrose lysis buffer	250 mM D(+)-Saccharose Protease inhibitor cocktail tablet (1 per 10 ml)
TE buffer	10 mM Tris/HCl pH 7,6 1 mM EDTA
Tissue lysis buffer	10% 10x PCR-buffer Mg-free 0.5 mM $MgCl_2$ 0.045% Tween-20 0.045% NP-40 Proteinase K 300 µg/ml

Agarose gel electrophoresis

DNA loading buffer (6x)	50% Glycerol 0.02% Bromophenol blue 0.04% Xylene Cyanol 1 mM EDTA
TAE buffer (50x)	2 M Tris 950 mM Acetic acid 62.5 mM EDTA

Agar plates

Ampicillin (100x)	10 mg/ml
Kanamycin (1000x)	50 mg/ml
LB (Lysogeny Broth) medium	10 g/l Bacto-tryptone 10 g/l NaCl 5 g/l yeast extract Adjust pH to 7.5 with NaOH
LB (Lysogeny Broth) agar plates	LB medium with 1.5% Bacto-Agar was

	autoclaved and cooled down to 50°C. 1% Ampicillin (100x) or 0.1% Kanamycin (1000x) was added. The media was mixed and poured into 90 mm Petri dishes. After hardening of the agar, plates were stored at 4°C

2.7.2 Cell culture

Supplements

Dulbecco's modified Eagle's medium (DMEM)	GIBCO®, Invitrogen™ (Karlsruhe, Germany)
Fetal Bovine Serum (FBS)	GIBCO®, Invitrogen™ (Karlsruhe, Germany)
KNOCKOUT™ DMEM	GIBCO®, Invitrogen™ (Karlsruhe, Germany)
L-Glutamine	GIBCO®, Invitrogen™ (Karlsruhe, Germany)
LIF (leukemia inhibitory factor)	ESGRO® mLIF; Merck KGaA (Darmstadt, Germany)
MEM-non-essential amino acids	GIBCO®, Invitrogen™ (Karlsruhe, Germany)
Nucleosides: adenosine, guanosine, uridine, cytidine, thymidine	Sigma-Aldrich Chemie GmbH (Steinheim, Germany)
100x Penicillin/streptomycin	GIBCO®, Invitrogen™ (Karlsruhe, Germany)
Sodium pyruvate	GIBCO®, Invitrogen™ (Karlsruhe, Germany)
Trypsin	GIBCO®, Invitrogen™ (Karlsruhe, Germany)

Media and buffers

Complete MEM	500 ml MEM 10% FBS 10 mM HEPES pH 7.4 2 mM L-Glutamine 1 mM Sodium pyruvate 0.1 mM Non-essential amino acids 1% 100x Penicillin/streptomycin
ES cell medium	500 ml Knockout-DMEM 0.1 mM Non-essential amino acids 0.1 mM 2-Mercaptoethanol 15% FBS 1% 100× Nucleosides 6000 U LIF 0.1 M L-Glutamine
ES cell freezing medium	20% DMSO 50% FBS 30% ES cell medium
10x HEPES-saline	200 mM HEPES 1.32 M NaCl 10 mM $CaCl_2$ 7 mM $MgCl_2$ 8 mM $MgSO_4$

	54 mM KCl
ES cell lysis buffer	100 mM Tris pH 8.3 5 mM EDTA 0.2% SDS 200 mM NaCl 0.1 µg/ml Proteinase K
Mouse Embryonic Fibroblast (MEF-) medium	440 ml KNOCKOUT™ DMEM, 50 ml Fetal Bovine Serum 5 ml L-Glutamine
100× nucleosides	3 mM Adenosine 3 mM Guanosine 3 mM Uridine 3 mM Cytidine 3 mM Thymidine
Phosphate Buffered Saline (PBS)	137 mM NaCl 2.7 mM KCl 7 mM $CaCl_2$ 0.8 mM $MgSO_4$ 1.4 mM KH_2PO_4 6.5 mM Na_2HPO_4 Adjust pH to 7.6
Trypsin	0.25% Trypsin 5 mM Glucose 1.3 mM EDTA in PBS

2.7.3 Biochemistry

Western Blotting

Alkaline wash buffer	100 mM Tris pH 9.5 100 mM NaCl
Blocking buffer	5% of non-fat dry milk powder in TBS-T (see below)
Running buffer	25 mM Tris 250 mM Glycine 0.1 % SDS
Running gel (10%)	3.75 ml Solution A (see below) 5.0 ml Solution B (see below) 6.11 ml H_2O 75 µl 20% SDS 30 µl TEMED 30 µl 10% APS in H_2O
SDS lysis buffer	25 mM HEPES pH 7.4 0.1% SDS 0.5% Deoxycholic acid 1% Triton X-100 10 mM EDTA 10 mM Sodium pyrophosphate

	10 mM Sodium fluoride 125 mM NaCl
SDS sample buffer (5x)	62.5 mM Tris pH 6.8, 10% Glycerol, 2% SDS, 0.04% Bromphenol blue 5% 2-Mercaptoethanol
Solution A	40% Acrylamide (39.2 g Acrylamide /100 ml; 0.8 g Bis-Acrylamide /100 ml)
Solution B	3M Tris pH 8.8
Solution C	3M Tris pH 6.8
Stacking gel	0.63 ml Solution A 0.21 ml Solution C 4.1 ml H_2O 0.025 ml 20% SDS 0.02 ml TEMED 0.02 ml 10% APS in H_2O
Transfer buffer	25 mM Tris 192 mM Glycine 20% Methanol
10 x Tris-buffered Saline supplemented with 0.1% Tween-20 (TBS-T)	200 mM Tris pH 7.4 1500 mM NaCl 1% Tween-20

2.8 Equipment

Cell culture incubator	ThermoFisher Scientific (Waltham, MA, USA)
Culture flasks and plates	TPP® (Trasadingen, Switzerland)
Cryotubes	ThermoFisher Scientific (Waltham, MA, USA)
Disposable polystyrene cuvettes	Sarstedt AG & Co (Nümbrecht, Germany)
DNA annotation and analysis software	Vector NTI 10.3.0; Invitrogen™ (Karlsruhe, Germany)
Electrophoretic transfer cell	Mini Trans-Blot® Cell; BioRad (München, Germany)
Electroporation cuvettes	Gene Pulser cuvettes 0,4 cm; BioRad
Electroporation device	Gene Pulser Xcell™; BioRad
Filter Paper	Whatman (Mainstone, United Kingdom)
Fluorescence microplate reader	BMG Labtech (Offenburg, Germany)
Gel-documentation device	AlphaImager® HP; Alpha Innotech/Biozym Scientific GmbH (Oldendorf, Germany)
Horizontal gel electrophoresis chamber	PEQLAB Biotechnology GmbH (Erlangen, Germany)
Hybond nitrocellulose membrane	GE Healthcare (Chalfont St Giles, United Kingdom)
Image analysis software	ImageJ; Rasband, W.S., U. S. National Institutes of Health (Bethesda, Maryland, USA); open-source software:

	http://imagej.nih.gov/ij/, (Schneider *et al.* 2012).
Laminar flow hood	Biohit/Sartorius Antares (Milano, Italy)
Neubauer chamber 0.1 mm	Marienfeld (Lauda-Königshofen, Germany)
Optical adhesive film	Sarstedt AG & Co (Nümbrecht, Germany)
Power source	PEQLAB Biotechnology GmbH (Erlangen, Germany)
Porcelain mortar	W.Haldenwanger Technische Keramik GmbH & Co. KG (Waldkraiburg, Germany)
Real-Time PCR System	ABI PRISM® 7300 Real-Time PCR System, Applied Biosystems (Foster City, CA, USA)
Shaking incubator	Eppendorf AG (Hamburg, Germany)
Sonicator	Model GE 50, 50 W model, ALLTECH Assoc. Inc. (Deerfield, IL, USA)
Thermal cycler	C1000™ thermal cycler; BioRad (München, Germany)
96 U-bottom well plate	Sarstedt AG & Co (Nümbrecht, Germany)
UV-spectrophotometer	Eppendorf AG (Hamburg, Germany)
Vertical protein electrophoresis system	Mini-PROTEAN® system; BioRad (München, Germany)

3. METHODS

3.1 Manipulation of DNA

3.1.1 Digestion of DNA by restriction enzymes

Restriction enzyme digests were performed for the purpose of plasmid identification, generation of DNA fragments for ligation, and linearization of DNA fragments prior to pronuclear injection. Digests of plasmid DNA (500-3000 ng) were performed in reaction volumes of 10 – 20 µl under conditions and durations that accounted for the enzyme(s) properties used in the reaction (according to the manufacturer`s protocols and compatibility table; New England BioLabs, Beverly, MA, USA).

3.1.2 Agarose gel electrophoresis

Agarose gel electrophoresis serves to separate linear DNA fragments according to their length. The concentration of agarose affects the separation properties of the negatively charged DNA in the gel matrix when an electric current is applied. For the analysis of DNA fragments with a size > 1 kb, 1% agarose was solved in 100 ml 1 x TAE buffer by boiling. To analyze DNA fragments with a size < 1 kb, 2% agarose was used. Furthermore, the DNA intercalating agent ethidium bromide (1 µl) was added to the agarose-matrix. The solution was poured into a gel tray with combs and left for 20 minutes to solidify. The tray was placed in a horizontal gel electrophoresis chamber connected to a power source. DNA samples were mixed with DNA loading buffer and loaded into the slots. Electrophoresis was started by applying an electric field with a constant voltage of 100 V. The fluorescence of ethidium bromide was visualized by excitation with ultraviolet (UV) light in a gel-documentation device. The length of the DNA fragments was deduced from a DNA standard ladder that was run parallel to the samples. Agarose gels served to identify and isolate desired DNA fragments.

3.1.3 DNA purification of agarose gels

DNA was extracted from agarose gels to isolate a fragment of interest and cleanup DNA from enzymatic reactions. The desired DNA fragment was excised from the agarose gel with a scalpel and processed according to the QIAquick Gel Extraction Kit protocol (buffers supplied with the kit: QG, PE). Briefly, the gel was solubilized at 50°C in buffer QG (3x gel volume) for

10 min. Isopropanol was added (1x gel volume) and mixed followed by application of the sample to a QIAquick column (supplied with the kit) and subsequent centrifugation at 13000 rpm. The column was washed once with 750 µl buffer PE. DNA was eluted into a clean Eppendorf-tube by applying 30 µl TE buffer to the column.

3.1.4 Filling of 5` protruding ends

The cloning strategy preferably was based on the ligation of compatible sticky ends. If this was not possible, the strategy relied on blunt-end cloning. To this end, fill-in reactions using the DNA polymerase I - large Klenow fragment were performed. Klenow is able to fill-in 5` overhangs. The reactions, involving linearized vectors or DNA fragments, were set up as follows:

DNA	20 µl
10 x Restriction enzyme buffer 2 (NEB)	3 µl
Klenow (5 U/µl)	1.5 µl
dNTP`s (10 mM)	5.5 µl

The reactions were carried out at RT for 30 minutes. Prior to using the DNA for ligation, Klenow was either inactivated at 75°C for 30 min or removed by purifying the DNA via gel electrophoresis and subsequent extraction.

3.1.5 Generation of linker from oligonucleotides

Two oligonucleotides were annealed to serve as a linker that yields two new restriction sites (PmeI and BsrGI) needed for following cloning steps. The reaction mixture, comprising 1 µl Tris (stock: 1 M) added to 10 µl PKLink1 and 10 µl PKLink2 (stocks: 100 µM) in a PCR tube, was put in a thermal cycler. The PCR program served to heat the reaction up to 95°C and subsequently cool it down with a ramp rate of 0.1°C/sec to RT. Slow cooling allowed annealing of the complementary strands. This yielded an adapter with four bases as overhangs on both sides.

3.1.6 Ligation of DNA fragments into plasmids

In order to incorporate a DNA fragment into a linearized plasmid vector backbone, a DNA ligase was utilized. The Ligase catalyzes the formation of phosphodiester bonds, thereby joining cohesive or blunt end termini. Ligations were performed with a molar insert: vector DNA ratio of 3:1 (about 100 ng vector backbone). The reaction was made up of 1 µl 10x DNA

ligase buffer, 1 µl DNA ligase, DNA and was filled up with ddH_2O to a final volume of 10 µl. For ligation of cohesive ends, reactions were performed at RT for 2 hours. To facilitate blunt end ligation, the reaction was left at RT overnight.

3.2 Transformation of competent bacteria with plasmid DNA

Plasmid DNA preparation was used to transform chemo-competent *E. coli* (DH10B). 1-4 µl of DNA was added to 100 µl of competent bacteria in a 1.5 ml reaction tube, gently mixed, and incubated for 20 minutes on ice. Bacteria were heat-shocked for 45 seconds at 42˚C. After the heat shock, the tube was incubated on ice for 10 minutes. Subsequently, 900 µl of LB medium was added and the tube incubated at 37°C for 30 minutes. Bacteria were pelleted by centrifugation at 3000 rpm for 2 minutes and the pellet resuspended in 50 µl of LB medium. The solution was distributed on a LB agar plate with appropriate antibiotic to select for bacteria that propagate the plasmid. Bacterial colonies were picked after 12-14 hours of incubation at 37°C.

3.3 Isolation of plasmid DNA

3.3.1 Mini-preparation

Single colonies were picked from a LB-agar plate with a pipette tip and added to 2 ml of LB medium with appropriate antibiotic. The culture was grown overnight at 37°C in a shaking incubator. After incubation, cells were transferred to a 2 ml reaction tube and pelleted by centrifugation at 13000 rpm for 1 minute. The supernatant was removed and the bacteria resuspended in 100 µl resuspension buffer. For cell lysis, 200 µl bacterial lysis buffer was added and mixed. Subsequently, 150 µl neutralization buffer was added and mixed by inverting 5 times. Tubes were centrifuged at 13000 rpm for 5 minutes. In the meantime, 1000 µl of 100% ethanol was added to new 1.5 ml Eppendorf-tubes. After centrifugation, the supernatant (~450 µl) was transferred to the Ethanol containing tubes for precipitation. Tubes were centrifuged at 13000 rpm for 15 minutes. Pellets were washed with 600 µl of 80% ethanol and air dried for 5 – 10 minutes prior to resuspension in 30 µl buffer TE.

3.3.2 Maxi-preparation

For large-scale plasmid preparation, 250 ml of LB medium with appropriate antibiotic were inoculated with bacteria to propagate the plasmid of interest. The culture was incubated in a

shaking incubator at 200 rpm overnight. The plasmid was harvested according to the protocol of the Endofree® plasmid Maxi kit based on alkaline lysis (the following reagents are supplied with the kit: P1, P2. P3, QBT, QC, QN, ER, and TE). Briefly, cells were centrifuged and the pellet resuspended in 10 ml buffer P1. 10 ml of buffer P2 were added, gently mixed and incubated for 5 minutes at RT. Following mixing with buffer P3, the solution was incubated on ice for 20 min. The lysate was poured into a QIAfilter Cartridge (supplied with the kit) and incubated for 10 min. The lysate was filtered into a 50 ml tube. Buffer ER, 2.5 ml, was added and incubated on ice for 30 min. The filtered lysate was applied to an equilibrated (buffer QBT) QIAGEN-tip 500 (supplied with the kit). The column was washed twice with 30 ml of buffer QC to dispose the plasmid DNA of proteins and RNA. DNA was eluted with 15 ml buffer QN and precipitated by adding 0.7 volumes isopropanol with subsequent centrifugation at 8000 rpm for 1 hour. Pellets were washed with 5 ml endotoxin-free 70% ethanol and air dried for 5 – 10 minutes. Plasmid DNA was dissolved in 50 µl endotoxin-free buffer TE (supplied with the kit). DNA concentrations were determined by means of a UV-spectrophotometer at a wavelength of 260 nm.

3.4 Analysis of ligation events by colony PCR

Plasmid DNA was screened for successful ligation events by colony PCR. To this end, plasmid DNA was added to a standard PCR reaction that included one primer hybridizing with its corresponding complementary DNA on the vector backbone and the other primer targeted to the inserted DNA fragment. The PCR reaction solely amplified a DNA fragment in the case that the DNA fragment was inserted with the correct orientation into the plasmid backbone. After transformation of plasmids into competent *E. coli* and overnight growth on LB agar plates at 37 °C, colonies were picked off with a pipette tip. The same tip was then dipped into a 0.2 ml tube containing reagents of the PCR reaction (10% PCR buffer (10x), 200 µM dNTPs, primers (150 pmol), standard Taq polymerase (1 unit/25 µl), and nuclease-free ddH_2O) and rubbed to the walls in a circular motion for 3 seconds. Subsequently, the same tip was used to inoculate an Eppendorf-tube with 1 ml fresh LB medium and selective antibiotic. The labeling of the Eppendorf-tubes corresponded to the labeling of the PCR reaction tubes. About 30 colonies per ligation were processed in this way. DNA amplification was performed in a thermal cycler. The lid was preheated to 104°C and the reactions were heated and cooled according to the following thermal protocol:

Thermal Protocol - "Standard PCR"

Step	Temperature	Time
1	**95°C**	**4:00 min**
2	**94°C**	**0:15**
3	**58°C**	**0:30**
4	**72°C**	**1:00**
5	**Go to step 2 (34x)**	
6	**72°C**	**9:00**
7	**4°C**	**"Forever"**

The PCR reaction product was analyzed by agarose gel electrophoresis. Inoculated LB-medium of colonies that showed successful amplification of a PCR product was used for Mini-preparation of plasmid DNA and further assessment by restriction enzyme digests.

3.5 Verification of recombination competence in bacteria

The pPS-Smpd1/KO plasmid contains recombination sites that flank the second exon of the *Smpd1* gene and the neomycin cassette. In order to verify at an early stage that the introduced sites are competent for recombination, the plasmid construct was transformed into *E. coli* strains 294-Cre and 294-FLP (Buchholz *et al.* 1996). The strains hold corresponding recombinase genes in their genome. After overnight growth of bacteria in LB medium at 37°C and subsequent isolation of plasmid DNA by mini-preparation (see above, paragraph 3.3.1), restriction enzyme digests with BstBI and XhoI were performed. The DNA fragments were separated on a 1% agarose gel.

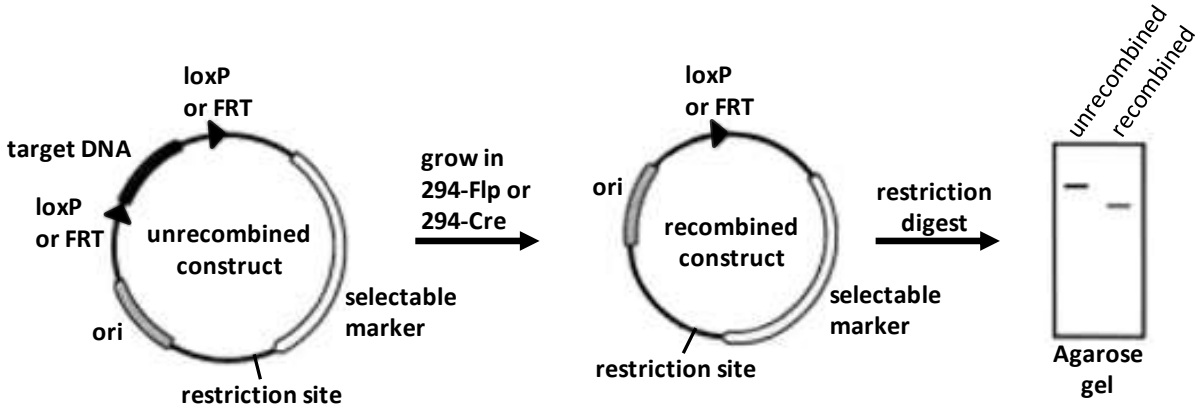

Figure 3.1: Scheme of the procedure to test for recombination competence. A DNA sequence of a plasmid is flanked by either loxP or FRT sites. The plasmid is transformed into recombinase expressing bacteria (Cre or FLP recombinase) and the bacteria left to grow. The enzymes recognize their respective recombination sites and remove the flanked DNA sequences. This can be confirmed by restriction enzyme digestion of purified plasmid DNA

and subsequent visualization of DNA fragments on an agarose gel. Figure adapted from (Buchholz et al. 1996), by permission of Oxford University Press.

3.6 Embryonic stem (ES-) cell culture methods

3.6.1 Preparation of mouse embryonic fibroblast (MEF) feeder layers

Prior to the culturing of ES cells, feeder cells were prepared. Mouse embryonic fibroblasts (MEFs) allow for the continuous growth of ES cells in an undifferentiated state. Thereby, pluripotency of ES cells is maintained which is crucial for effective contribution of modified ES cells to the germline. The surfaces of 6 tissue culture flasks, 225 cm^2, were coated with 20 ml of 0.2% gelatin in PBS for 2 hours. The gelatin was aspirated and flasks were washed once with 20 ml of PBS prior to adding 15 ml prewarmed MEF medium. Ready to use fibroblasts were removed from the liquid nitrogen (LN_2) –tank and the cryotubes thawed at 37°C in a water bath. Fibroblasts were diluted in 30 ml of prewarmed MEF medium in a sterile tube and 5 ml of the fibroblast solution was pipetted to each culture flask. Cells were grown in a cell culture incubator (5% CO_2 and 37°C) and split 1:3 after 3 days. Confluent monolayers (70 – 100%) were division-inactivated by mitomycin C. The mitomycin C stock (20x mitomycin C stock: 2 mg mitomycin C dissolved in 10 ml PBS) was diluted in MEF medium (1:20). The original medium in the culture flasks was aspirated and 20 ml of the mitomycin C containing medium was added. Cells were left for 2-3 hours in the incubator. Subsequently, the medium was removed and fibroblasts were washed twice with PBS to remove remains of the drug. Next, the cells were harvested and frozen (in medium supplemented with 20% DMSO). In order to use the MEFs as feeder layer for the culturing of ES cells, fibroblasts were thawed and plated with the previous MEF-concentration/plate area ratio on gelatin coated plastic ware to obtain a confluent layer. Prior to usage as a feeder plate, the MEF medium was aspirated, the culture plate washed once with PBS and ES cell medium added.

3.6.2 ES cell culture

Murine ES cells of the R1-129 line were cultured under a laminar flow hood under sterile conditions and kept in a cell culture incubator at 5% CO_2 and 37°C. In order to keep the stem cells in an undifferentiated, pluripotent state, cells were constantly cultured in ES cell medium and grown on MEF feederlayers. The medium was invariably changed every 24 hours. A vial of ES cells was thawed and diluted in 10 ml ES cell medium. The cells were centrifuged at 1200 rpm for 5 minutes and the pellet resuspended in 5 ml ES cell medium.

The cell solution was transferred to a T25 culture flask. After 24 hours, ES cells were split 1:6 by transferring the cells to two T75 culture flasks (à 150 cm^2). This involved trypsinization, spinning (5 min at 1200 rpm), resuspension (in 5 ml ES medium) and transfer (2.5 ml to each T75 culture flask) of ES cells. Cells were grown until the plate was dense with oval, shiny clones with clear boundaries (~ 5 x 10^7 cells/T75 flask) and used for electroporation.

3.6.3 Electroporation of ES cells

DNA was introduced into mouse embryonic stem cells by electroporation. An electrical pulse opens pores in the ES cells for a short time frame and suffices for the linearized DNA of the targeting construct to enter the cell.

Plasmid DNA (90 µg, EndoFree® Plasmid Maxi Kit derived) of the targeting construct, pPS-Smpd1/KO, was digested by the restriction enzyme KpnI. DNA was solved in a final volume of 150 µl in ddH_2O supplemented with KpnI (4 µl), and appropriate restriction buffer. The reaction was incubated at 37°C overnight. To remove contaminating proteins from the DNA, the sample volume was increased to 300 µl with ddH_2O and an equal volume phenol:chloroform 1:1 was added and the tube vortexed. The solution was centrifuged at 13000 rpm for 2 minutes and the protein-free aqueous phase removed into a fresh reaction tube. In order to precipitate the DNA, 0.1 volumes sodium acetate 3.0 M, pH 5.5, and 2.5 volumes cold 100% ethanol were added and the reaction tube put into a -20°C freezer and left overnight. The next day, the tube was centrifuged at 13000 rpm at 4°C for 15 minutes. The pellet was washed once with 500 µl 80% ethanol, air dried, and finally dissolved in 40 µl TE buffer. In order to ensure completeness of the DNA digestion by KpnI, 2 µl of linearized DNA were run in a 1% agarose gel and compared to an undigested pPS-Smpd1 plasmid DNA sample.

Cells of two T75 culture flasks (à 150 cm^2; ~ 5 x 10^7 cells) were trypsinized, centrifuged (1100 rpm, 5 minutes, RT) and suspended in 2 ml PBS (4°C). An electroporation cuvette was loaded with 30 µl DNA solution (~ 30 µg DNA) and 1 ml of cell suspension. The electroporation was carried out in “time constant” mode using an electroporation device with the following settings: voltage: 800 V, time constant: 0.2 ms, capacitor 10 µF, and resistor/pulse controller: infinity. Afterwards, the cuvettes were kept at 4°C for 20 minutes. The solution of each approach was diluted 1:10 with ES cell medium and divided over 14 petri dishes (1 ml/dish). Another 15 ml of ES cell medium was added to each dish. The medium was

changed every 24 hours. One day post electroporation, the medium was supplemented with 175 µg/ml geneticin (G418) to select for integration of the targeting construct. After 7 days of selection, ES cell clones were picked.

3.6.4 Collection of ES cell clones

After seven days of selection, single ES cell clones were visible under the microscope. The media of the first petri dish was aspirated and changed for PBS. Next, 15 µl of PBS were added to the wells of a new 96 U-bottom well plate. Microscope assisted, a single clone was freed from the feeder layer with a 20 µl pipette tip. The clone was sucked into the tip in a volume of 2.5 µl fluid and transferred to a well of the 96 well plate. The procedure was repeated and the 96 well plate filled with one clone per well. Every twelfth well, the procedure was interrupted to add 35 µl of trypsin to the clone containing wells. The plate was incubated at 37°C for 10 minutes. Afterwards, 75 µl of ES cell medium was added and the cells of the clones singularized by pipetting up and down (10x). The cells were transferred to a normal 96 well plate with MEF feeder layer. Then, the collection of ES cell clones was continued. The 14 petri dishes were processed in this way and three 96 well plates were filled with ES cell clones. When individual clones reached 60% percent confluence, cells were transferred to 24 well plates with feeder layer. At this stage, 148 clones showed normal growth in 24 well plates and were further processed. After 2 days of further culturing in the 24 well plate, cells were trypsinized and singularized in 750 µl ES cell medium. Three-quarter of cells (500 µl) were diluted in ES cell freezing medium 1:1 v/v, transferred to cryo tubes in a precooled cryo box, and kept at -80°C for one night. The next day, clones were frozen in liquid nitrogen. The other quarter of ES cells was left to grow for another 2 days in the 24 well plate and then lysed in 400 µl ES cell lysis buffer to obtain DNA samples.

3.6.5 ES cell screening by PCR

DNA of 148 ES cell clones was screened for the integration of the targeting construct at the *Smpd1* locus by PCR. DNA samples were heated to 95°C for 10 minutes in order to inactivate proteinase K which was a constituent of the ES cell lysis buffer. PCR master mixes were assembled and contained: 10% PCR buffer (10x), 200 µM dNTPs, 150 pmol primers, DNA Polymerase (1 unit/25 µl), and nuclease-free ddH_2O. DNA (1 µl, ca. 100 ng) was added to a 0.2 ml PCR reaction tube to yield a total reaction volume of 25 µl. Standard Taq polymerase

was used for the amplification of DNA templates up to 1 kb. Larger DNA fragments were amplified by AccuPrime™ DNA polymerase. Reaction tubes were put into the thermal cycler and reaction products were analyzed via agarose gel electrophoresis.

The following primerpairs, DNA polymerases, and thermal protocols were utilized:

Primer pair	**Polymerase**	**Thermal protocol**
Neo1F and Smpd1.3	AccuPrime™ DNA polymerase	"Long range" PCR
PB3 and Smpd1.16	AccuPrime™ DNA polymerase	"Long range" PCR
Smpd1.14 and Smpd1.15	Standard Taq polymerase	"Standard" PCR
DTA1 + DTA2	Standard Taq polymerase	"Standard" PCR

Thermal protocols:

"Standard" PCR: see paragraph 3.4

"Long range" PCR:

Step	Temperature	Time
1	**95°C**	**4:00 min**
2	**94°C**	**0:30**
3	**56°C**	**1:00**
4	**68°C**	**4:00**
5	**Go to step 2 (34x)**	
6	**68°C**	**5:00**
7	**4°C**	**"Forever"**

3.7 Blastocyst injections

Targeted R1-129 ES cells were injected into C57BL/6 blastocysts. Injected embryos were surgically transferred into the uterine horns of pseudopregnant recipient females. Chimeras were identified by patches of agouti (129 mouse strain) and black coat color (C57BL/6 mouse strain). Chimeras were mated with C57BL/6 mice. The agouti coat color of the R1-129 strain is dominant to the black coat color of C57BL/6 mice. In the case that R1-129 ES cells contributed to the germline of chimeras, the progeny were agouti. Genomic DNA of agouti offspring was examined by PCRs.

The blastocyst injections and surgical procedures were supervised by Dr. Ralph Waldschütz and performed by Wojziech Węgrzyn of the "Zentrales Tierlaboratorium" (ZTL), the Central Animal Facility of the University Hospital Essen.

3.8 Transfection of GL261 cells

The functionality of the AC expression construct was tested *in vitro.* To this end, GL261 cells were transfected with the CAG-Asah1/NeoR plasmid. Transfections were performed with the aid of Effectene® reagent according to the manufacturer`s protocol. Briefly, GL261 cells (1.5 x 10^5 cells/well) were seeded on a 6 well plate one day prior to transfection. At the day of transfection, cells displayed 60% confluence. Plasmid DNA (0.4 µg), purified by maxi-preparation (see above, paragraph 3.3.2), was diluted to a volume of 100 µl in buffer EC (supplied) and 3.2 µl Enhancer (supplied) were added. After 5 minutes of DNA condensation, 10 µl Effectene® reagent was added. For the formation of Effectene®-DNA complexes the solution was incubated for 10 minutes. The transfection mixture was diluted in 600 µl medium and added drop-wise to a 6 well plate. After 24 hours, medium was exchanged for selective medium containing the antibiotic geneticin (G418) at a concentration of 400 µg/ml in complete MEM. After one week of selection, an untransfected control well showed no more viable cells. Transfected cells were constantly grown in medium with the selective drug. Aliquots of transfected cells were frozen in liquid nitrogen. By this means, GL261 cells were transfected with the CAG-Asah1/NeoR or an empty pJK plasmid. Geneticin (G418) was removed 48 hours prior to any experiment.

3.9 Pronuclear injections

The CAG-Asah1 transgene cassette flanked by unique restriction enzyme sites (PmeI, AscI) was separated from the cloning vector. The transgene construct was purified of plasmid backbone DNA and the ethidium bromide dye, which is mutagenic and might alter the ES cell genome. To this end, the digested DNA was extracted twice from agarose gels. First, the 7274 bp transgene construct was purified of an ethidium bromide containing gel. The second agarose gel run was performed without ethidium bromide. In order to identify the construct on the DNA, the first lane, loaded with a DNA ladder, and a second lane, loaded with a small fraction of digested DNA, was dissected from the rest of the agarose gel and retroactively stained with ethidium bromide. To this end, the gel fragment was put into a 50 ml Falcon tube with 25 ml of TAE buffer and 2 µl of ethidium bromide and left for 15 minutes. The gel was reassembled and the ethidium bromide stained DNA ladder and digested DNA of the first two lanes were used as orientation for the excision of ethidium bromide -free DNA transgene construct from lane 3 to 5. The DNA was purified with the Qiaquick Gel Extraction Kit. Afterwards, the linearized transgene construct was injected into the pronuclei of

fertilized eggs of B6C3F1 mice (see figure 3.2). The eggs were transferred back to the uterus of pseudopregnant C57BL/6 recipients. Transgenic animals were identified by PCR (see paragraph 3.10) and crossed back to the C57BL/6 background.

The pronucleus injections and surgical procedures were supervised by Dr. Ralph Waldschütz and performed by Wojziech Węgrzyn of the "Zentrales Tierlaboratorium" (ZTL), the Central Animal Facility of the University Hospital Essen.

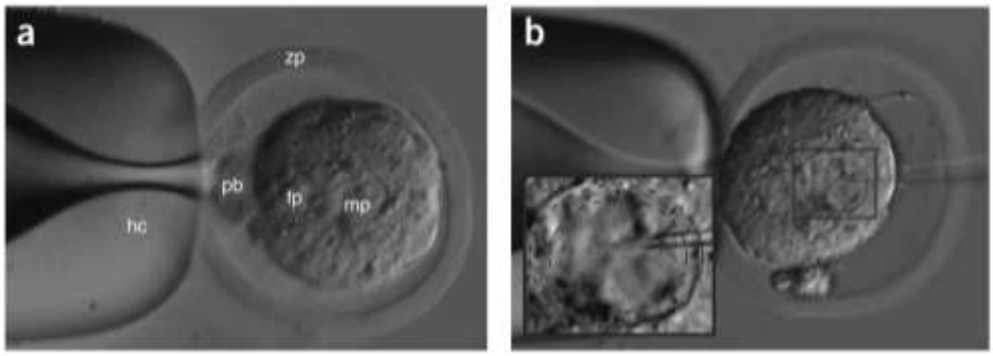

Figure 3.2: Pronuclear injection. a) Microscopic view of a holding capillary (hc) steadying a fertilized egg (zp: zona pelucida, pb: polar body, fp: female pronucleus, mp: male pronucleus). b) DNA of the linearized CAG-Asah1 transgene construct was injected into the male pronucleus of B6C3F1 derived eggs. Reprinted by permission from Macmillan Publishers Ltd: [Nature Protocols] (Ittner and Gotz 2007), copyright (2007).

3.10 Genotyping of mice

3.10.1 Isolation of genomic DNA from mouse tail tissue

Tail biopsies (0.5 – 1 cm) of candidate mice were taken 4 weeks after birth with a medical scalpel. The tissue was incubated in 100 µl tissue lysis buffer at 55°C on a shaker overnight. In order to inactivate proteinase K, samples were heated to 95°C for 15 minutes. Lysates were diluted with 900 µl nuclease-free ddH_2O to be ready for PCR-genotyping.

3.10.2 PCR detection of transgenic mice

Differentiation of wild type and transgenic mice was facilitated by PCRs in conjunction with the tail tissue derived genomic DNA templates. A master mix was assembled and contained: 10% PCR buffer (10x), 200 µM dNTPs, 150 pmol primers, standard Taq polymerase (1 unit/25 µl), and nuclease-free ddH_2O. Primers were designed to amplify wild type and transgene specific sequences. The DNA (2.5 µl) was added to a 0.2 ml PCR reaction tube to yield a total reaction volume of 25 µl. The reaction tubes were put into the thermal cycler and

temperated according to the “Standard” PCR protocol (see paragraph 3.4). Reaction products were analyzed via agarose gel electrophoresis. The identification of founders was performed by multi-plex PCR amplifying a CAG-Asah1 specific sequence (Asah1.2 and CAG4) and an endogenous control sequence (Ragf and Ragr; recombination activating gene 1 (Rag1), chromosome 2E2). General genotyping was performed with a single primer pair (Asah1.3 and Asah1.6) that allowed for reliable differentiation of transgenic and wild type mice.

3.11 Animal husbandry

Mice were maintained under specific pathogen free (SPF) conditions. Animals were provided with a standard rodent diet and had access to water ad libitum. The mice were kept in a room with a 12h/12h light/dark cycle, constant temperature (22°C), and constant humidity (55 ± 10%). Health monitoring was performed according to the guidelines of the Federation of European Laboratory Animal Science Associations (FELASA). The animal husbandry was policed by the "Zentrales Tierlaboratorium" (ZTL), the Central Animal Facility of the University Hospital Essen. All animal experiments were approved by the “Animal Care and Use Committee“ of the Bezirksregierung Düsseldorf, Germany in accordance with the german animal welfare act/„Tierschutz Gesetz“ (TSG).

Table 3.1: Approved animal experiment projects.

TSG-ID	Title
G 1157/10	„Analyse der Rolle von Ceramid bei Tumormetastasierung mit Hilfe eines konditionellen „Knock-out“ des Gens für die saure Sphingomyelinase und ubiquitärer Überexpression der sauren Ceramidase in der Maus“

3.12 Real-time PCR for the determination of transgene copies

The number of transgene copies in the genome of the four transgenic founder lines was determined by real-time PCR. For the quantitative measurement, a Rag primer pair (Ragf and Ragr) served as endogenous control. An *Asah1* primer pair (Asah1.3 and Asah1.4) was used for the amplification of a sequence within exon 11 of endogenous *Asah1* DNA as well as the *Asah1* cDNA template of the transgene cassette (see figure 3.3).

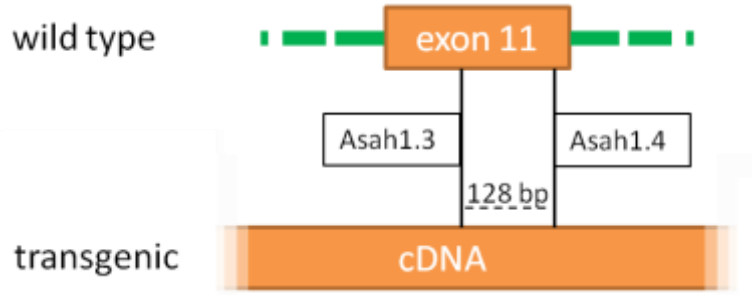

Figure 3.3: Strategy of CAG-Asah1 transgene copy number quantification. Primer Asah1.3 and Asah1.4 bind to sequences within exon 11 of the endogenous Asah1 gene (wild type) and amplify a template of 128 bp. In comparison to wild type mice, CAG-Asah1 transgenic animals hold additional PCR templates due to the cDNA sequence of the transgene cassette.

The PCR reactions were performed in a 96-well plate and carried out in triplicates using different vessels for the primer sets. The two master mixes contained the following components per PCR reaction: 10% PCR buffer (10x), 5% Evagreen® (20x), 200 µM dNTPs, primers (150 pmol), standard Taq polymerase (1 unit/25 µl), and nuclease-free ddH_2O. The mastermix was distributed in a 96 well plate and 2 µl of DNA template, isolated from mouse tail tissue (see paragraph 3.10.1), was added. The final volume was 25 µl per reaction. The plate was sealed with an optical adhesive film. Subsequently, the plate was inserted into a real-time PCR System. The fluorescence was analyzed during the run of the following thermal protocol:

Thermal protocol:

	Step	Temperature	Time
Amplification	1	**95°C**	**10:00 min**
	2	**94°C**	**0:15**
	3	**58°C**	**0:30**
	4	**72°C**	**1:00**
	5	**Go to step 2 (34x)**	
Dissociation	6	**95°C**	**0:15**
	7	**60°C**	**0:30**
	8	**95°C**	**0:15**

The specificity of the reaction was controlled by ascertaining the melting curves and visualization of the PCR fragments on an agarose gel. The analysis was performed according to the comparative $2^{-\Delta\Delta Ct}$ Ct method (Livak and Schmittgen 2001; Ballester *et al.* 2004a; Bubner and Baldwin 2004). Evagreen® acquires fluorescent properties upon intercalation with double stranded DNA. This signal is proportional to the quantity of DNA produced

during the PCR reaction. The amount of initial target sequence (X_0) determines the number of targets (X) at cycle n ($X_n = X_0 * 2^n$), and at which cycle a defined threshold (Ct value) of fluorescence intensity is reached. Hence, Ct values can be related to the initial amounts of DNA template (see figure 3.4). The Ct values observed for the *Asah1* reactions were normalized to the Ct values of an endogenous control amplicon (Rag primer) to compensate for variances in DNA template concentration. The Ct value was then set into relation to a calibrator – Ct values of a wild type mice holding two alleles of *Asah1*. The data were transferred to the linear form by $2^{-\Delta\Delta Ct}$ calculation.

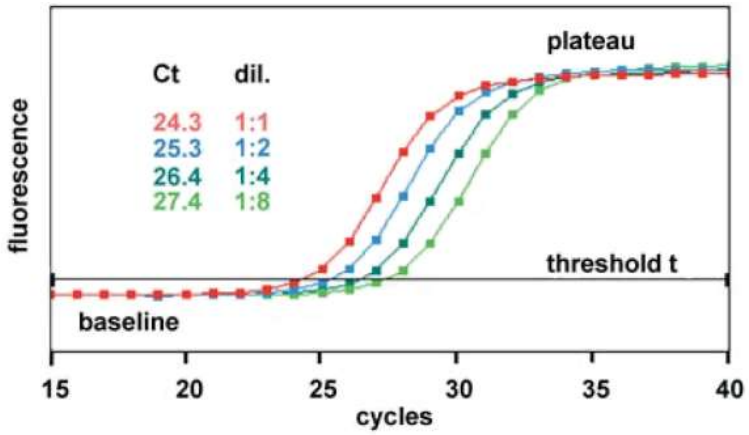

Figure 3.4: Fluorescence plot of a DNA dilution series during real-time PCR. The fluorescence accumulation of a marker that incorporates into the PCR product is recorded after each cycle (C) of the thermal protocol and plotted against the cycle number. Initial cycles define the baseline of background fluorescence. The threshold (t) is set above the baseline and is crossed at the beginning of the exponential phase. The cycle of threshold attainment represents the Ct value of a sample. In the dilution series, the Ct value increments one value with each 2 fold dilution of DNA template. Figure from (Bubner and Baldwin 2004), copyright 2004, with kind permission from Springer Science and Business Media.

3.13 Protein analysis

3.13.1 Protein extraction of culture cells

Protein extracts were obtained from cultured GL261 cells. GL261 cells were mobilized with trypsine and washed twice with PBS. For immunoblot analysis, cells were resolved in 500 µl SDS lysis buffer, supplemented with protease inhibitors aprotinin (10 µg/ml) and leupeptin (10 µg/ml). In order to determine AC activity, cells were lysed in 750 µl of sucrose lysis buffer. Next, cells were transferred to 1.5 ml reaction tubes, lysed on ice for 5 minutes and then sonicated, 3x 10 seconds at 25% output control. Subsequently, cell lysates were

centrifuged for 10 minutes at 13000 rpm and 4°C to remove cellular debris. The supernatant was transferred to a new Eppendorf tube and used for experiments or snap-frozen with liquid nitrogen and stored at -80°C.

3.13.2 Determination of protein concentrations

Concentrations of solubilized proteins were determined with a spectrophotometer by the Bradford method (Bradford 1976). The Bradford reagent contains an acidic dye with an absorbance maximum of 465 nm. However, when the dye binds to basic or aromatic amino acids of proteins, a color change occurs that shifts the absorbance maximum to 595 nm. Preliminary, the concentrated Bradford reagent was diluted with distilled water in a 1:5 ratio. A standard curve was established by usage of five BSA protein standards of 1, 3, 5, 10 and 20 µg/µl. Duplicates of standards and samples were added to 1 ml Bradford reagent in disposable polystyrene cuvettes. The absorbance was measured at 595 nm with a photometer. The absorbance of the samples was compared to the standard curve and protein concentrations deduced.

3.13.3 Immunoblot analysis

In order to quantify specific proteins, immunoblot analysis was performed. The method comprises sodium dodecyl sulfate polyacrylamide gel electrophoresis (SDS-PAGE), Western blotting, and antibody detection of proteins (Renart *et al.* 1979). During SDS-PAGE, proteins complexed with sodium dodecyl sulfate (SDS) are separated within a polyacrylamide gel according to their electrophoretic mobility. The mobility is antiproportional to the protein mass. The resulting protein pattern is subsequently immobilized by “Western blot” transfer to a nitrocellulose membrane. Primary antibodies are applied to specifically detect their epitope on a target protein. Polyclonal secondary antibodies, linked to reporter enzymes, bind specifically for the species of the primary antibody. The addition of a substrate results in a colorimetric conversion. The amount of visualized product is proportional to the amount of target protein on the nitrocellulose membrane.

3.13.3.1 Sodium dodecyl sulfate polyacrylamide gel electrophoresis

The acrylamide gel consists of two layers that polymerize within a glass chamber. First, the running gel solution was prepared and poured into the chamber to fill 4/5 of the space. A layer of distilled water ensures that the free edge of the gel is plane. After polymerization,

the water was removed and the solution of the stacking gel was poured into the remaining space of the chamber. A comb was inserted and the gel left for polymerization. The stacking gel ensures that proteins line up before they entry into the running gel. In the running gel, proteins are separated according to their mass. Proteins (25 µg) were solved in sodium dodecyl sulfate (SDS) sample buffer and boiled for 5 minutes. The denatured protein samples and a protein molecular weight marker were loaded into the wells of a 10% acrylamide gel. For the initial run through the stacking gel, a constant ampere of 50 mA was applied to the vertical protein electrophoresis system. When the bromphenol dye reached the running gel, the ampere was increased to 75 mA. Electricity was turned off when the bromophenol dye was leaking out of the running gel.

3.13.3.2 Western Blot and protein detection

The transfer onto a hybond nitrocellulose membrane was performed with aid of an electrophoretic transfer cell. A "gel sandwich" was prepared. Fiber pads, filter papers, the acrylamide gel, and the nitrocellulose membrane were equilibrated with transfer buffer and assembled in a plastic cassette according to the manufacturer`s instructions. The cassette was placed in the tank and the tank filled with transfer buffer. The blot was run at a voltage of 80 V for 2 hours at 4°C. Afterwards, the nitrocellulose membrane was retrieved from the "gel sandwich" and washed with TBS. The membrane was incubated in blocking buffer at 4°C overnight. The next day, the membrane was washed with TBS-T 3 x 10 minutes under constant shaking. The primary antibody was diluted in TBS-T (α-acid ceramidase 1:5000 and α-actin 1:2000) and incubated at 4°C overnight. Once again, the membrane was washed 3 x 10 minutes in TBS-T. The secondary antibody was diluted 1:30000 in TBS-T and incubated for 2 hours at 37°C. One more time, the membrane was washed 3 x 10 minutes in TBS-T. The secondary antibodies are coupled to an alkaline phosphatase. Accordingly, the membrane was then washed in an alkaline wash buffer, 2 x 5 minutes. Molecules labeled with alkaline phosphatase were detected with the chemiluminescent substrate CDP-*Star®*. The substrate was added to cover the membrane and incubated for 5 minutes. Excess substrate was removed and the blot placed in a film cassette. In a dark room, photographic films were exposed and developed. The signals on the films were quantified with an image analysis software.

3.13.4 Acid ceramidase activity assay

Acid ceramidase activity was determined in a fluorogenic assay according to the publications of Bedia et al. (Bedia *et al.* 2007; Bedia *et al.* 2010). The metabolic conversion of the substrate RBM14-12, a synthetic ceramide analog, was determined after 2 hours of incubation in an acidic buffer at 37°C. RBM14-12 holds a 2-oxo-2H-chromen-7-yloxy coumarin ring residue. Upon hydrolysis of the substrate by acid ceramidase, the residue can be transformed into the fluorescent molecule umbelliferone (see figure 3.5). Intermediary steps involve 1. periodate oxidation of the aminodiol at alkaline pH and 2. β-elimination of the aldehyde oxidation product. The kinetic characteristics of RBM14-12 hydrolysis were ascertained by Bedia et al. (Bedia *et al.* 2010). For the employed 25 µg of protein and 2 hours of incubation at 37°C, the linearity of the reaction kinetics has been previously reported (Bedia *et al.* 2010). Because the reaction is sensitive to the presence of detergents (Bedia *et al.* 2010), no detergents were utilized in the activity assay.

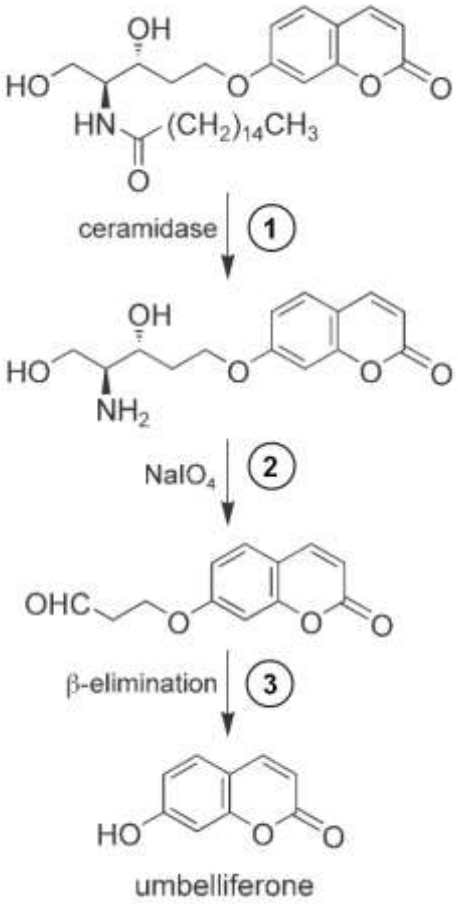

Figure 3.5: Enzymatic conversion of RBM14-12. The ceramide analog RBM14-12 holds a coumarin residue in the sphingoid base. 1) Acid ceramidase cleaves the amide bond that links the fatty acid to the sphingoid base. 2) The alkaline buffer containing $NaIO_4$ oxidizes the

remaining aminodiol of the sphingoid base, and 3) generates the fluorophore umbelliferone by β-elemination of the oxidized product. Figure from (Bedia et al. 2007), copyright 2007, with permission from WILEY-VCH Verlag GmbH & Co. KGaA, Weinheim.

Protein (25 µg) solved in 25 µl sucrose lysis buffer, 74.5 µl sodium acetate buffer (25 mM, pH 4.5) and 0.5 µl of Rbm14-12 substrate (final concentration 20 µM) were added to a well of a 96 well plate. "No substrate" (Protein solved in 25 µl sucrose lysis buffer + 75 µl sodium acetate buffer) and "No protein" (25 µl sucrose lysis buffer + 74.5 µl sodium acetate buffer and 0.5 µl of Rbm14-12 substrate) reactions served as negative controls. The plate was left for 2 hours in a 37°C incubator. The reactions were stopped by the addition of 50 µl methanol. Subsequently, 100 µl of a 2.5 mg/ml $NaIO_4$ fresh solution in 100 mM glycine/NaOH buffer, pH 10.6 was added. The plate was left in the dark for 2 hours. During this incubation step, the converted substrate undergoes oxidation and β-elimination. A plateau of florescence production was already seen after one hour (see appendix 9.1). This ensured that the produced fluorescence solely depended on the initial substrate conversion by AC. Fluorescence was quantified with a fluorescence microplate reader using an excitation of 360 nm and an emission of 446 nm. Umbelliferone standards were used to present the conversion of substrate by AC as pmol umbelliferone/hour/µg protein.

3.14 Mass spectrometry (MS) of sphingosine in mouse tissues

Sphingosine was quantified in murine tissue samples. To this end, mice were sacrificed and intracardially perfused with 0.9% NaCl to wash the blood out of the tissues. Skin and bone of the ribcage were removed to gain access to the heart. The aorta abdominalis infrarenalis was cut to allow for the efflux of blood. A butterfly needle (0.8 x 20 mm) was inserted into the left ventricle of the heart. NaCl was flowing through a standard infusion tube with a drop height of 80 cm into the mouse. Mice were perfused for 5 minutes. Subsequently, liver, kidney and spleen tissue (about 200 mg) were collected and snap frozen in liquid nitrogen. Tissues were mechanically pulverized with a porcelain mortar. Powdered samples were transferred to Eppendorf tubes and 1 ml of methanol was added. The samples were sonicated until the powder was completely dissolved. Protein concentrations were determined via Bradford assay (see above, paragraph 3.13.2). The samples were send on dry ice to the Department of Nutritional Toxicology, Institute of Nutritional Science, University

Potsdam, Germany. The quantification of sphingosine by mass spectrometry (MS) was performed by the group of Prof. Dr. Burkhard Kleuser.

3.15 Statistics

Data are given as mean ± SD. Statistical significances between organs from wild type and acid ceramidase transgenic mice were determined by Student`s t-test; *$p<0.05$.

4. RESULTS

4.1 Results of the CAG-Asah1 mouse model

4.1.1 General strategy for the generation of CAG-Asah1 transgenic mice

The plasmid expressing the *Asah1* cDNA was constructed by insertion of the following DNA fragments into the pNEB plasmid: (i) A polyadenylation signal (bGH-polyA) in order to prevent formation of hybrid proteins in the case that the construct integrates into coding genomic DNA. (ii) Two heterologous Drosophila melanogaster derived "SCS" insulator elements. Insulators protect gene expression from chromosomal positional effects and block enhancer activated transcription (Dunaway *et al.* 1997; Recillas-Targa *et al.* 2002; West *et al.* 2002). They frame the following elements of the transgene cassette. (iii) A CAG promoter. The CAG promoter is composed of the cytomegalovirus (CMV) early enhancer element and chicken beta-actin promoter. In transgenic models, the promoter is established and known to drive high expression levels of the gene next in line (Niwa *et al.* 1991; Okabe *et al.* 1997; Xu *et al.* 2001). (iv) The murine AC complementary DNA (cDNA). A plasmid containing the full-length *Asah1* cDNA was purchased from imaGenes (imaGenes GmbH, Berlin, Germany, Genbank accession: BC003204). (v) A polyadenylation signal from the human growth hormone (hGH polyA) at the 3` end of the mRNA is important for nuclear export, translation and stability of mRNA (Guhaniyogi and Brewer 2001).

4.1.2 Outline of the cloning procedures in detail

The pCMV-Sport6 plasmid contained the *Asah1* cDNA. In order to obtain applicable restriction enzyme sites flanking the *Asah1* cDNA, the DNA segment was inserted into the pBSpec2Z plasmid backbone. The cDNA fragment was mobilized by digesting the pCMV-Sport6 plasmid with the enzymes SacII and MscI (blunt end). The pBSpec2Z plasmid was opened by the enzymes BamHI and SacII. The 5` overhang of the BamHI site was filled by the polymerase I large Klenow fragment to generate blunt ends compatible to the MscI site. The resulting plasmid was denoted pBSpec2Z-Asah1. Now the cDNA was flanked by a BamHI and a XbaI restriction site. The cDNA was mobilized yet again by BamHI and XbaI and ligated into the pNeb-bGHpA/SCS/lck/iCre/hGHpA/FRT/SCS plasmid, opened by BamHI and NheI. In this cloning step, the XbaI and the NheI produce compatible overhangs. The resulting plasmid was denoted as pNeb-bGHpA/SCS/Asah1/hGHpA/FRT/SCS.

The CAG promoter was derived from the pLCAG-DnmtI plasmid. The promoter was subcloned into the pk18 plasmid. To this end, the CAG-fragment was obtained by restriction digest with DraI (blunt end) and XbaI. The DNA fragment was inserted to the pk18 plasmid that was linearized by XbaI and SmaI (blunt end). The resulting plasmid was denoted pk18-CAG.

In order to position the polyadenylation signal (bGHpA) and the insulator element (SCS) ”5`” of the CAG promoter, the corresponding elements were isolated from the pNEB193bGHpA/SCS/L2/SCS plasmid by KpnI and PmlI (blunt end). The pK18-CAG plasmid was digested with the endonucleases HincII (blunt end) and KpnI. The resulting plasmid was denoted pK18-bGHpA/SCS/CAG.

In the final cloning step, the fragment comprising the bGHpA/SCS/CAG segment of the pK18-bGHpA/SCS/CAG plasmid was inserted into the pNeb-bGHpA/SCS/Asah1/hGHpA/FRT/SCS. In this cloning step, the bGHpA and SCS element were exchanged and the CAG promoter was added upstream of the *Asah1* cDNA. The donor plasmid, pK18-bGHpA/SCS/CAG, as well as the destination plasmid, pNeb-bGHpA/SCS/Asah1/hGHpA/FRT/SCS, were cut by AscI and FseI. After ligation, the plasmid holding the complete transgene construct could be denoted as pNeb-bGHpA/SCS/CAG/Asah1/hGHpA/FRT/SCS, but is referred to as “CAG-Asah1” (see figure 4.1).

For cell culture experiments a neomycin resistance cassette was inserted into the CAG-Asah1 transgene construct. The neomycin cassette was derived from the pNEB-bGHpA/SCS/lck/Icre/hGHpA/NeoR/SCS plasmid and mobilized by the enzymes BamHI and PmeI. The CAG-Asah1 transgene construct was linearized by the same enzymes. The resulting plasmid was denoted as CAG-Asah1/NeoR.

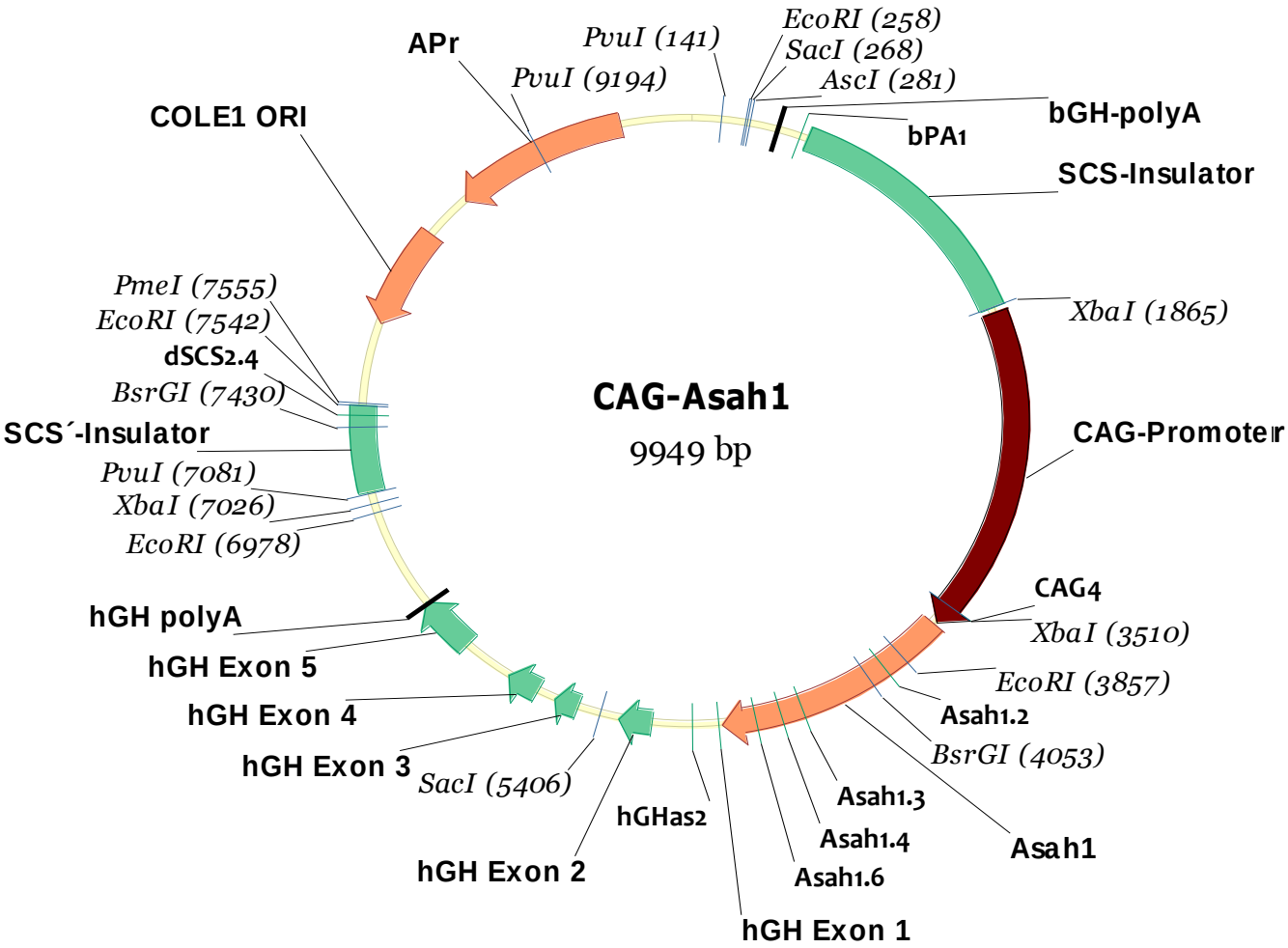

Figure 4.1: Graphical map of the CAG-Asah1 plasmid. The graphic displays the molecule map of the CAG-Asah1 plasmid. Functional features, restriction sites, and primer binding sites of the targeting vector are shown and labeled (see droplines). By molecular cloning techniques the following genetic elements were assembled: A polyadenylation signal (bGH-polyA), two heterologous Drosophila melanogaster derived "SCS" insulator elements (SCS-Insulator), a CAG promoter (CAG-Promoter), the acid ceramidase cDNA (Asah1), and a polyadenylation signal from the human growth hormone (hGH polyA). Transcripts of the Asah1 cDNA are driven by the CAG4 promoter and terminated by the bGH-polyA. The pNEB plasmid backbone further features a replication origin (COLE1-ORI) and an ampicillin resistance gene (APr). The specified restriction enzymes and primers allow to comprehend and review the hereinafter referred restriction enzyme digests and PCRs.

4.1.3 Verification of CAG-Asah1 expression vector generation

The Asah1 expression vector was generated according to the cloning strategy. Single cloning steps were controlled by diagnostic restriction enzyme digests and/or PCRs. The restriction enzymes were chosen to yield unique patterns of DNA fragments on the agarose gel that verified the integration of inserts in the plasmid backbone. The correct orientation of the

inserts was further confirmed by PCRs using plasmid DNA as a template. The PCRs were performed with one primer hybridizing with its corresponding complementary DNA on the vector backbone and the other primer targeted to the inserted DNA fragment. Only a correct orientation of the insert juxtaposes the primers and yields a DNA amplicon of a defined length. The same way, the final plasmid construct was reexamined. The CAG-Asah1 plasmid was digested with either BsrGI, SacI, XbaI or PvuI (see figure 4.2 A). Furthermore, the primer sets CAG4 + Asah1.6, Asah1.3 + hGHas2 and dScs 2.4 + bpA1 were used in PCR reactions (see figure 4.2 B). The DNA "fingerprint" of the CAG-Asah1 plasmid was expected to yield the following fragment patterns: BsrGI 6572 bp and 3377 bp, SacI 5138 bp and 4811 bp, XbaI 4788 bp, 3516bp and 1645 bp, PvuI 6940 bp, 2113 bp and 896 bp. Primer set CAG4 + Asah1.6: 1159 bp, primer set Asah1.3 + hGHas2: 564 bp, and primer pair dScs 2.4 + bpA1: 2961 bp. The signals on the agarose gels reflected the expected band patterns indicating successful realization of the CAG-Asah1 plasmid.

A)

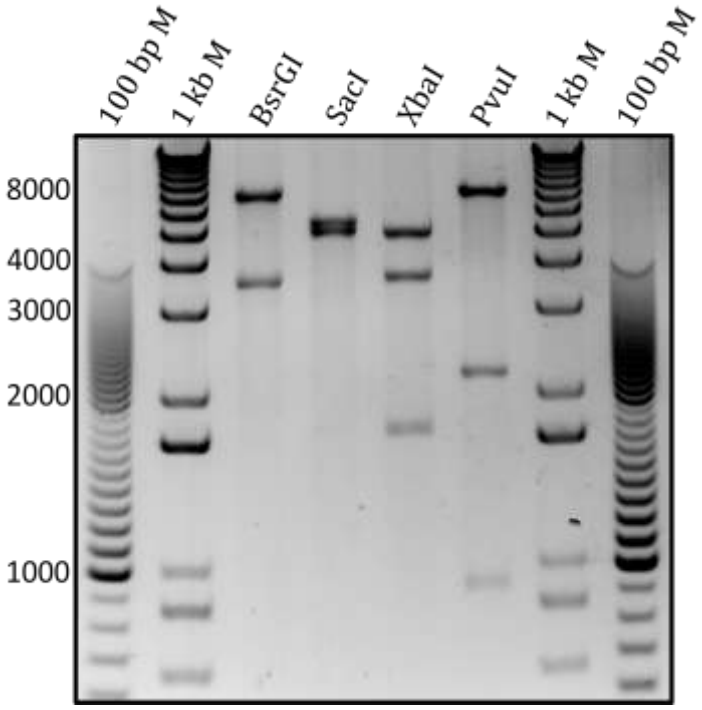

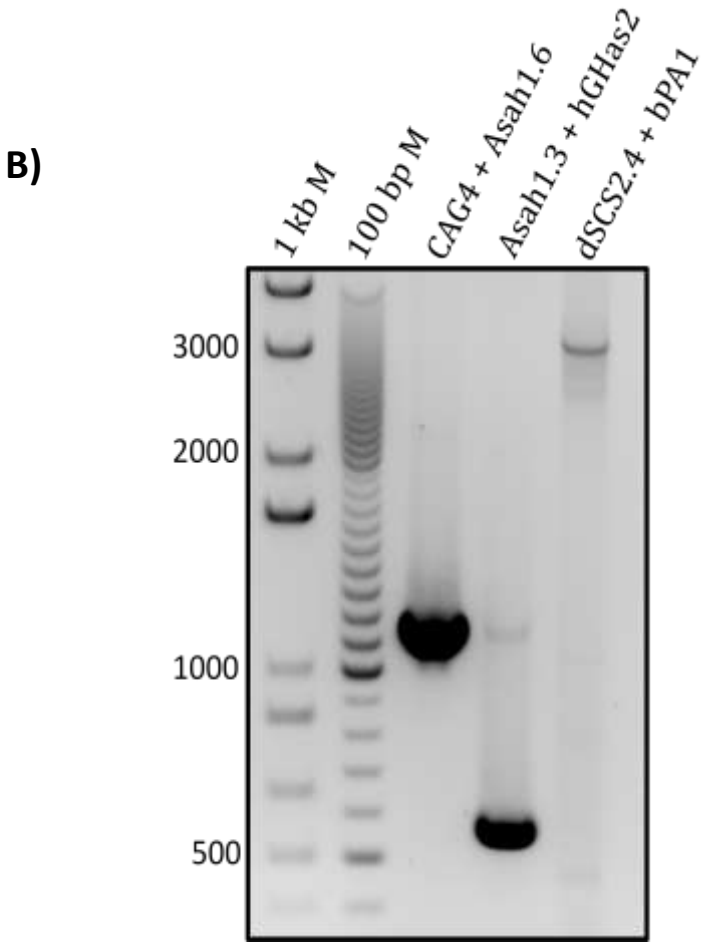

Figure 4.2: Verification of Asah1 expression vector generation. A) The CAG-Asah1 plasmid was digested with either BsrGI, SacI, XbaI or PvuI. Incubation and buffer conditions of the reactions conformed to the specifications of the manufacturer. The resulting DNA fragments and molecular markers (100 bp marker and 1 kb marker) were separated on an 1% agarose gel. BsrGI digestion yields fragments of 6572 bp and 3377 bp. The restriction enzyme SacI produces a 5135 bp and 4811 bp fragment. Three fragments of 4788 bp, 3516bp and 1645 bp are generated by XbaI digestion. PvuI digestion yields fragments of 6940 bp, 2113 bp and 896 bp. B) PCR reactions were performed with the CAG-Asah1 plasmid template and reaction products run on an 1% agarose gel. The primer set CAG4 + Asah1.6 produced an amplicon of 1159 bp. The PCR reaction with the primers Asah1.3 + hGHas2 resulted in a 564 bp fragment. Primers dScs 2.4 + bpA1 amplified a 2961 bp fragment.

4.1.4 AC expression and activity *in vitro*

"Plasmid fingerprinting" verified the generation of the CAG-Asah1 plasmid. Next, AC expression and activity was ascertained in CAG-Asah1 transfected cells. The *in vitro* experiments were performed one time (n = 1) and merely served to indicate the functionality of the CAG-Asah1 transgene cassette. In order to perform cell culture

experiments, a neomycin resistance cassette was inserted into the CAG-Asah1 plasmid. This cloning step was verified by restriction enzyme digestion with EcoRI and agarose gel analysis (see figure 4.3). The murine cell line GL261 was transfected with the CAG-Asah1/NeoR plasmid. Cells were cultured and selected in the presence of the antibiotic geneticin (G418). Geneticin was removed 48 hours prior to any experiment. AC protein expression and enzyme activity of whole cell lysates was investigated and compared to lysates of control-vector (pJK plasmid) transfected cells. Protein samples (25 µg) were analyzed by SDS-PAGE, subsequent Western blots, and detection of the murine acid ceramidase β-subunit with a specific antibody (see figure 4.4). The housekeeping protein actin was detected with an antibody to serve as a loading control. Immunoblots of GL261 lysates stably transfected with CAG-Asah1/NeoR showed increased levels of AC protein (1.7 fold, densitometric analysis) in comparison to control-vector transfected cells.

Moreover, the activity of AC was ascertained by quantification of fluorescent umbelliferone that was produced upon hydrolization of the synthetic RBM14-12 ceramide analog. RBM14-12 was incubated with 25 µg protein of GL261 cell lysates in an acidic buffer (pH 4.5) at 37°C. The enzymatic conversion was stopped with methanol after 2 hours. The coumarin residue of hydrolyzed RBM14-12 was transformed to fluorescent umbelliferone (see above, figure 3.5) and quantified with a fluorescence reader. Protein lysates of CAG-Asah1/NeoR stably transfected GL261 cells generated 2276 pmol umbelliferone/hour/mg protein (see figure 4.5). This was 6.1x higher than the AC activity of lysates derived from untransfected cells (370 pmol umbelliferone/hour/mg protein) and 4.9x higher than in lysates of control-vector (461 pmol umbelliferone/hour/mg protein) transfected cells.

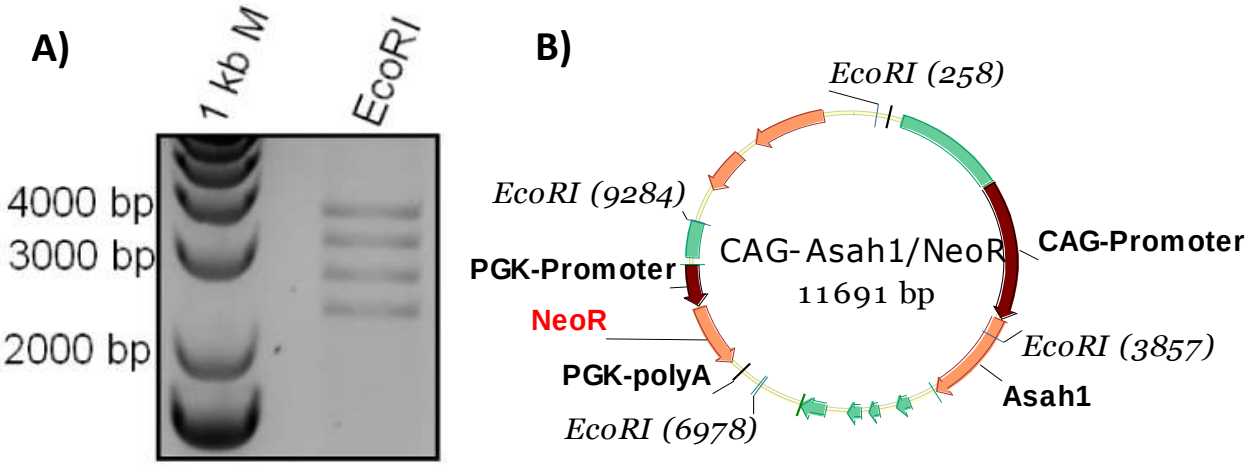

Figure 4.3: Generation of CAG-Asah1/NeoR. A neomycin resistance cassette was inserted into the CAG-Asah1 plasmid. The sequence of the antibiotic resistance gene was derived from the pNEB-bGHpA/SCS/lck/Icre/hGHpA/NeoR/SCS plasmid cut with the restriction enzymes BamHI and PmeI. Utilizing the same enzymes, the recipient CAG-Asah1 plasmid was opened. A) Generation of CAG-Asah1/NeoR was verified by digestion with EcoRI and subsequent agarose gel electrophoresis. The 1 kb molecular marker indicates the size of separated DNA fragments: 3599 bp, 3121 bp, 2665 bp, and 2306 bp. B) Graphical map of the CAG-Asah1/NeoR plasmid. The neomycin cassette consists of a PGK-promoter, the neomycin phosphotransferase gene (NeoR), and a PGK-polyA transcriptional stop signal. The CAG-Asah1 expression cassette remained intact as the neomycin cassette was positioned between the hGH-polyA and the distal SCS` insulator element. EcoRI restriction sites are indicated (see droplines).

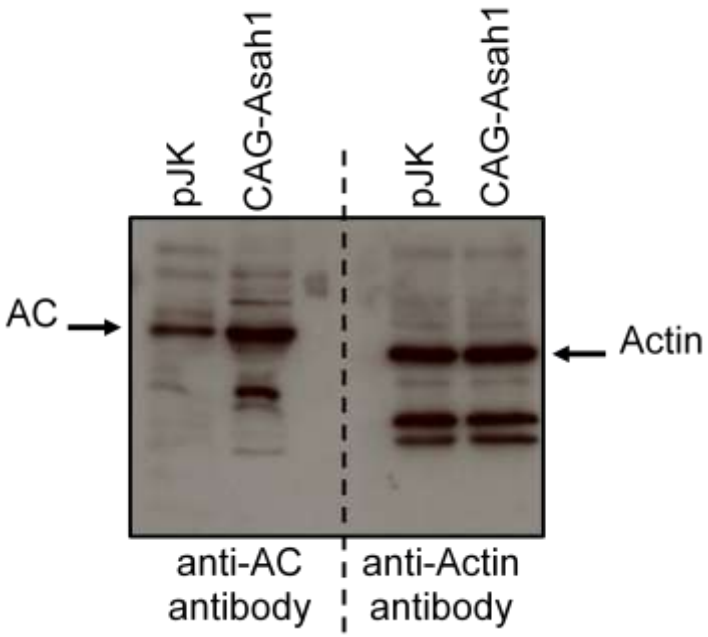

Figure 4.4: Immunoblot analysis of AC with whole cell lysates. GL261 cells that were either transfected with the CAG-Asah1/NeoR plasmid or an empty vector control plasmid (pJK) were lysed. Proteins (25 µg) were separated via SDS-PAGE and immobilized by subsequent Western blotting. *The AC protein of 53 kDa was detected using a murine acid ceramidase antibody that specifically binds to the* β-subunit*. The housekeeping protein actin (43 kDA) was detected to serve as a loading control.*

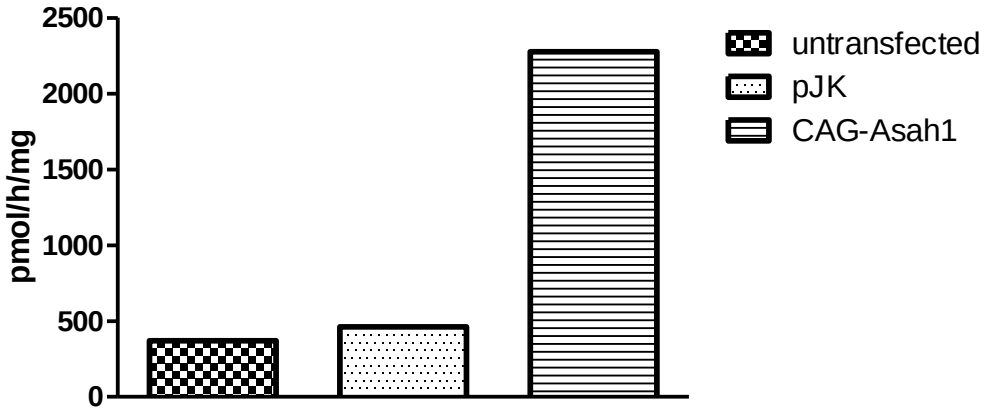

Figure 4.5: AC activity assay with whole cell lysates. The substrate RBM14-12 was incubated at 37°C for 2 hours in an acidic buffer (pH of 4.5) in the presence of protein lysates obtained from untransfected, empty vector control (pJK) transfected and CAG-Asah1/NeoR transfected GL261 cells. Hydrolysis rates were determined with a fluorescence reader (extinction 360 nm, emission 446 nm) detecting the fluorescent substrate conversion product umbelliferone. Results are denoted with the measurement unit pmol umbelliferone/hour/mg protein; n = 1.

4.1.5 Pronuclear injections of CAG-Asah1

The *in vitro* investigations of CAG-Asah1 functionality legitimized the deployment of the expression cassette for the generation of transgenic mice. The CAG-Asah1 expression cassette was separated from the vector backbone by restriction enzyme digestion with PmeI and AscI. The linearized fragment was extracted twice from agarose gels to clean the DNA of ethidium bromide and prevent cotransfer of vector backbone specific sequences (see figure 4.6). About 100 fertilized eggs were injected with the CAG-Asah1 DNA. The eggs were then transferred to the uterus of pseudopregnant recipients. Transgenic founders were identified by PCR using DNA of mouse tail tissue as a PCR template (see figure 4.7). In the PCR reaction, two primer sets were employed: One pair amplifies a CAG-Asah1 specific sequence (CAG4 + Asah1.2), the other pair (Ragf + Ragr) produces an amplicon of an endogenous control sequence in the murine genome. Consequentially, transgenic mice were expected to display a fragment of 476 bp in addition to the endogenous control fragment of 295 bp. PCR reactions were analyzed on an agarose gel. The outcome of two sessions (injections of 2 x 50 fertilized eggs) was the generation of 4 transgenic mice. All four mice were female. One mouse died at the age of 5 weeks. Three founder lines were established – denoted F1, F2 and F3. Two lines were backcrossed to the C57BL/6 background.

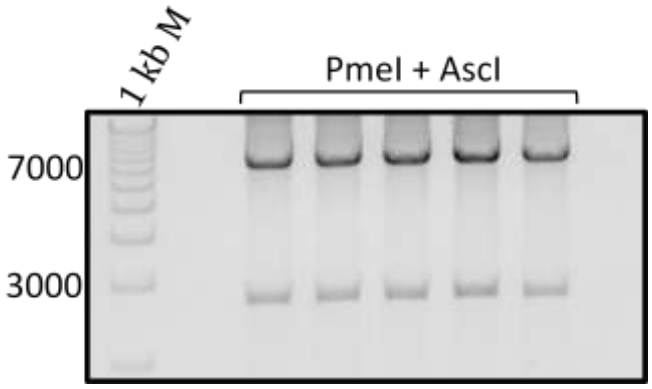

Figure 4.6: Linearization of the CAG-Asah1 expression cassette. The CAG-Asah1 plasmid was digested with the restriction enzymes PmeI and AscI. The resulting fragments were separated on a 1% agarose gel stained with ethidium bromide. The transgene construct DNA of 7274 bp was cut off the gel lanes and purified while the vector backbone of 2675 bp remained in the gel. In a second agarose gel run the expression cassette was extracted without the mutagenic ethidium bromide dye. The CAG-Asah1 DNA was purified and injected into the pronuclei of fertilized eggs of B6C3F1 mice.

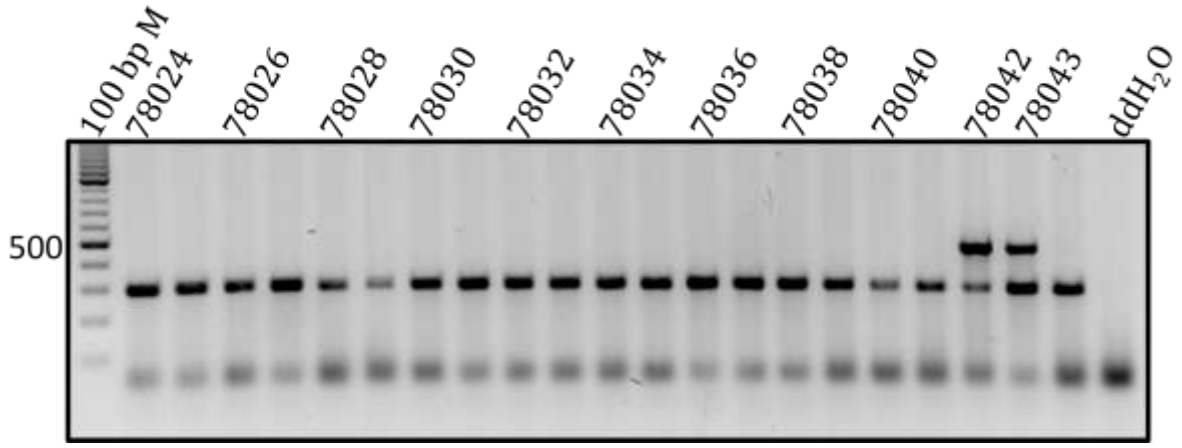

Figure 4.7: Outcome of the pronuclear injections with the CAG-Asah1 expression cassette. The CAG-Asah1 transgene construct was injected into the male pronuclei of fertilized eggs of B6C3F1 mice. Eggs were transferred back to the uterus of pseudopregnant recipients. After delivery, tail tissue derived DNA templates of the progeny were analyzed by multiplex PCRs and subsequent separation of DNA fragments on a 2% agarose gel. Mice with the ID number 78042 and 78043 display a transgene specific band (476 bp) generated by the primers Asah1.2 and CAG4 in addition to the signal (295 bp) of the endogenous control primers (Ragf + Ragr). The same way, two further transgenic founders were identified.

4.1.6 Genotyping of CAG-Asah1 transgenic mice

General genotyping of mice was performed with an optimized PCR approach. In comparison to the PCR that was used for the identification of founders, this PCR approach only required a single primer pair (Asah1.3 + Asah1.6) which allowed for reliable differentiation of transgenic and wild type mice. The primers were designed in a way that the intron between exon 11 and exon 12 was flanked (see figure 4.8 A). Amplification of a DNA template of wild type tissue solely yielded a fragment of 339 bp. In comparison, a DNA template of transgenic origin displayed a reaction product with reduced size (252 bp) due to the absence of the intron (87 bp) (see figure 4.8 B).

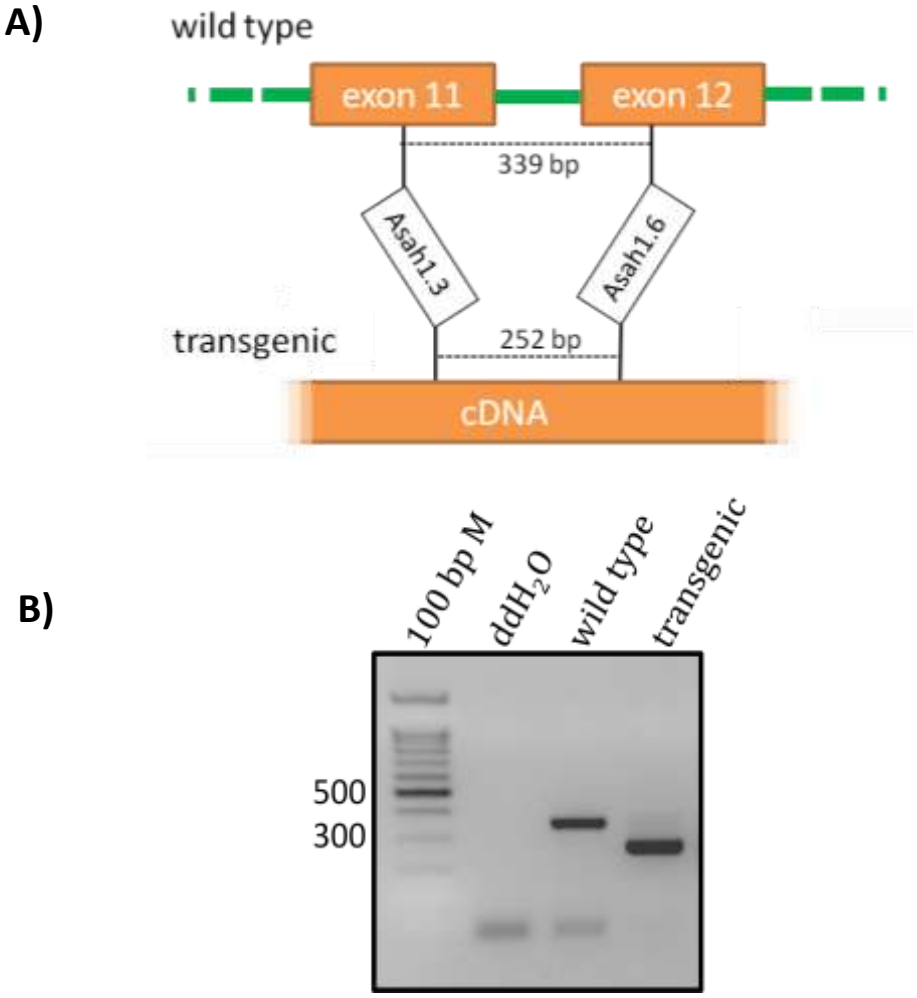

Figure 4.8: Genotyping of CAG-Asah1 transgenic mice. A) Strategy for the identification of CAG-Asah1 transgenic mice. The wild type Asah1 gene locus holds exonic and intronic sequences while in the cDNA of the transgene cassette intronic sequences are absent. Primer Asah1.3 and Asah1.6 bind to sequences within exon 11 and exon 12, respectively. The amplicon of a transgenic template is shorter by the size of the intron (87 bp) in comparison to a wild type template. B) Example of an agarose gel image. PCR amplification resulted in a

339 bp fragment for wild type DNA templates. A 252 bp fragment is visible in the case of transgenic DNA templates. PCR reactions without DNA template (ddH_2O) served as a negative control. A 100 bp marker indicates the sizes of PCR amplicons.

4.1.7 Determination of CAG-Asah1 copy quantity in founders

The number of transgene copies in the genome of the four transgenic founder lines was determined by real-time PCR. The chemical compound Evagreen® acquires fluorescent properties upon intercalation with double stranded DNA. This signal is proportional to the quantity of DNA produced during the PCR reaction. Tail tissue derived genomic DNA (n = 3 for each founder) was used as a template. An *Asah1* primer set (Asah1.3 + Asah1.4) was used for the amplification of a DNA fragment present on the wild type *Asah1* locus as well as the *Asah1* cDNA template of the transgene cassette. A Rag primer set served as endogenous control. Reactions were carried out in triplicates using different vessels for the two primer sets and fluorescence was analyzed with a real-time PCR System. Ct values, the cycle (C) at which a defined threshold (t) of fluorescence intensity is crossed, were determined. By means of the Ct values, the initial amounts of DNA template can be deduced. To this end, Ct values observed for the *Asah1* reactions were normalized to an endogenous control (Ragf +Ragr) to compensate for variances in DNA template concentration. The Ct value was then set into relation to a calibrator – a DNA template of a wild type mouse (holding two alleles of *Asah1*). The data were transferred to the linear form by $2^{-\Delta\Delta Ct}$ calculation (see table 4.1 and appendix).

In addition to the real-time PCR approach, the standard genotyping PCR allowed for an assessment of transgene copy numbers. The primer set Asah1.3 and Asah1.6 amplifies the intron spanning amplicon of 339 bp of the endogenous *Asah1* gene and in case of transgene presence an additional smaller amplicon (252 bp) of the cDNA templates. Therefore, the DNA templates “compete” for the resources in the PCR reaction. The number of PCR cycles was reduced to 28 and the signal ratios of the reaction products on the agarose gel were densitometrically determined. The more the ratio of the two DNA signals on the agarose gel shifts towards the transgene site, the more CAG-Asah1 template was present (see table 4.1). This technique is also termed semi-quantitative competitive PCR (cPCR) (Hubner *et al.* 1999). Genomic DNA samples of 3 animals (n = 3) were used for founder F1, F2 and F3, a single DNA sample of founder F4 was run in triplicate (n = 1).

qPCR analysis revealed that founder F2 derived animals display the highest numbers of CAG-Asah1 integrates (nAsah1 = 46.09 ± 5.18, including 2 endogenous *Asah1* copies). Founder F1 animals held 22.09 ± 1.22 copies of nAsah1, while the offspring of founder F2 bore 16.72 ± 1.98 nAsah1 copies. Semi-quantitative cPCR affirmed the qPCR results and *Asah1* gene dosage succession F2 > F1 > F3. The wild type signal in the PCR product of founder F4 template was nearly absent.

Table 4.1: Quantitative real-time PCR (qPCR)- and semi-quantitative competitive PCR (cPCR) results of transgene copy analysis in CAG-Asah1 founders. qPCR data represent the number of Asah1 copies (nAsah1 = cDNA Asah1 copies + 2 endogenous Asah1 copies) after $2^{-\Delta\Delta Ct}$ calculation. Signals of cPCR reaction products on the agarose were densitometrically determined and ratios of transgene to wild type signals calculated. Data are presented as mean ± SD.

		Founder 1	Founder 2	Founder 3	Founder 4
qPCR	*nAsah1*	22.09 ± 1.22	46.09 ± 5.18	16.72 ± 1.98	Not determined
cPCR	Ratio	0.65 ± 0.03	1.39 ± 0.02	0.20 ± 0.03	10.85 ± 0.76
	Gel image	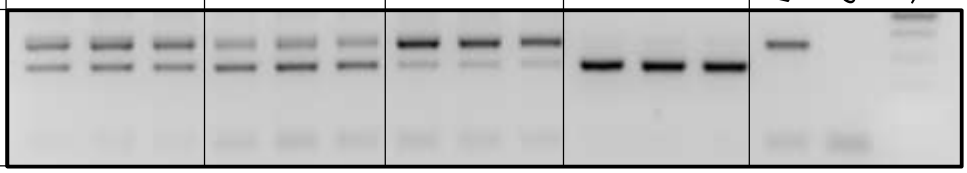			

4.1.8 Quantification of sphingosine by mass spectrometry

Sphingosine is the reaction product of ceramide hydrolysis by AC. An enhanced catalytic activity of AC in the CAG-Asah1 mouse model should result in elevated levels of its reaction product in comparison to wild type mice. To examine sphingosine levels, murine liver, kidney and spleen tissue samples were collected after perfusion of animals with 0.9% NaCl. Samples of wild type mice (liver: n = 3, kidney: n = 6 , and spleen: n = 3) and CAG-Asah1 mice of founder line F2 (liver: n = 3, kidney: n = 6, and spleen: n = 3) were snap frozen in liquid nitrogen and mechanically pulverized. Powdered tissue samples were diluted in 1 ml of methanol and solved by sonication. Quantification of sphingosine by mass spectrometry was performed by the group of Prof. Dr. Burkhard Kleuser (see figure 4.9).

Wild type liver samples display 29.4 ± 24.8 (mean ± SD) pmol sphingosine/mg protein. CAG-Asah1 liver samples showed 4.3 fold higher sphingosine levels (126.1 ± 38.2 pmol sphingosine/mg protein). There is a significant difference between the two groups (p =

0.021). CAG-Asah1 kidneys contained sphingosine levels of 99.5 ± 35.1 pmol sphingosine/mg protein, while wild type kidneys held 35.1 ± 13.3 pmol sphingosine/mg protein. Sphingosine levels were elevated 2.8 fold in CAG-Asah1 kidneys compared to wild types (p = 0.002). Spleen tissue of wild type (29.9 ± 24.5 3 pmol sphingosine/mg protein) and CAG-Asah1 animals (74.7 ± 10.9 3 pmol sphingosine/mg protein) were significantly different in their sphingosine concentrations (2.5 fold, p = 0.045).

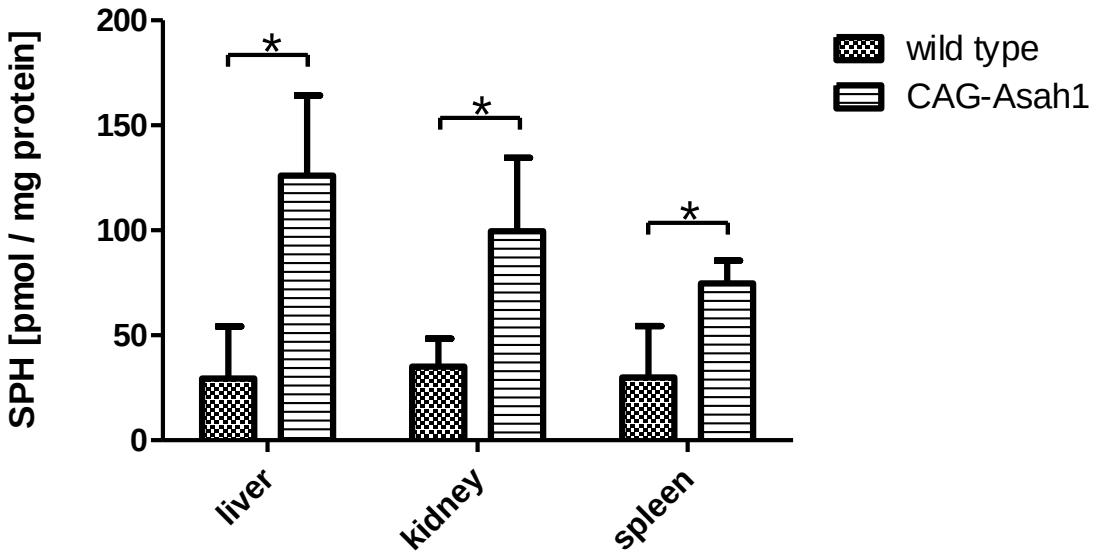

*Figure 4.9: Quantification of sphingosine by mass spectrometry. Murine livers, kidneys and spleens were collected after perfusion of animals with 0.9% NaCl via the heart. Tissue samples were snap frozen in liquid nitrogen, mechanically pulverized, and diluted in 1 ml methanol. Samples were sonicated until the powder was completely dissolved. Protein concentrations were determined via Bradford assay. Tissue samples of wild type mice (liver: n = 3, kidney: n = 6, and spleen: n = 3) and CAG-Asah1 mice (liver: n = 3, kidney: n = 6, and spleen: n = 3) were analyzed by mass spectrometry in the Department of Nutritional Toxicology, Institute of Nutritional Science, University Potsdam, Germany. The quantification of sphingosine by mass spectrometry was performed by the group of Prof. Dr. Burkhard Kleuser. Data are expressed as the mean ± SD with the measurement unit pmol/mg protein. * indicates a p value < 0.05 of a Student`s t-test.*

4.2 Results of the *Smpd1* conditional knockout mouse model

4.2.1 General strategy for the conditional knockout of the murine *Smpd1* gene

In order to generate mice with a conditional null mutation of the *Smpd1* gene, a targeting vector based on genomic DNA of the *Smpd1* locus on chromosome 7 of the mouse was designed. In addition to the phage library derived genomic DNA, the replacement vector

holds two loxP sites that flank exon 2. Upon homologous recombination, this will allow for Cre-recombinase mediated excision of exon 2. Disruption of exon 2 was chosen since this reportedly results in a functional null allele in the mouse and resembles an authentic model of Niemann-Pick disease type A and B (Horinouchi *et al.* 1995). Further features of the vector comprise a FRT flanked neomycin (NeoR) cassette and a diphtheria toxin A (DTA) cassette. Both allow for the selection towards the desired targeting events in ES cells (Yanagawa *et al.* 1999). The targeting construct was linearized by KpnI and electroporated into ES cells. With the antibiotic geneticin (G418), ES cells were positively selected for the presence of the neomycin phosphotransferase protein. The neomycin cassette can be deleted later in the process by the action of the FLP recombinase enzyme. DTA allows for the negative selection of insertional events that are not based on homologous recombination. ES cell clones were screened for homologous recombination events at the *Smpd1* locus. Positive ES cell clones were injected into C57BL/6 blastocysts. Germline transmission of the floxed allele was confirmed by the appearance of agouti fur, and PCRs. The neomycin cassette can be deleted later in the process by crossbreeding with mice expressing FLP recombinase. Following production of *Smpd1*-flox mice, it needs to be verified that the targeted allele still produces normal amounts of ASM protein. Finally, investigating Cre-mediated excision of the floxed sequence can confirm that deletion of exon 2 results in a functional null allele.

4.2.2 Outline of the cloning procedures in detail

The cloning strategy involved the sequential assembly of genetic features yielding the targeting vector pPS-Smpd1/KO. First, the DTA cassette was positioned 5` to the *Smpd1 genomic DNA*. Then exon 2 of *Smpd1* was flanked with loxP sites and a neomycin cassette was inserted.

4.2.2.1 Cloning of the DTA cassette into pPS-Smpd1

The DTA cassette was positioned at the 5´ end of the final targeting construct. The DTA cassette was excised of the pKO-DT vector by the activity of the restriction enzymes XbaI and RsrII. The 5` overhang of the RsrII site was filled by the polymerase I - large Klenow fragment to generate blunt ends. As an intermediate step in order to obtain convenient restriction sites (EcoRV and NotI), the 1177bp fragment was cloned into the pBlueSpec2SK plasmid. To this end, pBlueSpec2SK was linearized by XbaI and the blunt cutter SmaI. The resulting pBSpec2-DT was cleaved by EcoRV and NotI to re-isolate the DTA cassette and clone the

fragment (1201 bp) into the pPS-Smpd1 vector that was previously opened by NotI and SwaI. In this step, EcoRV and SwaI produce compatible blunt ends. The resulting plasmid was denoted as pPS-Smpd1/DT.

4.2.2.2 Modifications surrounding exon 2 of Smpd1

For the addition of features adjacent to exon 2, a better manageable portion of the genomic DNA, limited to exon 1 to exon 5, was isolated from pPS-Smpd1 and cloned into the multiple cloning site of a Litmus28 vector. The 4413 bp fragment was generated by XhoI and BstBI. Subsequently, Litumus28 was linearized by the same enzymes (XhoI and BstBI). The compatible DNA sequences were ligated and the resulting plasmid was denoted as Litmus28-Smpd1.

Addition of a loxP site 3` of exon 2: In order to obtain a vector with a loxP site 3` of exon 2, Litmus28-Smpd1 was linearized by NheI cutting its restriction site in the intron between exon 2 and 3. In addition, SacII with a cleavage site 3´ of exon 1 was utilized to result in a 1928 bp fragment comprising exon 1 and exon 2 of *Smpd1*. This fragment was cloned into the pBS-loxP vector, cleaved with XbaI and SacII. NheI and XbaI cohesive overhangs are compatible. The ligation resulted in a plasmid with a loxP site positioned according to the objective and was denoted as pBS-Smpd1/loxP.

Insertion of the neomycin cassette and second loxP site 5´ of exon 2: Applicable restrictions sites (BsrGI and PmeI), needed for the insertion of the neomycin cassette, were inserted into pBS-Smpd1/loxP by means of a linker (LK). This adapter was synthesized by the annealing of two oligonucleotides (see above, paragraph 3.1.5) and was cloned into a NsiI restriction site 5` of exon 2. The resulting plasmid was denoted as pBS-Smpd1/LK/loxP. Subsequently, pBS-Smpd1/LK/loxP was linearized by SacII and HindIII and the fragment comprising exon 1, exon 2 and the loxP site was cloned into the Litmus28-Smpd1 plasmid opened with NheI and SacII – denoted as Litmus28-Smpd1/LK/loxP. Subsequently, the restriction enzymes BsrGI and PmeI with cleavage sites included in the linker were employed to yield suited sites for the pK11rev2 plasmid derived neomycin cassette and loxP site. pK11rev2 was linearized by Acc65I and SmaI. Acc65I produced restriction overhangs, which are compatible with BsrGI derived cohesive ends. SmaI and PmeI form blunt ends. The resulting vector was denoted Litmus28-Smpd1/NeoR/loxP.

Finally, the DNA with the applied modifications had to replace the DNA that equates to the genomic locus. To this end, Litmus28-Smpd1/NeoR/loxP and pPS-Smpd1/DT were cut by

XhoI and BstBI. The 6341 bp fragment bearing the applied modifications in the surroundings of exon 2 replaced 4413 bp of the originating material in the pPS-Smpd1/DT vector. The final construct was simply denoted as pPS-Smpd1/KO (see figure 4.10).

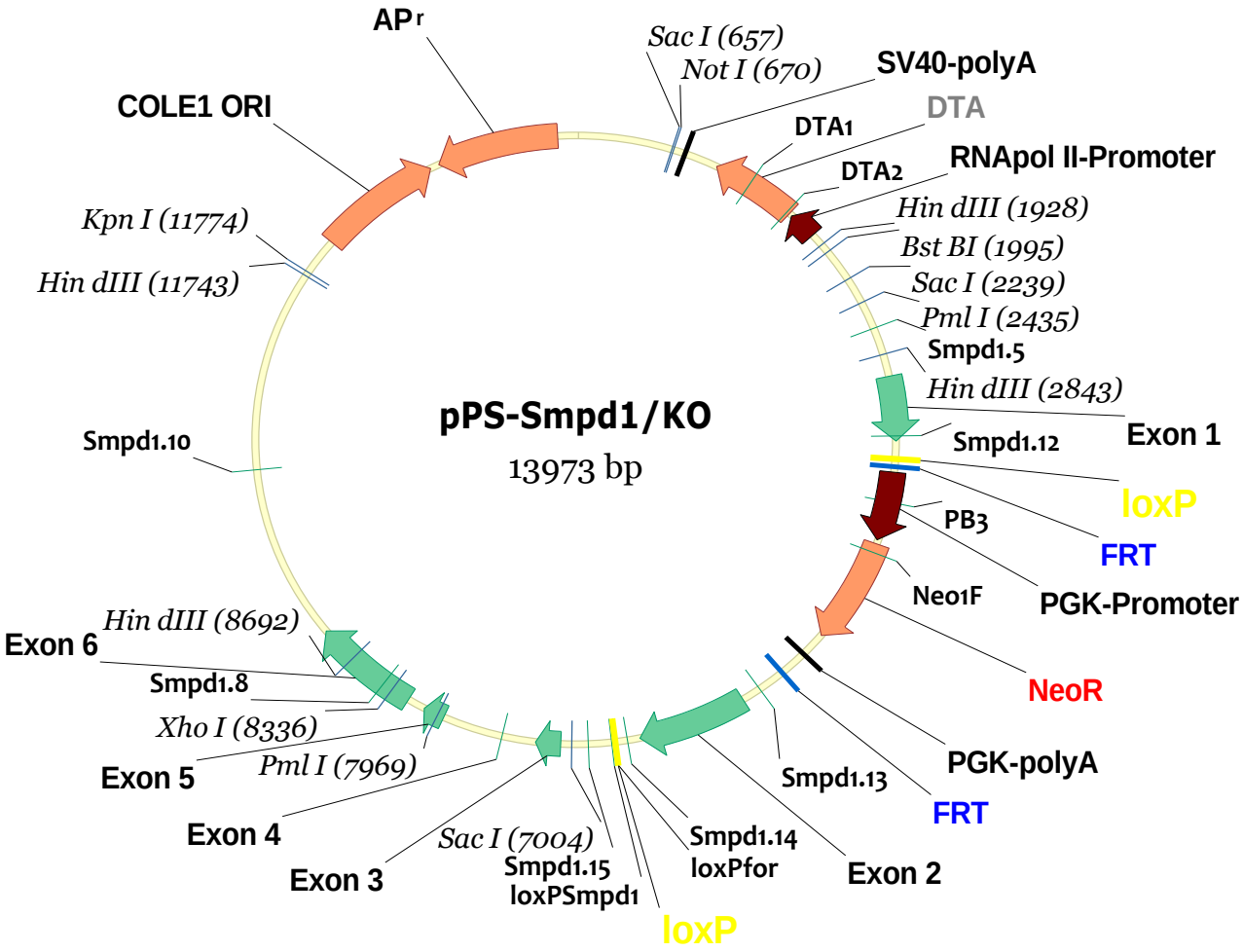

Figure 4.10: Graphical map of the pPS-Smpd1/KO plasmid. The graphic displays the molecule map of the pPS-Smpd1/KO plasmid. Functional features, restriction sites, and primer binding sites of the targeting vector are shown and labeled (see droplines). The replacement vector is based on genomic DNA of the Smpd1 locus of the mouse. The plasmid holds two loxP sites that flank exon 2 of Smpd1. Additional features of the vector comprise a FRT flanked neomycin cassette (PGK-promoter + NeoR gene + PGK –polyA) and a diphtheria toxin A cassette (RNApol II –promoter + DTA gene + SV40 poly A). Both allow for the selection towards the desired targeting events in ES cells. The pPS-Smpd1/KO plasmid backbone further features a replication origin (COLE1-ORI) and an ampicillin resistance gene (APr). The specified restriction enzymes and primers allow to comprehend and review the hereinafter referred restriction enzyme digests and PCRs.

4.2.3 Verification of pPS-Smpd1/KO targeting vector generation

In order to generate mice with a conditional null mutation of the *Smpd1* gene, a targeting vector based on genomic DNA of the *Smpd1* locus was designed. The cloning strategy involved the sequential addition of features to a pBlueScript plasmid. Single cloning steps were controlled by diagnostic restriction enzyme digests and PCRs. The completed targeting vector, pPS-Smpd1/KO, was also reexamined by restriction enzyme digests and PCRs. pPS-Smpd1/KO was digested with either SacI, HindIII, PmlI or (NotI + XhoI), (see figure 4.11 A). Furthermore, the primer sets Smpd 1.5 + PB3, Smpd 1.12 + PB3, loxP for + Smpd1.8, loxP for + Smpd1.10, loxPSmpd1 + Smpd1.8 and loxPSmpd1 + Smpd1.10 were used in PCR reactions (see figure 4.11 B). The "fingerprint" of the pPS-Smpd1/KO plasmid was expected to yield the following DNA fragment patterns: SacI 7626 bp, 4765 bp and 1582 bp, HindIII 5849 bp, 4158 bp, 3051 bp, and 915 bp, PmlI 8439bp and 5534 bp, NotI + XhoI 7666 bp and 6307 bp. Primer set Smpd1.5 + PB3: 1314 bp, Smpd 1.12 + PB3: 507 bp, loxP for + Smpd1.8: 1732 bp, loxP for + Smpd1.10: 3579 bp, loxPSmpd1 + Smpd1.8: 1704 bp and loxPSmpd1 + Smpd1.10: 3552 bp. The signals on the agarose gels reflected the expected band patterns. Restriction enzyme digests and PCR analysis confirmed the integrity of the pPS-Smpd1/KO targeting construct.

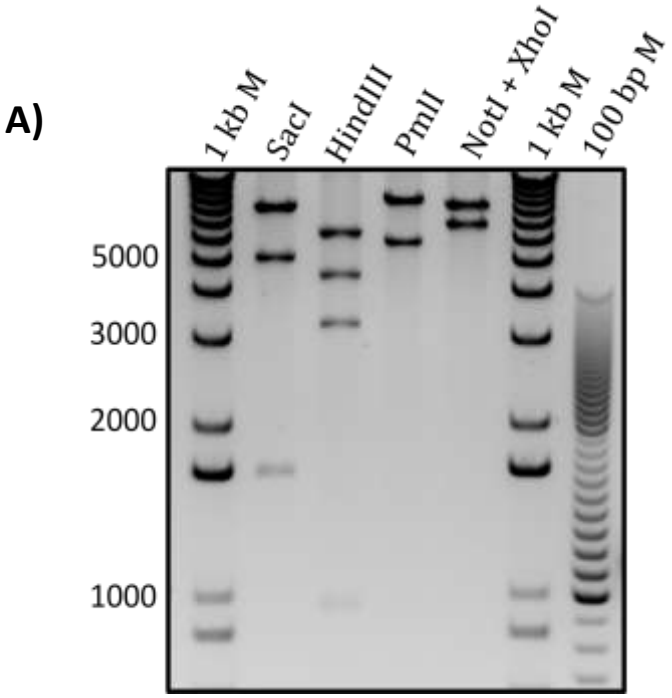

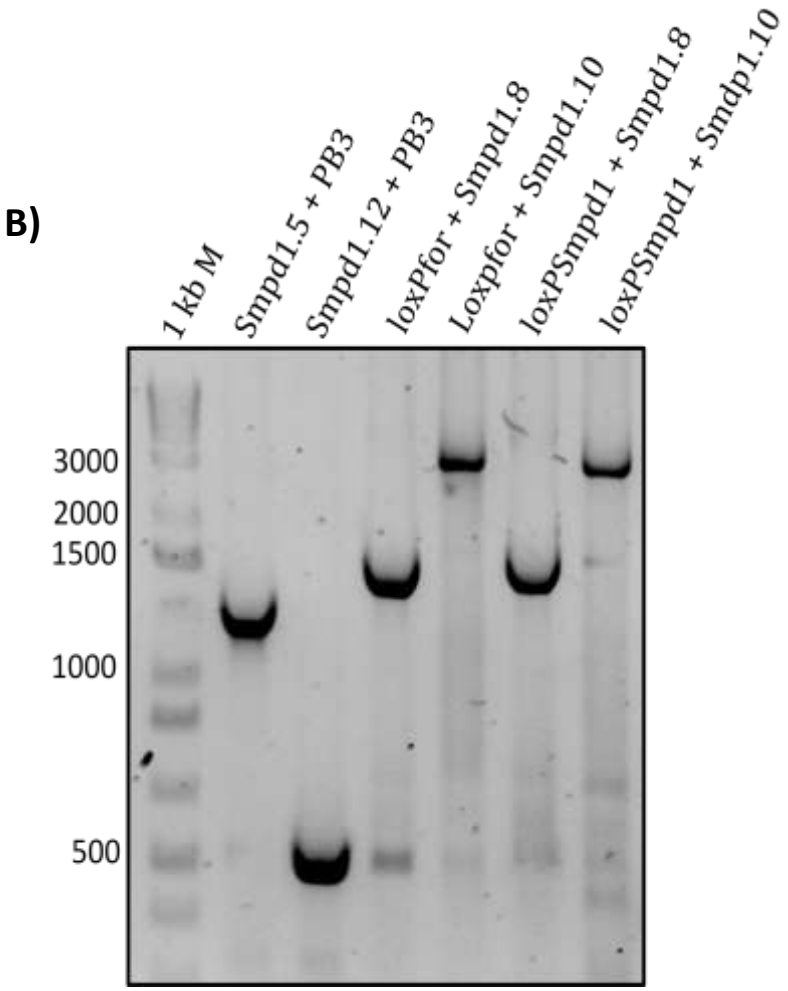

Figure 4.11: Verification of pPS-Smpd1/KO plasmid generation. A) The pPS-Smpd1/KO plasmid DNA was digested with restriction enzymes. Four reaction preparations with pPS-Smpd1/KO plasmid DNA and either SacI, HindIII, PmlI or (NotI + XhoI) were incubated. Conditions of the reactions (buffer, incubation temperature and duration) conformed to the specifications of the restriction enzyme supplier. The resulting DNA fragments and molecular markers (100 bp marker and 1 kb marker) were separated on an agarose gel. SacI digestion yields fragments of 7626 bp, 4765 bp and 1582 bp (lane 1). Four fragments of 5849 bp, 4158 bp, 3051 bp, and 915 bp were generated by HindIII digestion (lane 2). The restriction enzyme PmlI produced fragments of 8439bp and 5534 bp (lane 3). Double digestion with NotI and XhoI yielded fragments of 7666 bp and 6307 bp (lane 4). B) PCR reactions were performed with the pPS-Smpd1/KO plasmid template and reaction products run on an agarose gel. The primer set Smpd 1.5 + PB3 produced an amplicon of 1314 bp (lane 1). The PCR reaction with the primers Smpd 1.12 + PB3 resulted in a 507 bp fragment (lane 2). Primers loxP for + Smpd1.8 amplified a 1732 bp fragment (lane 3). A 3580 bp DNA fragment is produced by the primers loxP for + Smpd1.10 (lane 4). loxPSmpd1 + Smpd1.8 yielded a 1704 bp fragment (lane 5) and loxPSmpd1 + Smpd1.10 generated a 3552 bp fragment (lane 6).

4.2.4 Evaluation of the recombination competence of pPS-Smpd1/KO

The pPS-Smpd1/KO plasmid holds two loxP sites flanking exon 2 of the *Smpd1* sequence. Upon homologous recombination, this is supposed to allow for Cre recombinase mediated excision of the exon and produce a null-allele. Furthermore, the vector features a FRT flanked neomycin cassette. On the one hand, the cassette is essential for the selection of transfected ES cells. On the other hand, the neomycin phosphotransferase may cause unwanted phenotypic side effects in the mouse. The selection gene shall be deleted by crossbreeding the *Smpd1*-flox animals with FLP recombinase expressing transgenic mice. In order to verify at an early stage that the recombination sites of the targeting vector are competent for recombination, the pPS-Smpd1/KO plasmid was transformed into *E. coli* strains 294-Cre and 294-FLP. The strains hold the corresponding recombinase genes in their genome. After overnight growth at 37°C in LB medium and subsequent isolation of plasmid DNA, the recombination competence of the construct was ascertained. pPS-Smpd1/KO plasmid DNA harvested from *E. coli* DH10B (no recombinase), *E. coli* 294-Cre, and *E. coli* 294-FLP was digested by the restriction enzymes BstBI and XhoI. The DNA fragments were separated on an agarose gel and analyzed (see figure 4.12).

The pPS-Smpd1/KO plasmid DNA of *E. coli* DH10B yielded two DNA fragments of 7632 bp and 6341 bp. The 6341 bp fragment corresponds to the sequence that comprises the Cre and FRT recombination sites. DNA of *E. coli* 294-Cre and *E. coli* 294-FLP likewise displayed a fragment of 7632 bp. Cre-mediated excision of exon 2 of *E. coli* 294-Cre plasmid DNA was evident due to the presence of a second 3223 bp fragment. The DNA fragment size equates to a pPS-Smpd1/KO plasmid reduced by the size of the floxed DNA segment (3118 bp). Analogously, the *E. coli* 294-FLP derived plasmid DNA displayed a second signal of 4565 bp. The FRT-flanked neomycin cassette (1776 bp) was deleted. The Cre and FLP enzyme recognized the respective recombination sites within the pPS-Smpd1/KO plasmid and excise the flanked DNA sequences. Both recombination systems, Cre-loxP and FLP-FRT, were functional.

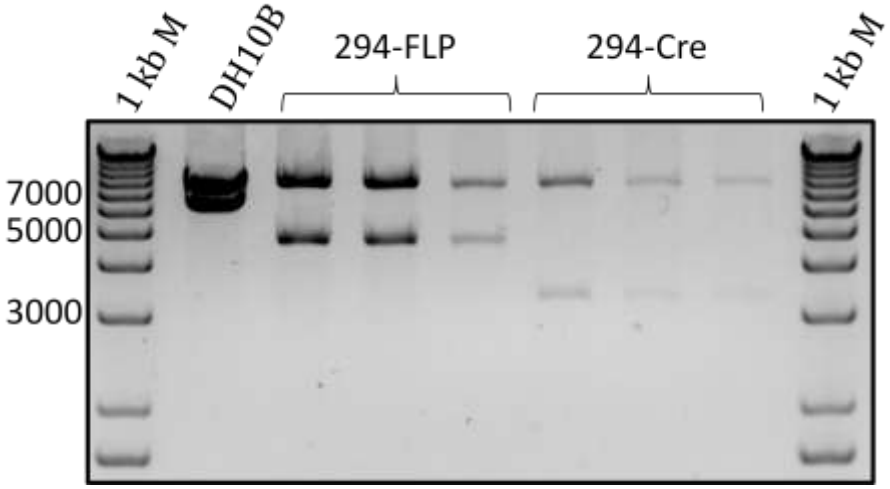

Figure 4.12: Recombination competence of pPS-Smpd1/KO plasmid. The ability of recombinases to remove FRT and loxP flanked DNA sequences of the pPS-Smpd1/KO plasmid was tested in E. coli. The pPS-Smpd1/KO plasmid was transformed into E. coli strains DH10B, 294-Cre and 294-FLP and the bacteria cultured. Upon recovery of the plasmid DNA, restriction enzyme digests with BstBI and XhoI were performed. DNA fragments and a 1 kb molecular marker were separated on an agarose gel. The pPS-Smpd1/KO plasmid DNA of E. coli DH10B displays two DNA fragments of 7632 and 6341 bp. DNA of E. coli 294-Cre and E. coli 294-FLP likewise show a fragment of 7632 bp. The second band of the E. coli 294-Cre plasmid DNA of 3223 bp equates to a pPS-Smpd1/KO plasmid reduced by the nucleotides of the floxed DNA segment (3118 bp). The second signal of the E. coli 294-FLP derived plasmid DNA of 4565 bp is reduced due to the removal of the FRT flanked neomycin cassette (1776 bp).

4.2.5 Linearization of the pPS-Smpd1/KO targeting construct

The plasmid design of the pPS-Smpd1/KO targeting construct included a singular KpnI restriction enzyme site between the short and long arm of homology. The restriction site was utilized to open the vector backbone and facilitate targeting of the *Smpd1* locus in ES cells. To this end, pPS-Smpd1/KO plasmid DNA was incubated with the KpnI restriction enzyme at 37°C overnight. The DNA was cleaned of the restriction enzyme by phenol:chloroform extraction, precipitated, and dissolved in TE buffer. In order to ensure completeness of the DNA digestion by KpnI, 2 µl of linearized DNA were run on an agarose gel and compared to an undigested pPS-Smpd1 plasmid DNA sample (see figure 4.13).

The gel image showed one defined signal of 13973 bp for the KpnI digested pPS-Smpd1/KO plasmid. Signals of circular plasmid conformations, as can be seen in the lane of the

undigested pPS-Smpd1/KO plasmid, were absent. This confirmed complete digestion and linearization of the targeting construct.

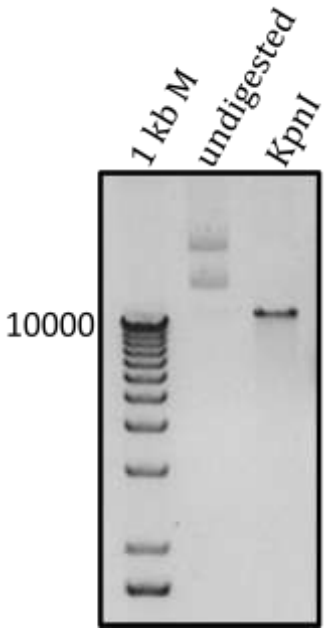

Figure 4.13: Linearization of the pPS-Smpd1/KO targeting construct. The pPS-Smpd1/KO plasmid was digested with the restriction enzyme KpnI. The reaction in a volume of 150 µl ddH_2O was incubated at 37°C overnight. The DNA was purified of the KpnI protein by phenol:chloroform extraction, precipitated, and dissolved in 40 µl TE buffer. In order to ensure completeness of the DNA digestion by KpnI, 2 µl of linearized DNA were run in a 1% agarose gel and compared to an undigested pPS-Smpd1 plasmid DNA sample and a 1 kb molecular marker. The KpnI digested pPS-Smpd1/KO plasmid of 13973 bp displays one defined signal. Signals of circular plasmid conformations are absent.

4.2.6 ES cell screening for targeting events

Generation of the pPS-Smpd1/KO plasmid was verified by restriction enzyme digests and its recombination competence validated in *E. coli.* DNA of the pPS-Smpd1/KO plasmid was linearized by KpnI and purified of contaminating proteins. The linearization of the pPS-Smpd1/KO plasmid DNA was controlled and considered suitable for the transfection of ES cells. Next, murine R1-129 ES cells were transfected with pPS-Smpd1/KO by electroporation. A single electrical pulse of 800 V and 10 µF was utilized to open the membranes of the ES cells allowing the exogenous DNA to enter the nucleus. One day post electroporation, ES cells were cultured in medium supplemented with geneticin (G418) to select for ES cells with integrated targeting construct. After 7 days, single ES cell clones were picked and separately

cultured. Part of ES cells from individual clones was transferred to cryo tubes and frozen. The other part was used to obtain genomic DNA samples. DNA of 148 ES cell clones was screened for the integration of the targeting construct at the *Smpd1* locus by PCR methods. First, PCRs over the "short arm of homology" were performed to test for homologous recombination at the *Smpd1* locus. Second, the presence of the distal loxP site was validated with primers that flank the recombination site. Finally, absence of the DTA cassette was checked by PCR. A correctly targeted ES cell clone should feature a single integration event of the targeting construct altering one allele of *Smpd1*.

4.2.6.1 Verification of homologous recombination

The ES clones were tested for the presence of the targeting construct at the *Smpd1* locus. In case of gene targeting, genomic DNA and targeting vector DNA interact. In order to test for the integration of vector specific sequences at the *Smpd1* locus, PCRs with primers that frame the "short arm of homology" were performed. Primer pairs were designed in a way that one primer binds to an endogenous DNA sequence outside of the targeting construct just beyond the "short arm" of homology while the other primer was positioned in a vector specific exogenous DNA sequence (see figure 4.14). Solely a homologous recombination event juxtaposes the primers and allows for PCR amplification of a sequence created by the novel junction. Long flanking regions decrease the efficiency of PCR amplification. In order to obviate this effect, a "nested PCR" approach was performed (Nitschke *et al.* 1993; Rolig *et al.* 1997). A nested PCR is achieved by performing a PCR reaction on a PCR reaction product. Therefore, two sets of primer pairs were used in frequency. The external primer pair Neo1F + Smpd1.3 produced a DNA fragment of 2558 bp. This fragment served as a template of the internal primer pair PB3 + Smpd1.16. An amplicon of 2220 bp was expected on the agarose gel. A total of 148 ES clone DNA samples were investigated by nested PCRs (see figure 4.15). Three ES cell clones were identified on the agarose gel image with a signal that matched the size of the spanned short arm of homology - 4A4, 4B4 and 1D5.

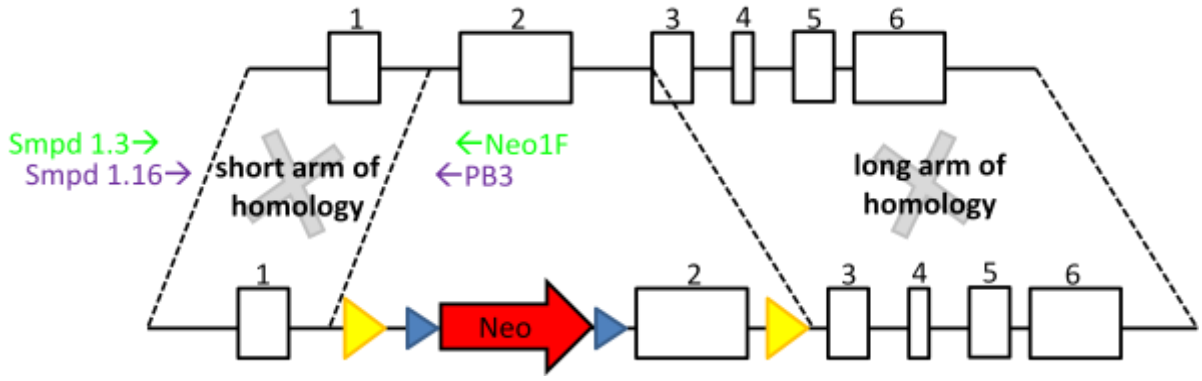

Figure 4.14: Verification of homologous recombination by PCR. Schematic representation of the strategy to detect homologous recombination events by PCR. The nested PCR approach comprises two primer sets framing the "short arm" of homology. In the case of gene targeting, genomic DNA and targeting vector DNA interact. Vector specific sequences integrate into the murine genome by homologous recombination. Primer pairs were designed in a way that one primer (Smpd1.3 and Smpd1.16) is located just beyond the "short arm" of homology, the other primer (Neo1F and PB3) is positioned in a vector specific sequence. Homologous recombination juxtaposes the primers and allows for PCR amplification of a sequence created by the novel junction. Two successive PCR runs ("nested" PCR) reduce non-specific signals. Primer Smpd1.16 + PB3 (purple) amplify a secondary target within the product of the first run (Smpd1.3 + Neo1F, green). Numbered boxes show exons of the Smpd1 locus. Yellow triangles represent loxP- and blue triangles FRT- recombination sites.

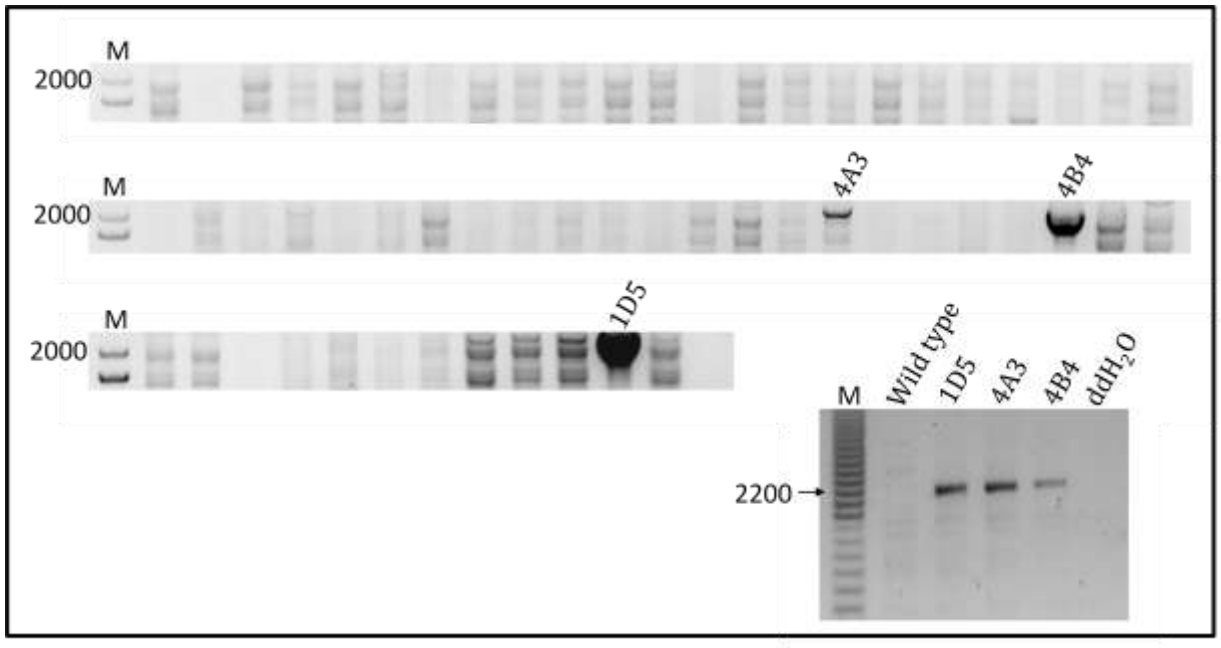

Figure 4.15: Homologous recombination at the Smpd1 locus. Genomic DNA of 148 ES cell clones was tested by a nested PCR approach for the exchange of DNA sequences by homologous recombination with the pPS-Smpd1/KO targeting vector. The internal primer pair (PB3 and Smpd1.16) frames the "short arm of homology" and amplifies a DNA fragment

of 2220 bp. Lanes of the agarose gel refer to the PCR signals of single ES cell clones (an extract of 58 PCR reactions is shown). Three clones display a signal of 2220 bp - 1D5, 4A3 and 4B4. (ES wt = clone with wild type genomic background; neg. = water added to the PCR reaction)

4.2.6.2 Confirming the presence of the distal loxP site

ES cell clones 4A3, 4B4, and 1D5 were further checked for the presence of the distal loxP site by PCR. Primers Smpd1.14 and Smpd1.15 flank the distal loxP site (see figure 4.16 A). Thus, next to the wild type *Smpd1* signal a further band was expected on the agarose gel due to the added bases of the loxP site (see figure 4.16 B).

The three clones were positive for the PCR signal of the distal loxP site. In addition to the wild type amplicon of 296 bp, a DNA amplicon with additional 34 bp due to the recombination site was present.

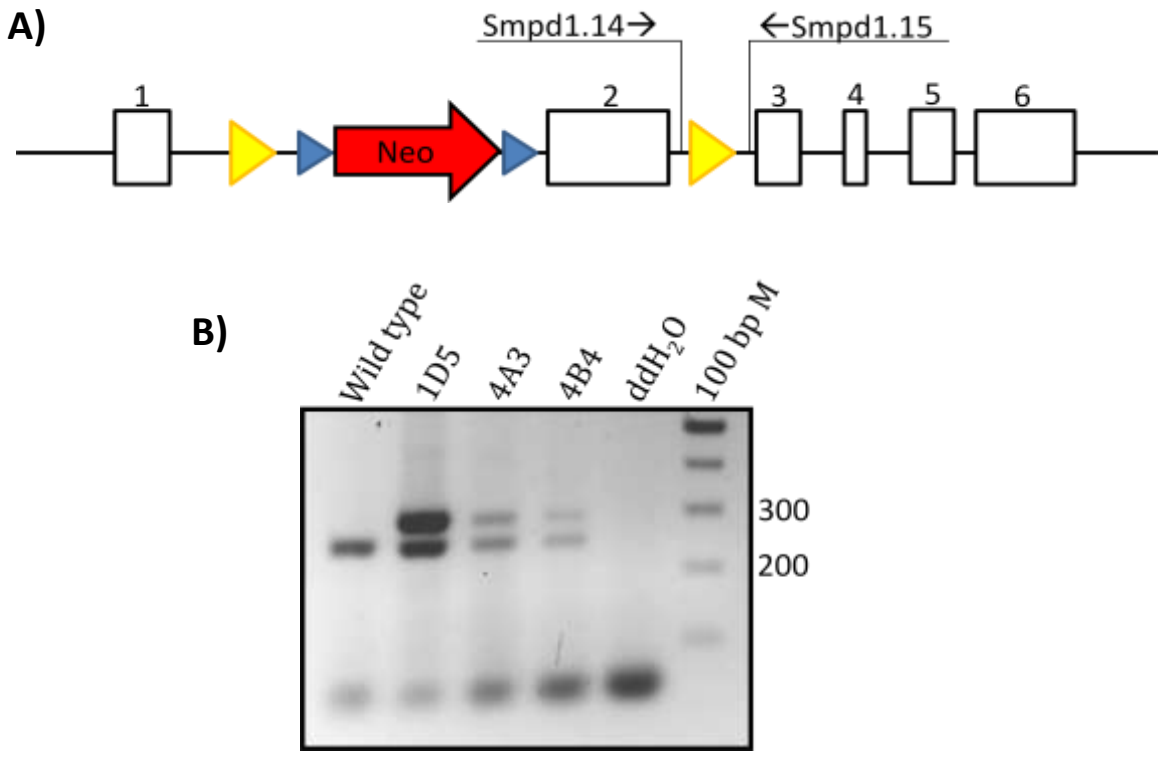

Figure 4.16: Confirming the presence of the distal loxp site in ES cell clones by PCR. A) Primers Smpd1.14 and Smpd1.15 flank the distal loxP site. A wild type Smpd1 allele produces a PCR signal of 262 bp. The template of a recombined allele generates a PCR product of 296 bp due to the 34 bp of the loxP sequence. Numbered boxes show exons of the Smpd1 locus. Yellow triangles represent loxP- and blue triangles FRT- recombination sites. B) DNA templates of the 3 candidate clones (1D5, 4A3 and 4B4) show a signal for the distal loxP site (296 bp) next

to the signal of the wild type configuration (262 bp) on the agarose gel image. A sample with no DNA template (ddH_2O) served as negative control. A 100 bp marker indicates the sizes of PCR amplicons.

4.2.6.3 Testing for presence of the diphteria toxin-A cassette signal

A diphteria toxin-A cassette (DTA cassette) was included in the targeting construct to induce apoptosis in cells that bear random integration events of the plasmid derived DNA in their genome. However, this selection procedure is not absolute. For instance, the integration into an epigenetically "shut down" locus may hinder the production of the toxin. The three ES clone candidates may possess the recombined allele and still hold random integration events in their genome. Therefore, the three clones were tested for the presence of the DTA-cassette. Primers (DTA1 + DTA2) that specifically bind to the DTA-cassette were utilized in PCRs (see figure 4.17 A). An additional endogenous control sequence was amplified (Ragf + Ragr) to facilitate the interpretation of the PCR outcome. A PCR signal for the DTA template of 386 bp in addition to the control fragment (295 bp) would exclude the corresponding ES cell clone from blastocyst injections (see figure 4.17 B).

The 386 bp PCR product of the DTA primers was present in the positive control. ES cell clones 4A3, 4B4, and 1D5 displayed the 295 bp fragment of the endogenous control while the signal of the DTA cassette was absent.

A)

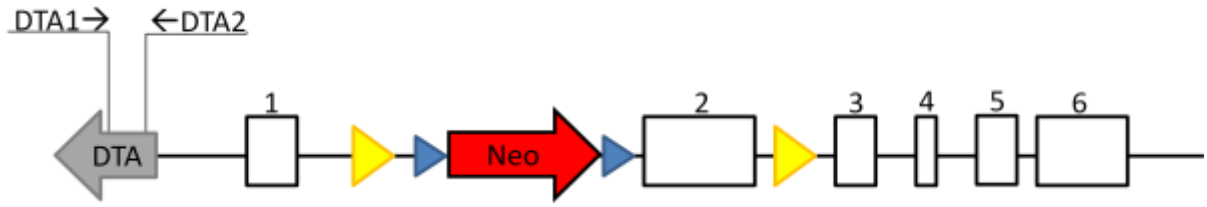

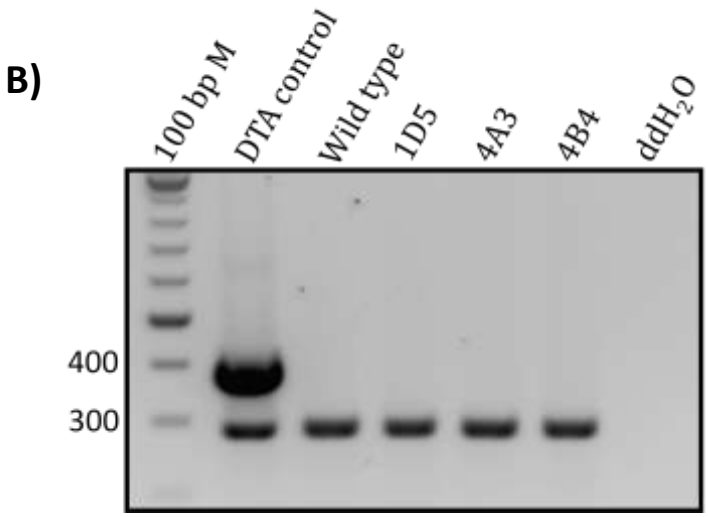

Figure 4.17: Testing for the presence of the diphteria toxin-A cassette signal in ES cell clones by PCR. A) A diphteria toxin-A cassette (DTA cassette) was included in the pPS-Smpd1/KO targeting construct (grey arrow). In the case of pPS-Smpd1/KO random integration, the DTA gene will produce the toxin and induce apoptosis of the ES cell. Primers DTA1 and DTA2 specifically bind to the DTA-cassette and were utilized in PCRs to indicate random integration events. Numbered boxes show exons of the Smpd1 locus. Yellow triangles represent loxP- and blue triangles FRT- recombination sites. B) Multiplex PCRs with the DTA cassette specific primer pair (DTA1 + DTA2) and a primer pair (Ragf + Ragr) that amplifies an endogenous control sequence were performed. The DNA of ES cell clones served as a template and reaction products were visualized on an agarose gel. ES cell clones 4A3, 4B4, and 1D5 display a PCR reaction product for the internal control fragment of 295 bp. The 386 bp PCR product of the DTA primers can be seen in the positive control (DTA control) and is absent in the reactions of the ES cell clones 4A3, 4B4, and 1D5. A 100 bp marker indicates the sizes of PCR amplicons.

4.2.3 Outcome of the blastocyst injections

The results of the ES cell screening legitimated the use of ES cell clones 4A4, 4B4 and 1D5 for the injection into murine blastocysts. The three clones displayed a PCR signal affirming recombination of the *Smpd1* locus. The presence of a distal loxP site and the loss of the DTA-cassette during recombination were affirmed by PCRs.

Frozen ES cells of clones 4A4, 4B4 and 1D5 were thawed, cultured and expanded. Three series of blastocyst injections were performed using ES cells of either clone 4A4, 4B4 or clone 1D5 (performed by Dr. Ralph Waldschütz and Wojziech Węgrzyn). Targeted R1-129 ES cells derived from an agouti mouse strain were injected into blastocysts of the black C57BL/6 strain. Injected embryos were transferred surgically to the uterine horns of pseudopregnant

recipient females. Two weeks after birth, contribution of targeted ES cells to the offspring was identified by patches of agouti coat color (see figure 4.18).

For each ES clone, mice with a high degree of chimerism, thus a high degree of R1-129 ES cell contribution, were generated.

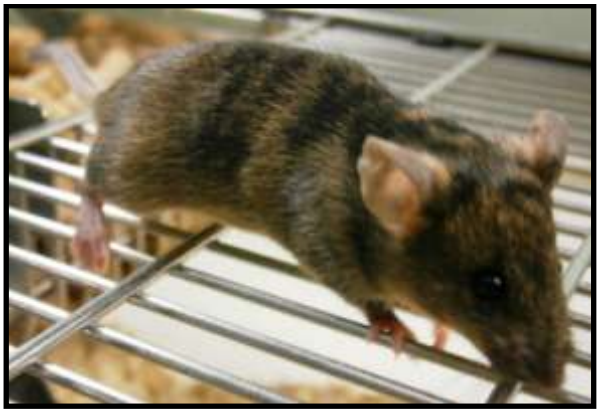

Figure 4.18: Photo of a chimeric mouse after injection of R1-129 ES cells into C57BL/6 blastocysts. R1-129 ES cells of clones 4A4, 4B4 and 1D5 were injected into C57BL/6 blastocysts. Injected embryos were transferred surgically to the uterine horns of pseudopregnant recipient females. Two weeks after birthing, contribution of ES cells to the offspring became apparent by patches of agouti coat color. An agouti coat is characteristic of the R1-129 strain, while C57BL/6 mice are black. The mouse in the photo was considered being 50% chimeric.

4.2.4 Germline transmission and reexamination of the *Smpd1* locus

Mice with a high degree of chimerism, ≥ 75% of R1-129 ES cell contribution, were mated with C57BL/6 mice. Contribution of the R1-129 ES cells to the germline was identified by the dominant agouti fur of the 129 strain. Mating pairs of each ES cell clone were able to litter agouti offspring. Tail biopsies of the agouti animals were taken and lysed to obtain DNA samples. The samples were used to repeat the previously described nested PCR over the short arm of homology and the PCR that identifies the distal loxP site (see table 4.2).

DNA samples of clone 4B4 derived animals were tested positive for the nested PCR signal. Germline animals of clone 1D4 and 4A4 did not display the signal of the short arm of homology. Genomic DNA of clone 1D4 and 4A4 was positive for the distal loxP PCR signal. Clone 4B4 derived animals on the other hand were negative for the distal loxP site

identifying PCR. All animals were excluded from further mating due to the incorrectly targeted *Smpd1* locus.

Table 4.2: Summary of blastocyst injections and analysis of germline animals.

ES Clone ID	Chimera generation with ≥ 75% ES cell contribution	Germline transmission	PCR analysis	
			Targeted *Smpd1* locus	Distal loxP site
4B4	Yes	Yes	Yes	No
1D5	Yes	Yes	No	Yes
4A3	Yes	Yes	No	Yes

5. DISCUSSION

5.1 Discussion on the transgenic CAG-Asah1 mouse model

In the present study, the CAG-Asah1 transgenic mouse model was established. In this gain of function model, an expression cassette was inserted into the murine genome. The expression cassette drives the transcription of an *Asah1* cDNA template under control of a CAG-promoter. AC hydrolyzes ceramide and produces sphingosine. Elevated sphingosine levels were affirmed in examined tissues of CAG-Asah1 animals. The mouse model therefore allows investigating the biological effects that result from enhanced ceramide consumption.

5.1.1 Design of the CAG-Asah1 expression cassette

In the CAG-Asah1 transgene design, DNA sequences were assembled that in conjunction constitute an expression cassette driving the synthesis of AC mRNA transcripts. The transcriptional start site resides in the CMV early enhancer/chicken β-actin (CAG) promoter sequence. The CAG promoter ubiquitously allows for the expression of the linked gene in transgenic mice (Okabe *et al.* 1997). The chicken insulator sequences of the CAG promoter decrement regulation by silencer elements (Niwa *et al.* 1991). Still, CAG driven transgenes were reported to display cell type and tissue specific expression due to chromosomal positional effects (Ida-Hosonuma *et al.* 2002; Hino *et al.* 2004; Wang *et al.* 2004; Baup *et al.* 2009). The heterologous Drosophila melanogaster derived “SCS” insulator elements were included in the CAG-Asah1 design to provide for additional shielding of the expression cassette from gene regulatory elements (Kellum and Schedl 1992; Dunaway *et al.* 1997; West *et al.* 2002; Gilbert *et al.* 2006). The shielding is mediated by the BEAF32 (boundary element-associated factor of 32kD) proteins which bind to the SCS sequences and constitute a barrier for regulatory elements (Zhao *et al.* 1995). Furthermore, SCS insulator elements block the formation of heterochromatin (Sun and Elgin 1999; West *et al.* 2002). A valid full-length complementary DNA (cDNA) sequence of *Asah1* was accessible from the cDNA library of the Mammalian Gene Collection (MGC) program of the National Institute of Health (NIH, Bethesda, MD, USA) (Strausberg *et al.* 1999). The sequence includes the translational start- and stop codon. The transcriptional stop signal was attached downstream of the *Asah1* cDNA. The polyadenylation signal from the human growth hormone (hGH polyA) at the 3` end of the mRNA is important for nuclear export, translation and stability of mRNA

(Guhaniyogi and Brewer 2001). In addition to the stretch of adenine bases, a GU-rich downstream sequence is required to stall transcription by RNA polymerase II and induce cleavage at the poly A site (Gromak *et al.* 2006). The importance of these nucleotides for the termination of transcription has been proven (Gromak *et al.* 2006), however the underlying mechanism is not fully known (Kuehner *et al.* 2011). Therefore, the entire hGH sequence was included in the CAG-Asah1 transgene design to grant transcriptional termination. Insertion of a transgene into coding genomic DNA may result in the production of hybrid mRNAs and proteins (Moyer *et al.* 1994; Ballester *et al.* 2004b). As an unintentional consequence, enzyme functions of the endogenous protein may be ascribed to the protein of interest. Another polyadenylation signal (bGH-polyA), upstream of the expression cassette, was included in the CAG-Asah1 design to prevent synthesis of hybrid proteins.

5.1.2 Cloning and validation of the CAG-Asah1 expression cassette

Serial assemblage of DNA segments was achieved by single cloning steps that each involved the following actions: 1. restriction enzyme digestion of the donor and destination plasmid, 2. purification and ligation of the DNA sequences, 3. transformation of bacteria with the ligation product, and 4. screening of antibiotic resistant bacterial colonies. Preferentially, the cloning strategy looked out for restriction enzyme sites that allowed joining DNA segments by directional cloning. This implies that both donor and destination plasmid are digested with two different restriction enzymes producing noncomplementary cohesive ends at either site of the DNA fragment. DNA segments are forced to ligate in the desired orientation while self-ligation is prevented. Directional cloning was reported to produce high numbers of recombinant plasmids (Revie *et al.* 1988). Alternatively, cohesive-end ligation was combined with blunt end ligation. Partially, the blunt ends had to be procured by Klenow filling of 5` protruding ends with dNTPs. After transformation, *E. coli* were selected based on the antibiotic resistance provided by the plasmid. Subsequently, plasmid DNA of resistant *E. coli* was screened for the correct joining of the DNA segments by PCRs. Frequently in this study, high numbers of antibiotic resistant *E. coli* transformants were observed on the agar plates. Much of the growing *E. coli* colonies were false positives due to recircularization of excess linearized plasmid backbones. In order to characterize a large scale of antibiotic resistant *E. coli* in a rapid and effective way, colony PCRs were performed using the bacteria directly for PCR amplification (Zon *et al.* 1989). If about 2% of the *E. coli* on

the plate held a recombinant plasmid, this was sufficient to identify an appropriately sized PCR product on an agarose gel indicative of a correct clone. The plasmid DNA of these clones was purified and further investigated by restriction enzyme digests. Finally, the realization of the expression cassette in accordance to the cloning strategy was accurately tested. After completion of the last cloning step, restriction enzyme digests and PCR analysis confirmed the integrity of the construct.

Prior to the pronuclear injection, the functionality of the expression cassettes was validated. In order to ascertain the ability to increase protein levels and activity of AC, the construct was transfected into GL261 cells. Prior to transfection, a neomycin resistance cassette was inserted into the CAG-Asah1 expression plasmid to allow for selection of cells with expression cassette DNA. Western Blots with cell lysates showed that CAG-Asah1 transfected cells displayed a 1.7 fold increase in AC protein levels in comparison to control-vector transfected cells. For the determination of AC activity, a recently described fluorogenic ceramide analog was employed (Bedia *et al.* 2007; Bedia *et al.* 2010). In contrast to the hitherto utilized radioactive (Mitsutake *et al.* 1997) and fluorogenic assays (Tani *et al.* 1998; He *et al.* 1999), the current assay does not require chromatography. The enzymatic conversion of the substrate can be directly read from a microtiter plate in a fluorescence reader. The data showed that AC activity of CAG-Asah1 transfected cells was increased 6.1 fold in comparison to untransfected and 4.9 fold in comparison to vector control transfected cells. The *in vitro* results indicated that the CAG-Asah1 construct was functional and justified to proceed in the use the CAG-Asah1 expression plasmid for the generation of transgenic mice. However, validating a transgene construct *in vitro* does not guarantee its expression *in vivo* (Haruyama *et al.* 2009).

5.1.3 Generation and identification of CAG-Asah1 transgenic mice

Prior to pronuclear injection, the expression construct was linearized and prokaryotic sequences (bacterial ori) removed. Transfection with linear DNA was reported to result in a five-fold higher integration efficiency (Brinster *et al.* 1985) and improve the transgene expression rate (Kjer-Nielsen *et al.* 1992) in comparison to transfection with supercoiled DNA. Furthermore, linearization secures that the DNA strand integrates with the required topology of the CAG-Asah1 expression cassette into the genome. Integration of the transgene is presumed to occur at sites in the genome with a spontaneous double strand

break (Palmiter and Brinster 1986). The 7274 bp long DNA of the CAG-Asah1 transgene cassette was injected into fertilized eggs of B6C3F1 mice. The length of the exogenous DNA is not a factor influencing transgene generation efficiency (Haruyama *et al.* 2009). Eggs of B6C3F1 mice were utilized as they, in comparison to the C57BL/6 strain, yield higher numbers of embryos after superovulation with superior visual and mechanical properties with regard to microinjection procedures (Teboul 2009). Intact eggs, about 60% of injected, were transferred into 8 pseudopregnant foster animals (performed by Dr. Ralph Waldschütz and Wojziech Węgrzyn). Per animal 30 fertilized eggs were transferred. At this point of the project, it was uncertain whether embryos that bear the CAG-Asah1 transgene in their genome are able to complete the complex developmental program despite potentially enhanced AC expression levels. A genetic knockout of both *Asah1* alleles in the mouse genome was reported to be lethal at the 2 cell stage (Li *et al.* 2002; Eliyahu *et al.* 2007) and mortality of early embryos was ascribed to increased ceramide levels (Perez *et al.* 2005; Eliyahu *et al.* 2007). In conclusion, regulation of ceramide levels by AC is critical during early embryogenesis. Therefore, enhanced AC protein levels in our mouse model and disturbed ceramide levels could have resulted in lethality. On the other hand, a study of Eliyahu et al. showed that enrichment of the oocyte environment with a source of recombinant AC protein during *in vitro* fertilization improved survival rates of embryos (Eliyahu *et al.* 2010). Therefore, it was feasible that incorporation of the CAG-Asah1 trangene and elevated AC protein levels may be beneficial for embryos. Eventually, four transgenic founders holding copies of the CAG-Asah1 expression cassette in their genome were identified by PCR. Founder F4 died at the age of 5 weeks. The carcass was disposed of without pathological investigation. The three remaining founders showed no evident phenotypical abnormalities and passed the transgene to their offspring.

5.1.4 Characterization of CAG-Asah1 transgene integration

It is difficult to elucidate and characterize the integration sites in the genome of mice generated by transgene technology. The genetic modification occurs in a non-targeted manner and expression cassettes randomly integrate into the genome. The formation of concatemers, multiple copies of the expression cassette linked in a head-to-tail array, is feasible (Costantini and Lacy 1981; Bishop and Smith 1989). Single and multiple chromosomal integration sites were reported (Wagner *et al.* 1983; Brinster *et al.* 1985).

However, the determination of transgene copy numbers allows investigating the functional impact of gene dosage effects in future experiments and can aid with the maintenance of transgenic mouse strains. Therefore, an attempt was made to answer this question and obtain an estimate for the number of CAG-Asah1 expression cassettes that integrated into the genome of the founder lines. To this end, quantitative real-time PCR was performed. The quantification of transgene copies in animals by real-time PCR was previously employed in studies of Tesson et al. and Ballester et al. (Tesson *et al.* 2002; Ballester *et al.* 2004a). A wild type mouse holds two endogenous copies of the *Asah1* gene. Accordingly, if a DNA fragment within an exon of the *Asah1* gene is amplified, one has to expect that the transgenic mice hold additional templates for the initial round of PCR amplification. In the PCR reaction, the flurophore binds to double stranded DNA synthesized by the Taq polymerase. The more initial template, the earlier a certain threshold of fluorescence is reached. The cycle of threshold attainment relative to a wild type DNA template gives an estimate of transgene copies. The analysis of Ct values was performed according to the comparative $2^{-\Delta\Delta Ct}$ Ct method (Livak and Schmittgen 2001; Ballester *et al.* 2004a; Bubner and Baldwin 2004). Founder F2 derived animals displayed the highest number of CAG-Asah1 integrates (nAsah1 = 46.09 ± 5.18, including 2 endogenous *Asah1* copies). Founder F1 animals held 22.09 ± 1.22 copies of nAsah1, while the offspring of founder F3 bore 16.72 ± 1.98 nAsah1 copies. For organisms with a high number of transgene copies, the quantification was reported to be less accurate (Ballester *et al.* 2004a; Bubner and Baldwin 2004). This is due to the nature of the PCR technique following a 2^n amplification of DNA within the exponential phase. If a transgene reaction sample reaches the threshold one cycle earlier than the wild type sample, the genome of the transgenic animal holds a double (2^1) amount of template. Yet another cycle earlier would imply that four times (2^2) the amount of DNA compared to wild type is present. In conclusion, the Ct difference between high-copy animals is very small. Mancini et al. quantified transgene copies in murine ES cells in an analogous way and observed comparable numbers of integrated transgene copies. It was stated that although exact numbers cannot be determined, values “probably reflect the amount of cassettes” (Mancini *et al.* 2011).

In addition to the real-time PCR approach, our standard genotyping PCR allowed for an assessment of transgene copies. The single primer set amplified the intron spanning amplicon of 339 bp of the endogenous *Asah1* gene and in case of transgene presence an

additional smaller amplicon of the cDNA templates (252 bp). Therefore, DNA templates "compete" for the resources in the PCR reaction. The densitometric analysis of the signal ratios can be interpreted. The more the ratio of the two DNA signals on the agarose gel shifts towards the transgene site, the more CAG-Asah1 template was present. This technique is also termed semi-quantitative competitive PCR (cPCR) (Hubner *et al.* 1999). One might argue that classical PCR is an endpoint measurement and as such is either positive or negative. However, it was clearly observed that the ratio of the two PCR signals varied between the four founders. The only reasonable explanation for the differences observed is the amount of the initial DNA template. The PCR techniques, real-time PCR and competitive PCR, point to the following succession of CAG-Asah1 gene dosage in founders: F4 > F2 > F1 > F3. Gene dosage may be one factor that determines protein expression levels (Friend *et al.* 1992; Liu *et al.* 1998). Linear relationships of transgene copy number and transcription levels have been reported (Swift *et al.* 1984; Grosveld *et al.* 1987). Regarding the results, one might speculate whether a high gene dosage in founder F4 may have correlated with high AC protein expression levels and activity, eventually causing death.

5.1.5 Sphingosine levels in transgenic tissues

The integration of CAG-Asah1 transgene cassettes into the mouse genome was proven. Next, the functionality of the expression cassette in the CAG-Asah1 mouse model was tested. To this end, sphingosine levels of CAG-Asah1 tissues were determined by mass spectrometry and compared to wild type tissues. Liver, kidney and spleen tissue of the founder F2 line were investigated as F2 animals held the highest gene dosage of CAG-Asah1 (tissues of founder F4 were not available). Sphingosine is the reaction product of ceramide hydrolysis by AC. The analysis revealed that sphingosine levels were elevated in tissues of the CAG-Asah1 genetic background. Sphingosine levels of the liver were 4.3 fold higher, kidney 2.8 fold higher, and spleen 2.5 fold higher than in wild type tissues. The results can be explained by an enhanced catalytic activity of AC. *In vitro* transfection of cells with the CAG-Asah1/NeoR plasmid resulted in increased AC protein levels and activity. Therefore, it seems reasonable to conclude that CAG-Asah1 transgene dependent AC expression is responsible for the altered sphingolipid metabolism *in vivo*. This allows for the qualitative statement that the CAG-Asah1 mouse model is functional. In conclusion, CAG-Asah1 transgenic mice were generated holding an altered ceramide metabolism.

5.1.6 Considerations regarding the CAG-Asah1 mouse model

In this project, CAG-Asah1 transgenic animals were generated displaying enhanced levels of the AC enzyme reaction product, sphingosine, in examined tissues. It has to be mentioned, however, that about 10% of transgenic animals that were generated by pronuclear injections show a phenotype due to disruption of host genome sequences (Gross and Stablewski 2013). Still, it is unlikely that the aberrant sphingosine levels observed, that can be logically explained by AC gain of function, are caused by disruption of another gene.

While mutations that limit AC activity result in Farber lipogranulomatosis (Farber *et al.* 1957; Sugita *et al.* 1972), the CAG-Asah1 gain of function model seems to be without major obvious consequences for the mice and does not result in severe phenotypic changes, although further studies on the phenotype of these mice are required. The feasibility of elevating AC activity and levels of sphingosine *in vivo* may be explained by the observation that even in wild type animals AC expression and activity is variable between different cell types, as was reported by Li et al. (Li *et al.* 1998). There are multiple potential sites of AC activity regulation in the cell. Protein levels can be fine-tuned by the government of AC synthesis, maturation, trafficking, and degradation. Kinetics of AC enzyme reactions in the cell depend on pH, cofactors and lipid composition (see above, paragraph 1.4). The observed sphingosine levels, however, show that the lipid composition of CAG-Asah1 cells differs from corresponding wild type cells and is not maintained by potential regulation of AC.

Regarding the transgene technology in general, the following knowledge was gained in the past that may concern the CAG-Asah1 mouse model: In gain of function models, the transcription level of a transgene within a founder line can change over time. For instance, a whole concatemer can be silenced by epigenetic changes such as DNA methylation and heterochromatin formation (Garrick *et al.* 1998; Henikoff 1998; Muskens *et al.* 2000; Calero-Nieto *et al.* 2010). Furthermore, gene copies of a transgene may be lost (Gordon 1993). Concatemers are unstable and copies of the transgene and/or adjacent DNA sequences may be deleted (Chen *et al.* 1995; Pravtcheva and Wise 1995; Scrable and Stambrook 1999; Pravtcheva and Wise 2003). Suspicious variances in future scientific results between generations of CAG-Asah1 animals may be attributed to these issues of the transgene technology. The real-time PCR methods, which were established in this project, allow quantifying CAG-Asah1 transgene copy numbers and testing the persistence of the transgene.

Despite these inconveniences resulting from the technology, transgenic mouse models have led to a variety of important scientific findings (Conn 2011). The CAG-Asah1 mouse model can be a valuable tool in the scientific contexts described in the following paragraph.

5.1.7 Perspectives of the CAG-Asah1 mouse model

The crucial role of ceramide induced endothelial apoptosis and microvascular dysfunction in the context of single dose radio therapy was investigated by Kolesnick et al. (Fuks and Kolesnick 2005; Garcia-Barros *et al.* 2010; Truman *et al.* 2010). Studies which investigated tumor transplants in immunodeficient SCID mice with either ASM wild type or knockout background showed that tumor cure by radiation does not exclusively depend on DNA breakage induced apoptosis of malignant tumor cells, but may be ascribed to a ceramide mediated reduction of microcvascular density (Garcia-Barros *et al.* 2010). Furthermore, tumor cell resistance to radiotherapy can be mediated by upregulation of AC (Liu *et al.* 2009). Collectively these studies led to the concept that radiotherapy depends on the ceramide pathway, reviewed in Henry et al. (Henry *et al.* 2013). In this context, studies with the CAG-Asah1 mouse model may lead to new insights that further clarify the molecular mechanism which underlie the concept and determine roles of ceramide and sphingosine in radiotherapy. Transgenic animals can be deployed as hosts for tumor transplants. According to this concept, reduced ceramide levels in endothelial cells of the microvasculature may confer resistance to tumor therapy.

In cystic fibrosis (CF), patients lack of a functional cystic fibrosis transmembrane conductance regulator (CFTR) which increases the pH of intracellular vesicles to pH 5.9 (Teichgraber *et al.* 2008). As a consequence, the enzyme kinetics of ASM and AC are modulated. On the one hand, ceramide production by ASM is lightly inhibited. On the other hand, AC switches from “forward” to “reverse” mode and produces ceramide. As an overall result, ceramide accumulates in epithelial cells of the lung. Apoptosis of ceramide-engorged epithelial cells leads to deposition of DNA and generation of a viscous mucus in the bronchi (Teichgraber *et al.* 2008). CF patients become highly susceptible to pulmonary inflammation. Normalization of pulmonary ceramide levels by ASM inhibition has become a clinical option for the treatment of cystic fibrosis (Riethmuller *et al.* 2009). A transfer of the CFTR knockout, (Dorin *et al.* 1992), to the CAG-Asah1 mouse model may show in how far modulation of AC can affect the CF phenotype. Small molecules that render AC activity might also be able to

normalize pulmonary ceramide levels in CF patients and provide a treatment option for the disease.

Internalization of many pathogens into mammalian cells was reported to critically depend on formation of CRDs (Grassmé *et al.* 2003b; Grassmé *et al.* 2005). The exact mechanisms of how CRD induced signalosomes facilitate internalization is not yet known. Clustering of receptors, exclusion of receptors and recruitment of intracellular signaling molecules are processes discussed in the literature (Grassmé *et al.* 2003b; Grassmé *et al.* 2005). Independent of pathogen internalization, the host cell defense is likewise conducted by CRDs (Grassmé *et al.* 2003b). Exemplarily, CRD formation has been shown to be essential for the clearance of acute *Pseudomonas aeruginosa* infections. This is achieved by CRDs balancing the cytokine response and mediating apoptosis of infected cells (Grassmé *et al.* 2003b). In accordance with this, Jan et al. reported that expression of AC by a recombinant *Sindbis virus* reduced intracellular ceramide levels upon infection and prohibited apoptosis of host cells (Jan *et al.* 2000). It has been proposed that infections with human pathogens may be treated with drugs that modulate the activity of enzymes of ceramide metabolism (Gulbins *et al.* 2004). Therefore, AC poses a candidate target for the treatment of infections. Investigations of host-pathogen interactions in CAG-Asah1 mice may deliver new insights in underlying mechanisms and validate AC as a drug target.

Continuous loss of oocytes during the development of female mice, finalizing in menopause, is mediated by ceramide (Perez *et al.* 2005; Kujjo *et al.* 2013). In this context, Morita et al. demonstrated that the reserve of oocytes in young *Smpd1* knockout mice was enhanced in comparison to wild type mice (Morita *et al.* 2000). In fertilized eggs, AC reduces the levels of ceramide and facilitates embryo survival past the two cell stage (Eliyahu *et al.* 2007). Furthermore, Eliayahu et al. showed that exogenous administration of AC protects murine oocytes as well as embryos *in vitro* (Eliyahu *et al.* 2010). Elementary pathways of oocyte and embryo protection by AC can be investigated in CAG-Asah1 animals.

5.2 Discussion on the *Smpd1* conditional knockout mouse model

ASM catalyzes the conversion of sphingomyelin to ceramide. Stress induced formation of ceramide-rich domains by ASM and subsequent reorganization of membrane proteins has been observed in *Smpd1* knockout mice (Cremesti *et al.* 2001; Grassmé *et al.* 2001; Dumitru and Gulbins 2006). This conventional *Smpd1* knockout mouse model, generated by

Hourinochi et al., affects every cell of the organism at any time (Horinouchi *et al.* 1995). As a consequence, the function of the enzyme cannot be analyzed in a single cell type, tissue, or at a defined time point of development or disease. In order to have temporal and spatial control of the *Smpd1* gene disruption, the current project aimed for the generation of a conditional knockout mouse model. To this effect, the following steps were taken and results obtained. The pPS-Smpd1/KO targeting vector was assembled by DNA cloning techniques. Diagnostic restriction enzyme digests and PCRs confirmed the realization of the targeting plasmid. Functionality of the Cre/loxP and FLP/FRT recombination system was validated in bacteria. The targeting vector was linearized and electroporated into murine ES cells. Integration of the exogenous DNA into the genome by homologous recombination at the *Smpd1* locus was tested by PCR. ES cells of three clones were injected into blastocysts and germline competent chimeras obtained. Unfortunately, required genetic modifications of the *Smpd1* locus were absent in offspring of chimeras. Recombination by Cre-recombinase and the knockout of the *Smpd1* gene cannot be achieved with the mice generated in this study.

Therefore, the following discussion deals with the crucial points that may have caused failure of this project. First, the low number of targeted clones is discussed and the targeting vector design reviewed. Then, the rationale for observing partial gene targeting vector integration at the *Smpd1* locus is provided. Furthermore, it is reasoned why discrepancies between PCR results with genomic DNA of ES cells and DNA of germline animals were observed. Finally, consequential insights enable recommending adjustments that can lead to the accomplishment of the knockout project.

5.2.1 Homologous recombination efficiency at the *Smpd1* locus

Exchange of plasmid and genomic DNA by homologous recombination is an essential and critical step in gene targeting experiments. The mechanism of homologous recombination is based on the alignment of the linear targeting construct DNA to the genomic DNA via base pairing of the homology arms. Enzymes of the DNA repair machinery facilitate the exchange of DNA sequences (Vasquez *et al.* 2001). Targeting event frequency in mouse ES cells is rather low, 10^{-5} to 10^{-6} targeting events per transfected ES cell (Bollag *et al.* 1989), while random integration events occur at a 30000 fold higher frequency (Hasty *et al.* 1991b). In the present study, merely 3 out of 148 ES cell clones were identified with a signal that

matched the size of the spanned short arm of homology - 4A4, 4B4 and 1D5. In case the other 145 ES clones were true negatives for the PCR over the short arm of homology, the targeting frequency within geneticin resistant ES clones was very low (3/148 ~ 2%). A large-scale mouse knockout program from the Wellcome Trust Sanger Institute reported 12% targeting efficiency for targeting constructs with 10 kb of homologous DNA and a DTA negative selection cassette (Skarnes *et al.* 2011). Thus, expectations of detecting targeted *Smpd1* loci were considerably higher than observed in the present study. Therefore, in the following paragraph, parameters of homologous recombination efficiency, which could be optimized, are discussed.

The design of the pPS-Smpd1/KO targeting vector particularly considered the following factors, which influence targeting frequency in ES cells. Recombination efficiency was reported to be higher in case the exogenous plasmid DNA is syngenic to the DNA of ES cells used for electroporation (te Riele *et al.* 1992). Therefore, genomic *Smpd1* DNA of the 129 strain was isolated from a Lambda phage library (done by Dr. Ralph Waldschütz). The length of the homologous sequences is another important determinant of recombination efficiency. Two arms of homology were created in the pPS-Smpd1/KO plasmid. A short arm of 1718 bp and a long arm of 4999 bp flank the heterologous DNA sequences. The short arm of homology included the sequence of exon 1 and the long arm of homology comprised the sequences of exon 3 to exon 6. It was reported that the short arm of homology can be as short as 0.5 kb without an effect on the quantity of recombination events (Hasty *et al.* 1991a). However, recombination efficiency is higher when the sequence of the long arm of homology is longer (Thomas and Capecchi 1987; Shulman *et al.* 1990; Hasty *et al.* 1991a). If the sequence extends to 8 kb, recombination efficiency reaches a maximum (Lu *et al.* 2003). Therefore, extending the long arm of homology in the pPS-Smpd1/KO plasmid to 8 kb offers the possibility to enhance recombination efficiency.

Positive and negative selection procedures allow enriching the fraction of targeted ES cells 2000 fold (Mansour *et al.* 1988). A FRT flanked neomycin cassette was positioned in the intron upstream of exon 2. The neomycin phosphotransferase protein can be present in the ES cells either due to random integration of the pPS-Smpd1/KO plasmid into the genome or homologous recombination of the targeting construct at the *Smpd1* locus. Looking at the neomycin selection in retrospect, it is conspicuous that of the 288 clones that were picked after selection, only 148 clones showed normal growth in the 24 well plates. The deviation

may be explained by untransfected ES cells that, due to a low metabolism, were able to survive selection but unable to proliferate. Geneticin was reported to be a differentiation inducing agent (Cuevas *et al.* 2004), and may compromise pluripotency of stem cells. Hence, the leeway of enhancing the drug dose rate seems marginal. Still, this could be an option to reduce the background of untransfected and enhance the fraction of targeted ES cells.

A diphtheria toxin A cassette was included in the strategy to selectively eliminate ES cells that bear random integration events in their genome. Expression of the DTA polypeptide inhibits RNA translation, protein synthesis, and specifically eliminates the ES cell (Palmiter *et al.* 1987). In case of homologous recombination, the DTA cassette detaches from the targeting vector, while the sequences that are flanked by the "arms of homology" integrate into the genome. This selection ought to enrich the quantity of ES cells with a recombined *Smpd1* locus. Effectiveness of DTA counter selection in gene targeting experiments was reported by several studies (Yagi *et al.* 1990; Yanagawa *et al.* 1999; Skarnes *et al.* 2011). Utilization of an alternative negative selection system in the pPS-Smpd1/KO plasmid does not seem promising. For instance, viral thymidine kinase/ganciclovir selection was reported to be less effective than selection with diphtheria toxin (Yanagawa *et al.* 1999).

Finally, linear DNA increases the chance of vector integration via homologous recombination (Hasty *et al.* 1992). For that reason, the plasmid design provided for a singular restriction site (KpnI) between the arms of homology. Overnight restriction enzyme digestion and visualization of the DNA on an agarose gel ensured linearity of the targeting plasmid. After linearization, vector backbone elements and the DTA cassette were situated external to the short arm of homology and can detach from the homologous sequences during recombination. This design was reported to be optimal in gene targeting experiments (LePage and Conlon 2006).

Also with regard to the transfection method, it was aimed to facilitate maximum recombination efficiency in ES cells. Electroporation was the DNA delivery method of choice seeing that this simple technique was reported to be more effective in terms of recombination frequency than other DNA transfer methods (Nairn *et al.* 1993; Yanez and Porter 1999). High purity plasmid DNA was utilized. The concentration of vector DNA, about 30 µg linear DNA were loaded into the electroporation cuvette, was reported not to be a critical factor for effective gene targeting (Thomas and Capecchi 1987). The electroporation pulse permeabilizes the membranes of the cell for a short fraction of a time and exogenous

DNA is able to enter the nucleus. In order to avoid the induction of karyotype alterations, a comparably mild electroporation pulse of 800 V, 10 µF for 0.2 ms was utilized for the transfection (e.g. in comparison to Nagy et al.: 250 V, 500 µF, 6-7 seconds (Nagy *et al.* 2003)). Still, these settings were established to be efficient for gene targeting experiments (Tompers and Labosky 2004). Nevertheless, utilizing a more intense pulse and taking the risk of genomic aberrations could on the other hand produce more targeted ES cell clones.

Furthermore, chromosome double strand breaks induced by DNA sequence detecting zinc finger nucleases promote homologous recombination (Rouet *et al.* 1994; Urnov *et al.* 2005; Meyer *et al.* 2010). Consequently, co-transfection with zinc finger mRNAs coding for nucleases that specifically cut within the *Smpd1* locus may boost the exchange of DNA sequences.

The sophisticated vector design and transfection method tried to take into account essential factors affecting targeting frequency. However, next to these variables, the chromatin structure of the targeted gene locus influences recombination efficiency (Capecchi 1989; Nickoloff 1992). Loci that are transcriptionally active in the ES cells are better accessible for the enzymatic machinery of homologous recombination (Muller 1999). Generation of the *Smpd1* knockout mouse by Horinouchi et al. (Horinouchi *et al.* 1995) and generation of animals with a partially targeted *Smpd1* gene in this study prove that, in general, the *Smpd1* locus allows for gene targeting.

5.2.2 Loss of the distal loxP site in the process of *Smpd1* gene targeting

Although cells of animals referring to clone 1D5 and 4A4 displayed a specific PCR signal for the distal loxP site, the *Smpd1* locus was unchanged. PCR signals over the short arm of homology could not be reproduced. The results suggest that these animals hold random integrations of the pPS-Smpd1/KO plasmid in their genome. In contrast, offspring referring to clone 4B4 displayed a targeted *Smpd1* locus. However, the genetic modifications were only partially integrated. The distal loxP site appears to have detached from the targeting vector during the homologous recombination event. Loss of the distal loxP site and partially recombinant alleles are frequently observed in gene targeting experiments. A high-throughput gene targeting pipeline for the generation of conditional knockout alleles reported that approximately half of the targeted clones miss the distal loxP site due to the internal homology region (Skarnes *et al.* 2011). Therefore, the internal arm of homology in

the pPS-Smpd1/KO plasmid is a potential cause of the observed configuration (see figure 5.1). In the non-conditional knockout model of Horinouchi et al., the *Smpd1* gene was disrupted by insertion of a neomycin cassette into exon 2. This resulted in a null allele and resembled an authentic model of Niemann-Pick disease type A and B (Horinouchi *et al.* 1995). For this reason, the strategy of the conditional knockout model in this study aimed for an inducible disruption of exon 2 by flanking the sequence with loxP sites. Exon 2 is the largest exon (775 bp) and encodes about 44% of the ASM protein (Newrzella and Stoffel 1992). Consequently, the floxed DNA sequence creates a relatively large internal arm of homology in the pPS-Smpd1/KO plasmid of 1228 bp. Unfortunately, longer sequences of homology promote recombination (Thomas and Capecchi 1987; Shulman *et al.* 1990; Hasty *et al.* 1991a) and may lead to loss of distal segments. Therefore, it would be prudent to flank a smaller *Smpd1* exon with loxP sites. For instance, mutations in exon 4 of human *SMPD1*, the smallest exon (80 bp), were reported to result in aberrant ASM protein and Niemann-Pick phenotype (Simonaro *et al.* 2002). The shorter sequence of internal homology may avert the loss of the distal loxP site.

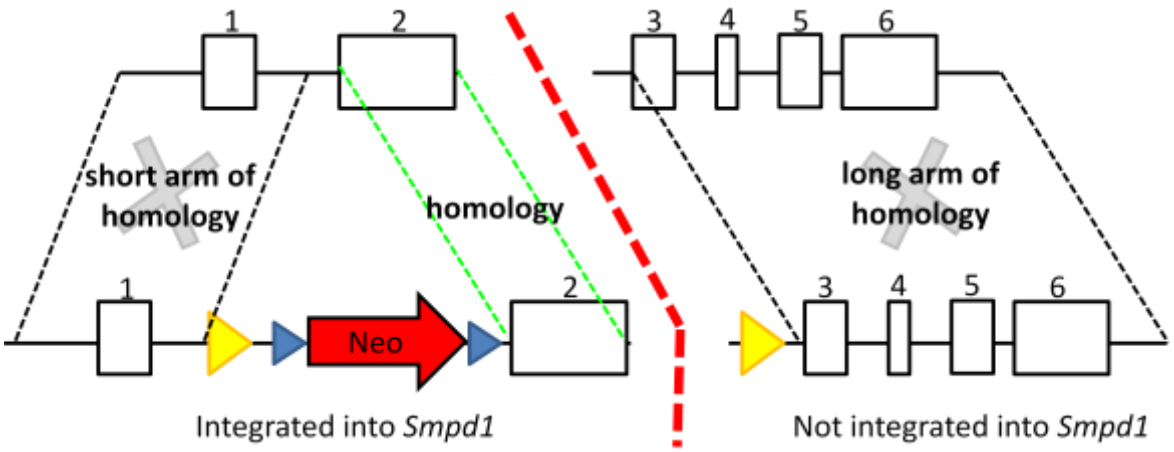

Figure 5.1: Schematic representation of the partially targeted Smpd1 locus. Mice derived from clone 4B4 were tested positive for the PCR signal of the template that is created by the novel junction of the recombined pPS-Smpd1/KO DNA sequence at the Smpd1 locus. The neomycin cassette and 5` loxP cassette are integrated into the murine genome. The distal loxP site could not be detected by PCR. Presumably, the distal loxP site detached from the targeting vector due to a recombination event between the short arm of homology (1718 bp) and the homology region comprising exon 2 (1228 bp, green lines). Integration of the pPS-Smpd1/KO plasmid at the Smpd1 locus is incomplete.

5.2.3 Incongruent ES cell screening results by PCR methods

The PCR based ES cell screening strategy was designed to indicate which ES clones bear a single integration of the targeting construct at the *Smpd1* locus. Comparable conventional PCR based screening strategies have let to the generation of gene targeted mice (Collinson *et al.* 2002; Nguyen *et al.* 2005; Gao *et al.* 2010). Homologous recombination events at the *Smpd1* locus were detected by nested PCRs over the short arm of homology. The second PCR served to exclude the scenario in which the DTA cassette is retained in the ES cells genome and disrupts the *Smpd1* locus. Presence of the distal loxP site was confirmed by a third PCR.

In order to frame the short arm of homology, it was unavoidable to amplify a DNA fragment of about 2 kb. The nested PCR method compensates for variations in quantity and quality of genomic DNA samples and enhances the specificity of the amplification reaction (Nitschke *et al.* 1993; Neumaier *et al.* 1998; Wienholds *et al.* 2003). A drawback of two step PCRs is an increased risk of contamination. Another shortcoming is that the PCR screen lacks a positive control. Still, targeting events were detected at the *Smpd1* locus as was confirmed for the ES cells and germline offspring referring to clone 4B4. However, positive PCR signals with DNA of ES cell clones 1D5 and 4A4 could not be reproduced with genomic DNA of corresponding germline animals. This incongruity could be ascribed to the increased contamination risk of the two step PCR resulting in amplification of non-specific templates during the ES cell screening. Mixed ES cell clones may provide an alternative explanation. ES cell clones, composed of targeted as well as non-targeted cells, can produce the observed ES cell PCR signals and result in transmission of a non-targeted genome. Plasmid DNA residues in the genomic DNA samples of the ES cell clones may also explain deceptive PCR results. After electroporation, the ES cell medium was changed several times. In spite of this, plasmid DNA could have served as templates for the PCR amplification of the distal loxP site. Arguing against contamination of the DNA samples, however, are the PCR results of the diphtheria toxin A cassette detection. Plasmid contamination of the genomic DNA samples would have resulted in a cassette-specific PCR signal. Contamination of other PCR reaction components with plasmid DNA can be excluded on the basis of the utilized negative controls.

ES cell screening by standard PCR is not without alternative. Modifications of the genome can be detected either by loss of allele (LOA-) assay (Frendewey *et al.* 2010) or Southern blot (Southern 1975). However, the LOA assay is based on allele quantification by real-time PCR and in turn bears similar pitfalls as standard PCR. Southern blot strategies must be

accounted for in the targeting vector design and labeled hybridization probes need to be generated and established.

In the present study, the PCR screening was not able to identify the ES cell clones, which were utilized for blastocyst injections, as non-recombined. The PCR detecting the distal loxP site confirmed the presence of the recombination site, but did not prove its integration at the *Smpd1* locus. Providing this missing information seems vital for detecting targeted ES cell clones and making a success of the project. Long-range PCRs over the long arm of homology or Southern blots may complement the ES cell screening strategy in order to detect incorporation of the distal loxP site at the *Smpd1* locus.

5.2.4 Perspectives of the conditional *Smpd1* knockout mouse model

A range of options emerges from the discussion and encourages proceeding with the project. Adjustments can increase recombination efficiency, reduce the risk of losing the distal loxP site, and improve the screening of ES cells.

Regarding recombination efficiency, it was emphasized that extension of the long arm of homology can produce more targeted clones. Additionally, a more intense electroporation pulse and stronger geneticin selection could enhance the fraction of recombined ES cell clones. Application of the novel zinc finger technology could also constitute a solution. In order to prevent the loss of the distal loxP site, it has been suggested to flank the short exon 4 with loxP sites to minimize the region of internal homology. Furthermore, the ES cell screening strategy could be reconsidered. Either a long-range PCR over the long arm of homology or a Southern Blot may complement the current ES cell screening strategy to affirm the integration of the distal loxP site at the *Smpd1* locus. By means of the suggested adoptions, it may be feasible to generate the conditional knockout mouse model in the future and selectively deplete the *Smpd1* gene.

7. SUMMARY

Ceramide self-association in cell membranes gives rise to formation of ceramide-rich domains, which in turn reorganize membrane proteins and affect reaction yields of signal transduction pathways. Deregulated ceramide metabolism and membrane organization has been shown in many disease pathologies. The present study aimed to generate transgenic mouse models for the enzymes acid ceramidase and acid sphingomyelinase which both modulate ceramide levels. Genetic mouse models are valuable scientific tools for studying physiological and pathological processes *in vivo*.

In a “gain of function” model, acid ceramidase expression cassettes were introduced into the murine genome. The expression cassette comprised a CAG-promoter driving the transcription of acid ceramidase complementary DNA. Genetic components of the CAG-Asah1 expression cassette were assembled by DNA cloning techniques. Functionality of the construct was tested *in vitro* proving CAG-Asah1 dependent enhancement of acid ceramidase protein levels and activity. The transgene cassette was delivered to the murine genome by pronuclear injections into fertilized eggs. Transgenic offspring was identified by PCRs and three founder lines were established. The gene dosage of transgene copies in distinct founder lines was determined by quantitative PCR methods. Sphingosine levels of liver, kidney and spleen tissue homogenates were determined by mass spectrometry. The data revealed that tissues of CAG-Asah1 transgenic animals displayed significantly higher levels of the acid ceramidase reaction product in comparison to wild type tissues. The results can be explained by an enhanced catalytic activity of acid ceramidase in CAG-Asah1 animals. In conclusion, my research generated a CAG-Asah1 transgenic mouse model which may reveal important scientific findings with regard to the biological effects resulting from ceramide consumption by acid ceramidase.

In an attempt to develop a conditional knockout model, the acid sphingomyelinase gene was targeted with a replacement vector. The design of pPS-Smpd1/KO vector aimed to enable the insertion of loxP recombination sites to the acid sphingomyelinase gene via homologous recombination in embryonic stem cells. The genetic sequences of pPS-Smpd1/KO were assembled by DNA cloning techniques and the completed plasmid reexamined by PCRs and

restriction enzyme digests. Recombination competence of the Cre/loxP system was confirmed in *E. coli.* Subsequently, murine ES cells were transfected with the pPS-Smpd1/KO plasmid DNA. Individual ES cell clones were screened by PCR for homologous recombination events and integration of the targeting construct at the acid sphingomyelinase gene locus. Three ES cell clones were assumed to hold a recombined acid sphingomyelinase gene and were utilized for injection into murine blastocysts. Examination of transgenic animals, however, revealed random and partial integration events of the targeting construct. In this study, knowledge was acquired which allows adapting the targeting construct and/or ES cell screening method to facilitate the generation of the conditional knockout model for the acid sphingomyelinase in the future.

8. REFERENCES

Abdel Shakor AB, Kwiatkowska K and Sobota A (2004). Cell surface ceramide generation precedes and controls FcgammaRII clustering and phosphorylation in rafts. *J Biol Chem* **279**(35): 36778-87.

Accili D, Drago J, Lee EJ, Johnson MD, Cool MH, Salvatore P, Asico LD, Jose PA, Taylor SI and Westphal H (1996). Early neonatal death in mice homozygous for a null allele of the insulin receptor gene. *Nat Genet* **12**(1): 106-9.

Alayoubi AM, Wang JC, Au BC, Carpentier S, Garcia V, Dworski S, El-Ghamrasni S, Kirouac KN, Exertier MJ, Xiong ZJ, Prive GG, Simonaro CM, Casas J, Fabrias G, Schuchman EH, Turner PV, Hakem R, Levade T and Medin JA (2013). Systemic ceramide accumulation leads to severe and varied pathological consequences. *EMBO Mol Med* **5**(6): 827-42.

Allen ND, Cran DG, Barton SC, Hettle S, Reik W and Surani MA (1988). Transgenes as probes for active chromosomal domains in mouse development. *Nature* **333**(6176): 852-5.

Artetxe I, Sergelius C, Kurita M, Yamaguchi S, Katsumura S, Slotte JP and Maula T (2013). Effects of sphingomyelin headgroup size on interactions with ceramide. *Biophys J* **104**(3): 604-12.

Auerbach C (1947). The induction by mustard gas of chromosomal instabilities in Drosophila melanogaster. *Proc R Soc Edinb Biol* **62**: 307-20.

Auerbach C and Robson JM (1947). The production of mutations by chemical substances. *Proc R Soc Edinb Biol* **62**: 271-83.

Avota E, Gulbins E and Schneider-Schaulies S (2011). DC-SIGN mediated sphingomyelinase-activation and ceramide generation is essential for enhancement of viral uptake in dendritic cells. *PLoS Pathog* **7**(2): e1001290.

Azuma N, O'Brien JS, Moser HW and Kishimoto Y (1994). Stimulation of acid ceramidase activity by saposin D. *Arch Biochem Biophys* **311**(2): 354-7.

Bagatolli LA, Ipsen JH, Simonsen AC and Mouritsen OG (2010). An outlook on organization of lipids in membranes: searching for a realistic connection with the organization of biological membranes. *Prog Lipid Res* **49**(4): 378-89.

Bai J and Pagano RE (1997). Measurement of spontaneous transfer and transbilayer movement of BODIPY-labeled lipids in lipid vesicles. *Biochemistry* **36**(29): 8840-8.

Ballester M, Castello A, Ibanez E, Sanchez A and Folch JM (2004a). Real-time quantitative PCR-based system for determining transgene copy number in transgenic animals. *Biotechniques* **37**(4): 610-3.

Ballester M, Molist J, Lopez-Bejar M, Sanchez A, Santalo J, Folch JM and Ibanez E (2004b). Disruption of the mouse phospholipase C-beta1 gene in a beta-lactoglobulin transgenic line affects viability, growth, and fertility in mice. *Gene* **341**: 279-89.

Bao JX, Xia M, Poklis JL, Han WQ, Brimson C and Li PL (2010). Triggering role of acid sphingomyelinase in endothelial lysosome-membrane fusion and dysfunction in coronary arteries. *Am J Physiol Heart Circ Physiol* **298**(3): H992-H1002.

Bar J, Linke T, Ferlinz K, Neumann U, Schuchman EH and Sandhoff K (2001). Molecular analysis of acid ceramidase deficiency in patients with Farber disease. *Hum Mutat* **17**(3): 199-209.

Baup D, Moser M, Schurmans S and Leo O (2009). Developmental regulation of the composite CAG promoter activity in the murine T lymphocyte cell lineage. *Genesis* **47**(12): 799-804.

Bedia C, Camacho L, Abad JL, Fabrias G and Levade T (2010). A simple fluorogenic method for determination of acid ceramidase activity and diagnosis of Farber disease. *J Lipid Res* **51**(12): 3542-7.

Bedia C, Casas J, Garcia V, Levade T and Fabrias G (2007). Synthesis of a novel ceramide analogue and its use in a high-throughput fluorogenic assay for ceramidases. *Chembiochem* **8**(6): 642-8.

Bernardo K, Hurwitz R, Zenk T, Desnick RJ, Ferlinz K, Schuchman EH and Sandhoff K (1995). Purification, characterization, and biosynthesis of human acid ceramidase. *J Biol Chem* **270**(19): 11098-102.

Bezombes C, Grazide S, Garret C, Fabre C, Quillet-Mary A, Muller S, Jaffrezou JP and Laurent G (2004). Rituximab antiproliferative effect in B-lymphoma cells is associated with acid-sphingomyelinase activation in raft microdomains. *Blood* **104**(4): 1166-73.

Bionda C, Hadchity E, Alphonse G, Chapet O, Rousson R, Rodriguez-Lafrasse C and Ardail D (2007). Radioresistance of human carcinoma cells is correlated to a defect in raft membrane clustering. *Free Radic Biol Med* **43**(5): 681-94.

Bishop JO and Smith P (1989). Mechanism of chromosomal integration of microinjected DNA. *Mol Biol Med* **6**(4): 283-98.

Bollag RJ, Waldman AS and Liskay RM (1989). Homologous recombination in mammalian cells. *Annu Rev Genet* **23**: 199-225.

Bradford MM (1976). A rapid and sensitive method for the quantitation of microgram quantities of protein utilizing the principle of protein-dye binding. *Anal Biochem* **72**: 248-54.

Brady RO, Kanfer JN, Mock MB and Fredrickson DS (1966). The metabolism of sphingomyelin. II. Evidence of an enzymatic deficiency in Niemann-Pick diseae. *Proc Natl Acad Sci U S A* **55**(2): 366-9.

Bretscher MS (1972). Asymmetrical lipid bilayer structure for biological membranes. *Nat New Biol* **236**(61): 11-2.

Bretscher MS and Raff MC (1975). Mammalian plasma membranes. *Nature* **258**(5530): 43-9.

Brinster RL, Chen HY, Trumbauer ME, Yagle MK and Palmiter RD (1985). Factors affecting the efficiency of introducing foreign DNA into mice by microinjecting eggs. *Proc Natl Acad Sci U S A* **82**(13): 4438-42.

Brown DA and London E (1998). Functions of lipid rafts in biological membranes. *Annu Rev Cell Dev Biol* **14**: 111-36.

Bubner B and Baldwin IT (2004). Use of real-time PCR for determining copy number and zygosity in transgenic plants. *Plant Cell Rep* **23**(5): 263-71.

Buchholz F, Angrand PO and Stewart AF (1996). A simple assay to determine the functionality of Cre or FLP recombination targets in genomic manipulation constructs. *Nucleic Acids Res* **24**(15): 3118-9.

Calero-Nieto FJ, Bert AG and Cockerill PN (2010). Transcription-dependent silencing of inducible convergent transgenes in transgenic mice. *Epigenetics Chromatin* **3**(1): 3.

Capecchi MR (1989). Altering the genome by homologous recombination. *Science* **244**(4910): 1288-92.

Charruyer A, Grazide S, Bezombes C, Muller S, Laurent G and Jaffrezou JP (2005). UV-C light induces raft-associated acid sphingomyelinase and JNK activation and translocation independently on a nuclear signal. *J Biol Chem* **280**(19): 19196-204.

Chen CM, Choo KB and Cheng WT (1995). Frequent deletions and sequence aberrations at the transgene junctions of transgenic mice carrying the papillomavirus regulatory and the SV40 TAg gene sequences. *Transgenic Res* **4**(1): 52-9.

Cohen SN, Chang AC, Boyer HW and Helling RB (1973). Construction of biologically functional bacterial plasmids in vitro. *Proc Natl Acad Sci U S A* **70**(11): 3240-4.

Collinson N, Kuenzi FM, Jarolimek W, Maubach KA, Cothliff R, Sur C, Smith A, Otu FM, Howell O, Atack JR, McKernan RM, Seabrook GR, Dawson GR, Whiting PJ and Rosahl TW (2002). Enhanced learning and memory and altered GABAergic synaptic transmission in mice lacking the alpha 5 subunit of the GABAA receptor. *J Neurosci* **22**(13): 5572-80.

Conn PM (2011). Animal Models of Molecular Pathology. Progress in Molecular Biology & Translational Science. *Academic Press*. London. First edition

Contreras FX, Basanez G, Alonso A, Herrmann A and Goni FM (2005). Asymmetric addition of ceramides but not dihydroceramides promotes transbilayer (flip-flop) lipid motion in membranes. *Biophys J* **88**(1): 348-59.

Costantini F and Lacy E (1981). Introduction of a rabbit beta-globin gene into the mouse germ line. *Nature* **294**(5836): 92-4.

Cremesti A, Paris F, Grassmé H, Holler N, Tschopp J, Fuks Z, Gulbins E and Kolesnick R (2001). Ceramide enables fas to cap and kill. *J Biol Chem* **276**(26): 23954-61.

Cuevas P, Diaz-Gonzalez D and Dujovny M (2004). Differentiation-inducing activity of neomycin in cultured rat glioma cells. *Neurol Res* **26**(4): 401-3.

Cuschieri J, Bulger E, Billgrin J, Garcia I and Maier RV (2007). Acid sphingomyelinase is required for lipid Raft TLR4 complex formation. *Surg Infect (Larchmt)* **8**(1): 91-106.

da Veiga Pereira L, Desnick RJ, Adler DA, Disteche CM and Schuchman EH (1991). Regional assignment of the human acid sphingomyelinase gene (SMPD1) by PCR analysis of somatic cell hybrids and in situ hybridization to 11p15.1----p15.4. *Genomics* **9**(2): 229-34.

de Laat SW, van der Saag PT, Elson EL and Schlessinger J (1979). Lateral diffusion of membrane lipids and proteins is increased specifically in neurites of differentiating neuroblastoma cells. *Biochim Biophys Acta* **558**(2): 247-50.

Devi AR, Gopikrishna M, Ratheesh R, Savithri G, Swarnalata G and Bashyam M (2006). Farber lipogranulomatosis: clinical and molecular genetic analysis reveals a novel mutation in an Indian family. *J Hum Genet* **51**(9): 811-4.

Doetschman T, Gregg RG, Maeda N, Hooper ML, Melton DW, Thompson S and Smithies O (1987). Targetted correction of a mutant HPRT gene in mouse embryonic stem cells. *Nature* **330**(6148): 576-8.

Dorin JR, Dickinson P, Alton EW, Smith SN, Geddes DM, Stevenson BJ, Kimber WL, Fleming S, Clarke AR, Hooper ML and et al. (1992). Cystic fibrosis in the mouse by targeted insertional mutagenesis. *Nature* **359**(6392): 211-5.

Dumitru CA and Gulbins E (2006). TRAIL activates acid sphingomyelinase via a redox mechanism and releases ceramide to trigger apoptosis. *Oncogene* **25**(41): 5612-25.

Dunaway M, Hwang JY, Xiong M and Yuen HL (1997). The activity of the scs and scs' insulator elements is not dependent on chromosomal context. *Mol Cell Biol* **17**(1): 182-9.

Durfee T, Nelson R, Baldwin S, Plunkett G, 3rd, Burland V, Mau B, Petrosino JF, Qin X, Muzny DM, Ayele M, Gibbs RA, Csorgo B, Posfai G, Weinstock GM and Blattner FR (2008). The complete genome sequence of Escherichia coli DH10B: insights into the biology of a laboratory workhorse. *J Bacteriol* **190**(7): 2597-606.

Eliyahu E, Park JH, Shtraizent N, He X and Schuchman EH (2007). Acid ceramidase is a novel factor required for early embryo survival. *FASEB J* **21**(7): 1403-9.

Eliyahu E, Shtraizent N, Martinuzzi K, Barritt J, He X, Wei H, Chaubal S, Copperman AB and Schuchman EH (2010). Acid ceramidase improves the quality of oocytes and embryos and the outcome of in vitro fertilization. *FASEB J* **24**(4): 1229-38.

Elojeimy S, Liu X, McKillop JC, El-Zawahry AM, Holman DH, Cheng JY, Meacham WD, Mahdy AE, Saad AF, Turner LS, Cheng J, T AD, Dong JY, Bielawska A, Hannun YA and Norris JS (2007). Role of acid ceramidase in resistance to FasL: therapeutic approaches based on acid ceramidase inhibitors and FasL gene therapy. *Mol Ther* **15**(7): 1259-63.

Emmelot P and Van Hoeven RP (1975). Phospholipid unsaturation and plasma membrane organization. *Chem Phys Lipids* **14**(3): 236-46.

Farber S, Cohen J and Uzman LL (1957). Lipogranulomatosis; a new lipo-glycoprotein storage disease. *J Mt Sinai Hosp N Y* **24**(6): 816-37.

Farese RV, Jr., Ruland SL, Flynn LM, Stokowski RP and Young SG (1995). Knockout of the mouse apolipoprotein B gene results in embryonic lethality in homozygotes and protection against diet-induced hypercholesterolemia in heterozygotes. *Proc Natl Acad Sci U S A* **92**(5): 1774-8.

Fassler R and Meyer M (1995). Consequences of lack of beta 1 integrin gene expression in mice. *Genes Dev* **9**(15): 1896-908.

Ferlinz K, Hurwitz R, Moczall H, Lansmann S, Schuchman EH and Sandhoff K (1997). Functional characterization of the N-glycosylation sites of human acid sphingomyelinase by site-directed mutagenesis. *Eur J Biochem* **243**(1-2): 511-7.

Ferlinz K, Kopal G, Bernardo K, Linke T, Bar J, Breiden B, Neumann U, Lang F, Schuchman EH and Sandhoff K (2001). Human acid ceramidase: processing, glycosylation, and lysosomal targeting. *J Biol Chem* **276**(38): 35352-60.

Frendewey D, Chernomorsky R, Esau L, Om J, Xue Y, Murphy AJ, Yancopoulos GD and Valenzuela DM (2010). The loss-of-allele assay for ES cell screening and mouse genotyping. *Methods Enzymol* **476**: 295-307.

Friend WC, Clapoff S, Landry C, Becker LE, O'Hanlon D, Allore RJ, Brown IR, Marks A, Roder J and Dunn RJ (1992). Cell-specific expression of high levels of human S100 beta in transgenic mouse brain is dependent on gene dosage. *J Neurosci* **12**(11): 4337-46.

Fuks Z and Kolesnick R (2005). Engaging the vascular component of the tumor response. *Cancer Cell* **8**(2): 89-91.

Gallala HD and Sandhoff K (2011). Biological function of the cellular lipid BMP-BMP as a key activator for cholesterol sorting and membrane digestion. *Neurochem Res* **36**(9): 1594-600.

Gao X, Eladari D, Leviel F, Tew BY, Miro-Julia C, Cheema FH, Miller L, Nelson R, Paunescu TG, McKee M, Brown D and Al-Awqati Q (2010). Deletion of hensin/DMBT1 blocks conversion of beta- to alpha-intercalated cells and induces distal renal tubular acidosis. *Proc Natl Acad Sci U S A* **107**(50): 21872-7.

Garcia-Barros M, Paris F, Cordon-Cardo C, Lyden D, Rafii S, Haimovitz-Friedman A, Fuks Z and Kolesnick R (2003). Tumor response to radiotherapy regulated by endothelial cell apoptosis. *Science* **300**(5622): 1155-9.

Garcia-Barros M, Thin TH, Maj J, Cordon-Cardo C, Haimovitz-Friedman A, Fuks Z and Kolesnick R (2010). Impact of stromal sensitivity on radiation response of tumors implanted in SCID hosts revisited. *Cancer Res* **70**(20): 8179-86.

Garrick D, Fiering S, Martin DI and Whitelaw E (1998). Repeat-induced gene silencing in mammals. *Nat Genet* **18**(1): 56-9.

Gatt S (1963). Enzymic Hydrolysis and Synthesis of Ceramides. *J Biol Chem* **238**: 3131-3.

Gilbert MK, Tan YY and Hart CM (2006). The Drosophila boundary element-associated factors BEAF-32A and BEAF-32B affect chromatin structure. *Genetics* **173**(3): 1365-75.

Goldkorn T, Chung S and Filosto S (2013). Lung cancer and lung injury: the dual role of ceramide. *Handb Exp Pharmacol* **216**: 93-113.

Gordesky SE and Marinetti GV (1973). The asymetric arrangement of phospholipids in the human erythrocyte membrane. *Biochem Biophys Res Commun* **50**(4): 1027-31.

Gordon JW (1993). Production of transgenic mice. *Methods Enzymol* **225**: 747-71.

Gordon JW and Ruddle FH (1981). Integration and stable germ line transmission of genes injected into mouse pronuclei. *Science* **214**(4526): 1244-6.

Gordon JW, Scangos GA, Plotkin DJ, Barbosa JA and Ruddle FH (1980). Genetic transformation of mouse embryos by microinjection of purified DNA. *Proc Natl Acad Sci U S A* **77**(12): 7380-4.

Grassmé H, Bock J, Kun J and Gulbins E (2002). Clustering of CD40 ligand is required to form a functional contact with CD40. *J Biol Chem* **277**(33): 30289-99.

Grassmé H, Cremesti A, Kolesnick R and Gulbins E (2003a). Ceramide-mediated clustering is required for CD95-DISC formation. *Oncogene* **22**(35): 5457-70.

Grassmé H, Jekle A, Riehle A, Schwarz H, Berger J, Sandhoff K, Kolesnick R and Gulbins E (2001). CD95 signaling via ceramide-rich membrane rafts. *J Biol Chem* **276**(23): 20589-96.

Grassmé H, Jendrossek V, Riehle A, von Kurthy G, Berger J, Schwarz H, Weller M, Kolesnick R and Gulbins E (2003b). Host defense against Pseudomonas aeruginosa requires ceramide-rich membrane rafts. *Nat Med* **9**(3): 322-30.

Grassmé H, Riehle A, Wilker B and Gulbins E (2005). Rhinoviruses infect human epithelial cells via ceramide-enriched membrane platforms. *J Biol Chem* **280**(28): 26256-62.

Grassmé H, Riethmuller J and Gulbins E (2007). Biological aspects of ceramide-enriched membrane domains. *Prog Lipid Res* **46**(3-4): 161-70.

Gromak N, West S and Proudfoot NJ (2006). Pause sites promote transcriptional termination of mammalian RNA polymerase II. *Mol Cell Biol* **26**(10): 3986-96.

Gross K and Stablewski A (2013). FAQs about Transgenics. Roswell Park Cancer Institute (RPCI), Buffalo (NY), from http://www.roswellpark.edu/shared-resources/gene-targeting-and-transgenics

Grosveld F, van Assendelft GB, Greaves DR and Kollias G (1987). Position-independent, high-level expression of the human beta-globin gene in transgenic mice. *Cell* **51**(6): 975-85.

Gu H, Marth JD, Orban PC, Mossmann H and Rajewsky K (1994). Deletion of a DNA polymerase beta gene segment in T cells using cell type-specific gene targeting. *Science* **265**(5168): 103-6.

Guhaniyogi J and Brewer G (2001). Regulation of mRNA stability in mammalian cells. *Gene* **265**(1-2): 11-23.

Gulbins E, Dreschers S, Wilker B and Grassmé H (2004). Ceramide, membrane rafts and infections. *J Mol Med (Berl)* **82**(6): 357-63.

Gulbins E, Szabo I, Baltzer K and Lang F (1997). Ceramide-induced inhibition of T lymphocyte voltage-gated potassium channel is mediated by tyrosine kinases. *Proc Natl Acad Sci U S A* **94**(14): 7661-6.

Hannun YA and Obeid LM (2011). Many ceramides. *J Biol Chem* **286**(32): 27855-62.

Haruyama N, Cho A and Kulkarni AB (2009). Overview: engineering transgenic constructs and mice. *Curr Protoc Cell Biol* **Chapter 19**: Unit 19 10.

Hasty P, Rivera-Perez J and Bradley A (1991a). The length of homology required for gene targeting in embryonic stem cells. *Mol Cell Biol* **11**(11): 5586-91.

Hasty P, Rivera-Perez J and Bradley A (1992). The role and fate of DNA ends for homologous recombination in embryonic stem cells. *Mol Cell Biol* **12**(6): 2464-74.

Hasty P, Rivera-Perez J, Chang C and Bradley A (1991b). Target frequency and integration pattern for insertion and replacement vectors in embryonic stem cells. *Mol Cell Biol* **11**(9): 4509-17.

He X, Huang Y, Li B, Gong CX and Schuchman EH (2010). Deregulation of sphingolipid metabolism in Alzheimer's disease. *Neurobiol Aging* **31**(3): 398-408.

He X, Li CM, Park JH, Dagan A, Gatt S and Schuchman EH (1999). A fluorescence-based high-performance liquid chromatographic assay to determine acid ceramidase activity. *Anal Biochem* **274**(2): 264-9.

He X, Okino N, Dhami R, Dagan A, Gatt S, Schulze H, Sandhoff K and Schuchman EH (2003). Purification and characterization of recombinant, human acid ceramidase. Catalytic reactions and interactions with acid sphingomyelinase. *J Biol Chem* **278**(35): 32978-86.

Heinrich M, Wickel M, Schneider-Brachert W, Sandberg C, Gahr J, Schwandner R, Weber T, Saftig P, Peters C, Brunner J, Kronke M and Schutze S (1999). Cathepsin D targeted by acid sphingomyelinase-derived ceramide. *EMBO J* **18**(19): 5252-63.

Henikoff S (1998). Conspiracy of silence among repeated transgenes. *Bioessays* **20**(7): 532-5.

Henry B, Moller C, Dimanche-Boitrel MT, Gulbins E and Becker KA (2013). Targeting the ceramide system in cancer. *Cancer Lett* **332**(2): 286-94.

Hino H, Araki K, Uyama E, Takeya M, Araki M, Yoshinobu K, Miike K, Kawazoe Y, Maeda Y, Uchino M and Yamamura K (2004). Myopathy phenotype in transgenic mice expressing mutated PABPN1 as a model of oculopharyngeal muscular dystrophy. *Hum Mol Genet* **13**(2): 181-90.

Hoekstra D and Kok JW (1992). Trafficking of glycosphingolipids in eukaryotic cells; sorting and recycling of lipids. *Biochim Biophys Acta* **1113**(3-4): 277-94.

Hoess RH, Wierzbicki A and Abremski K (1986). The role of the loxP spacer region in P1 site-specific recombination. *Nucleic Acids Res* **14**(5): 2287-300.

Hoess RH, Ziese M and Sternberg N (1982). P1 site-specific recombination: nucleotide sequence of the recombining sites. *Proc Natl Acad Sci U S A* **79**(11): 3398-402.

Holopainen JM, Subramanian M and Kinnunen PK (1998). Sphingomyelinase induces lipid microdomain formation in a fluid phosphatidylcholine/sphingomyelin membrane. *Biochemistry* **37**(50): 17562-70.

Horinouchi K, Erlich S, Perl DP, Ferlinz K, Bisgaier CL, Sandhoff K, Desnick RJ, Stewart CL and Schuchman EH (1995). Acid sphingomyelinase deficient mice: a model of types A and B Niemann-Pick disease. *Nat Genet* **10**(3): 288-93.

Huang HW, Goldberg EM and Zidovetzki R (1996). Ceramide induces structural defects into phosphatidylcholine bilayers and activates phospholipase A2. *Biochem Biophys Res Commun* **220**(3): 834-8.

Hubner P, Studer E and Luthy J (1999). Quantitation of genetically modified organisms in food. *Nat Biotechnol* **17**(11): 1137-8.

Hui SW and Parsons DF (1975). Direct observation of domains in wet lipid bilayers. *Science* **190**(4212): 383-4.

Hurwitz R, Ferlinz K, Vielhaber G, Moczall H and Sandhoff K (1994). Processing of human acid sphingomyelinase in normal and I-cell fibroblasts. *J Biol Chem* **269**(7): 5440-5.

Huwiler A, Fabbro D and Pfeilschifter J (1998). Selective ceramide binding to protein kinase C-alpha and -delta isoenzymes in renal mesangial cells. *Biochemistry* **37**(41): 14556-62.

Ida-Hosonuma M, Iwasaki T, Taya C, Sato Y, Li J, Nagata N, Yonekawa H and Koike S (2002). Comparison of neuropathogenicity of poliovirus in two transgenic mouse strains expressing human poliovirus receptor with different distribution patterns. *J Gen Virol* **83**(Pt 5): 1095-105.

Ittner LM and Gotz J (2007). Pronuclear injection for the production of transgenic mice. *Nat Protoc* **2**(5): 1206-15.

Jaenisch R and Mintz B (1974). Simian virus 40 DNA sequences in DNA of healthy adult mice derived from preimplantation blastocysts injected with viral DNA. *Proc Natl Acad Sci U S A* **71**(4): 1250-4.

Jain MK and White HB, 3rd (1977). Long-range order in biomembranes. *Adv Lipid Res* **15**: 1-60.

Jan JT, Chatterjee S and Griffin DE (2000). Sindbis virus entry into cells triggers apoptosis by activating sphingomyelinase, leading to the release of ceramide. *J Virol* **74**(14): 6425-32.

Jenkins RW, Idkowiak-Baldys J, Simbari F, Canals D, Roddy P, Riner CD, Clarke CJ and Hannun YA (2011). A novel mechanism of lysosomal acid sphingomyelinase maturation: requirement for carboxyl-terminal proteolytic processing. *J Biol Chem* **286**(5): 3777-88.

Jin S, Zhang Y, Yi F and Li PL (2008). Critical role of lipid raft redox signaling platforms in endostatin-induced coronary endothelial dysfunction. *Arterioscler Thromb Vasc Biol* **28**(3): 485-90.

Kellum R and Schedl P (1992). A group of scs elements function as domain boundaries in an enhancer-blocking assay. *Mol Cell Biol* **12**(5): 2424-31.

Kitatani K, Idkowiak-Baldys J and Hannun YA (2008). The sphingolipid salvage pathway in ceramide metabolism and signaling. *Cell Signal* **20**(6): 1010-8.

Kjer-Nielsen L, Holmberg K, Perera JD and McCluskey J (1992). Impaired expression of chimaeric major histocompatibility complex transgenes associated with plasmid sequences. *Transgenic Res* **1**(4): 182-7.

Klein A, Henseler M, Klein C, Suzuki K, Harzer K and Sandhoff K (1994). Sphingolipid activator protein D (sap-D) stimulates the lysosomal degradation of ceramide in vivo. *Biochem Biophys Res Commun* **200**(3): 1440-8.

Koch J, Gartner S, Li CM, Quintern LE, Bernardo K, Levran O, Schnabel D, Desnick RJ, Schuchman EH and Sandhoff K (1996). Molecular cloning and characterization of a full-length complementary DNA encoding human acid ceramidase. Identification Of the first molecular lesion causing Farber disease. *J Biol Chem* **271**(51): 33110-5.

Kolesnick RN, Goni FM and Alonso A (2000). Compartmentalization of ceramide signaling: physical foundations and biological effects. *J Cell Physiol* **184**(3): 285-300.

Kowluru A and Metz SA (1997). Ceramide-activated protein phosphatase-2A activity in insulin-secreting cells. *FEBS Lett* **418**(1-2): 179-82.

Kuehner JN, Pearson EL and Moore C (2011). Unravelling the means to an end: RNA polymerase II transcription termination. *Nat Rev Mol Cell Biol* **12**(5): 283-94.

Kujjo LL, Acton BM, Perkins GA, Ellisman MH, D'Estaing SG, Casper RF, Jurisicova A and Perez GI (2013). Ceramide and its transport protein (CERT) contribute to deterioration of mitochondrial structure and function in aging oocytes. *Mech Ageing Dev* **134**(1-2): 43-52.

Lacour S, Hammann A, Grazide S, Lagadic-Gossmann D, Athias A, Sergent O, Laurent G, Gambert P, Solary E and Dimanche-Boitrel MT (2004). Cisplatin-induced CD95 redistribution into membrane lipid rafts of HT29 human colon cancer cells. *Cancer Res* **64**(10): 3593-8.

Lang PA, Schenck M, Nicolay JP, Becker JU, Kempe DS, Lupescu A, Koka S, Eisele K, Klarl BA, Rubben H, Schmid KW, Mann K, Hildenbrand S, Hefter H, Huber SM, Wieder T, Erhardt A, Haussinger D, Gulbins E and Lang F (2007). Liver cell death and anemia in Wilson disease involve acid sphingomyelinase and ceramide. *Nat Med* **13**(2): 164-70.

LePage DF and Conlon RA (2006). Animal models for disease: knockout, knock-in, and conditional mutant mice. *Methods Mol Med* **129**: 41-67.

Lepple-Wienhues A, Belka C, Laun T, Jekle A, Walter B, Wieland U, Welz M, Heil L, Kun J, Busch G, Weller M, Bamberg M, Gulbins E and Lang F (1999). Stimulation of CD95 (Fas) blocks T lymphocyte calcium channels through sphingomyelinase and sphingolipids. *Proc Natl Acad Sci U S A* **96**(24): 13795-800.

Lewandoski M (2001). Conditional control of gene expression in the mouse. *Nat Rev Genet* **2**(10): 743-55.

Li CM, Hong SB, Kopal G, He X, Linke T, Hou WS, Koch J, Gatt S, Sandhoff K and Schuchman EH (1998). Cloning and characterization of the full-length cDNA and genomic sequences encoding murine acid ceramidase. *Genomics* **50**(2): 267-74.

Li CM, Park JH, He X, Levy B, Chen F, Arai K, Adler DA, Disteche CM, Koch J, Sandhoff K and Schuchman EH (1999). The human acid ceramidase gene (ASAH): structure, chromosomal location, mutation analysis, and expression. *Genomics* **62**(2): 223-31.

Li CM, Park JH, Simonaro CM, He X, Gordon RE, Friedman AH, Ehleiter D, Paris F, Manova K, Hepbildikler S, Fuks Z, Sandhoff K, Kolesnick R and Schuchman EH (2002). Insertional mutagenesis of the mouse acid ceramidase gene leads to early embryonic lethality in homozygotes and progressive lipid storage disease in heterozygotes. *Genomics* **79**(2): 218-24.

Linke T, Wilkening G, Sadeghlar F, Mozcall H, Bernardo K, Schuchman E and Sandhoff K (2001). Interfacial regulation of acid ceramidase activity. Stimulation of ceramide degradation by lysosomal lipids and sphingolipid activator proteins. *J Biol Chem* **276**(8): 5760-8.

Liu JL, Grinberg A, Westphal H, Sauer B, Accili D, Karas M and LeRoith D (1998). Insulin-like growth factor-I affects perinatal lethality and postnatal development in a gene dosage-dependent manner: manipulation using the Cre/loxP system in transgenic mice. *Mol Endocrinol* **12**(9): 1452-62.

Liu X, Cheng JC, Turner LS, Elojeimy S, Beckham TH, Bielawska A, Keane TE, Hannun YA and Norris JS (2009). Acid ceramidase upregulation in prostate cancer: role in tumor development and implications for therapy. *Expert Opin Ther Targets* **13**(12): 1449-58.

Livak KJ and Schmittgen TD (2001). Analysis of relative gene expression data using real-time quantitative PCR and the 2(-Delta Delta C(T)) Method. *Methods* **25**(4): 402-8.

Lu ZH, Books JT, Kaufman RM and Ley TJ (2003). Long targeting arms do not increase the efficiency of homologous recombination in the beta-globin locus of murine embryonic stem cells. *Blood* **102**(4): 1531-3.

Mahdy AE, Cheng JC, Li J, Elojeimy S, Meacham WD, Turner LS, Bai A, Gault CR, McPherson AS, Garcia N, Beckham TH, Saad A, Bielawska A, Bielawski J, Hannun YA, Keane TE, Taha MI, Hammouda HM, Norris JS and Liu X (2009). Acid ceramidase upregulation in prostate cancer cells confers resistance to radiation: AC inhibition, a potential radiosensitizer. *Mol Ther* **17**(3): 430-8.

Mancini C, Messana E, Turco E, Brussino A and Brusco A (2011). Gene-targeted embryonic stem cells: real-time PCR assay for estimation of the number of neomycin selection cassettes. *Biol Proced Online* **13**: 10.

Mandon EC, Ehses I, Rother J, van Echten G and Sandhoff K (1992). Subcellular localization and membrane topology of serine palmitoyltransferase, 3-dehydrosphinganine reductase, and sphinganine N-acyltransferase in mouse liver. *J Biol Chem* **267**(16): 11144-8.

Mansour SL, Thomas KR and Capecchi MR (1988). Disruption of the proto-oncogene int-2 in mouse embryo-derived stem cells: a general strategy for targeting mutations to non-selectable genes. *Nature* **336**(6197): 348-52.

Marchesini N and Hannun YA (2004). Acid and neutral sphingomyelinases: roles and mechanisms of regulation. *Biochem Cell Biol* **82**(1): 27-44.

Melo EC, Lourtie IM, Sankaram MB, Thompson TE and Vaz WL (1992). Effects of domain connection and disconnection on the yields of in-plane bimolecular reactions in membranes. *Biophys J* **63**(6): 1506-12.

Merrill AH, Jr. and Wang E (1992). Enzymes of ceramide biosynthesis. *Methods Enzymol* **209**: 427-37.

Metzger D and Chambon P (2001). Site- and time-specific gene targeting in the mouse. *Methods* **24**(1): 71-80.

Meyer M, de Angelis MH, Wurst W and Kuhn R (2010). Gene targeting by homologous recombination in mouse zygotes mediated by zinc-finger nucleases. *Proc Natl Acad Sci U S A* **107**(34): 15022-6.

Mitsutake S, Kita K, Okino N and Ito M (1997). [14C]ceramide synthesis by sphingolipid ceramide N-deacylase: new assay for ceramidase activity detection. *Anal Biochem* **247**(1): 52-7.

Momoi T, Ben-Yoseph Y and Nadler HL (1982). Substrate-specificities of acid and alkaline ceramidases in fibroblasts from patients with Farber disease and controls. *Biochem J* **205**(2): 419-25.

Morita Y, Perez GI, Paris F, Miranda SR, Ehleiter D, Haimovitz-Friedman A, Fuks Z, Xie Z, Reed JC, Schuchman EH, Kolesnick RN and Tilly JL (2000). Oocyte apoptosis is suppressed by disruption of the acid sphingomyelinase gene or by sphingosine-1-phosphate therapy. *Nat Med* **6**(10): 1109-14.

Moser H, Moser A and Chen W (1989). The Metabolic Basis of Inherited Disease. Ceramidase deficiency:

Farber lipogranulomatosis. *McGraw-Hill*. New York. Sixth edition

Moyer JH, Lee-Tischler MJ, Kwon HY, Schrick JJ, Avner ED, Sweeney WE, Godfrey VL, Cacheiro NL, Wilkinson JE and Woychik RP (1994). Candidate gene associated with a mutation causing recessive polycystic kidney disease in mice. *Science* **264**(5163): 1329-33.

Muller HJ (1955). Genetic damage produced by radiation. *Science* **121**(3155): 837-40.

Muller U (1999). Ten years of gene targeting: targeted mouse mutants, from vector design to phenotype analysis. *Mech Dev* **82**(1-2): 3-21.

Muskens MW, Vissers AP, Mol JN and Kooter JM (2000). Role of inverted DNA repeats in transcriptional and post-transcriptional gene silencing. *Plant Mol Biol* **43**(2-3): 243-60.

Nagy A, Gertsenstein M and Vintersten K (2003). Manipulating the mouse embryo: a laboratory manual. *Cold Spring Harbor*. New York. Third edition

Nairn RS, Adair GM, Porter T, Pennington SL, Smith DG, Wilson JH and Seidman MM (1993). Targeting vector configuration and method of gene transfer influence targeted correction of the APRT gene in Chinese hamster ovary cells. *Somat Cell Mol Genet* **19**(4): 363-75.

Neumaier M, Braun A and Wagener C (1998). Fundamentals of quality assessment of molecular amplification methods in clinical diagnostics. International Federation of Clinical Chemistry Scientific Division Committee on Molecular Biology Techniques. *Clin Chem* **44**(1): 12-26.

Newrzella D and Stoffel W (1992). Molecular cloning of the acid sphingomyelinase of the mouse and the organization and complete nucleotide sequence of the gene. *Biol Chem Hoppe Seyler* **373**(12): 1233-8.

Newrzella D and Stoffel W (1996). Functional analysis of the glycosylation of murine acid sphingomyelinase. *J Biol Chem* **271**(50): 32089-95.

Nguyen NM, Kelley DG, Schlueter JA, Meyer MJ, Senior RM and Miner JH (2005). Epithelial laminin alpha5 is necessary for distal epithelial cell maturation, VEGF production, and alveolization in the developing murine lung. *Dev Biol* **282**(1): 111-25.

Nickoloff JA (1992). Transcription enhances intrachromosomal homologous recombination in mammalian cells. *Mol Cell Biol* **12**(12): 5311-8.

Niemann A (1914). Ein unbekanntes Krankheitsbild. *Jahrb. Kinderheilkd.* **79**: 1-10.

Nitschke L, Kopf M and Lamers MC (1993). Quick nested PCR screening of ES cell clones for gene targeting events. *Biotechniques* **14**(6): 914-6.

Niwa H, Yamamura K and Miyazaki J (1991). Efficient selection for high-expression transfectants with a novel eukaryotic vector. *Gene* **108**(2): 193-9.

Okabe M, Ikawa M, Kominami K, Nakanishi T and Nishimune Y (1997). 'Green mice' as a source of ubiquitous green cells. *FEBS Lett* **407**(3): 313-9.

Okino N, He X, Gatt S, Sandhoff K, Ito M and Schuchman EH (2003). The reverse activity of human acid ceramidase. *J Biol Chem* **278**(32): 29948-53.

Orban PC, Chui D and Marth JD (1992). Tissue- and site-specific DNA recombination in transgenic mice. *Proc Natl Acad Sci U S A* **89**(15): 6861-5.

Palmiter RD, Behringer RR, Quaife CJ, Maxwell F, Maxwell IH and Brinster RL (1987). Cell lineage ablation in transgenic mice by cell-specific expression of a toxin gene. *Cell* **50**(3): 435-43.

Palmiter RD and Brinster RL (1986). Germ-line transformation of mice. *Annu Rev Genet* **20**: 465-99.

Park JH and Schuchman EH (2006). Acid ceramidase and human disease. *Biochim Biophys Acta* **1758**(12): 2133-8.

Perez GI, Jurisicova A, Matikainen T, Moriyama T, Kim MR, Takai Y, Pru JK, Kolesnick RN and Tilly JL (2005). A central role for ceramide in the age-related acceleration of apoptosis in the female germline. *FASEB J* **19**(7): 860-2.

Perrotta C, Bizzozero L, Cazzato D, Morlacchi S, Assi E, Simbari F, Zhang Y, Gulbins E, Bassi MT, Rosa P and Clementi E (2010). Syntaxin 4 is required for acid sphingomyelinase activity and apoptotic function. *J Biol Chem* **285**(51): 40240-51.

Pravtcheva DD and Wise TL (1995). A postimplantation lethal mutation induced by transgene insertion on mouse chromosome 8. *Genomics* **30**(3): 529-44.

Pravtcheva DD and Wise TL (2003). Transgene instability in mice injected with an in vitro methylated Igf2 gene. *Mutat Res* **529**(1-2): 35-50.

Quintern LE, Weitz G, Nehrkorn H, Tager JM, Schram AW and Sandhoff K (1987). Acid sphingomyelinase from human urine: purification and characterization. *Biochim Biophys Acta* **922**(3): 323-36.

Rajewsky K, Gu H, Kuhn R, Betz UA, Muller W, Roes J and Schwenk F (1996). Conditional gene targeting. *J Clin Invest* **98**(3): 600-3.

Recillas-Targa F, Pikaart MJ, Burgess-Beusse B, Bell AC, Litt MD, West AG, Gaszner M and Felsenfeld G (2002). Position-effect protection and enhancer blocking by the chicken beta-globin insulator are separable activities. *Proc Natl Acad Sci U S A* **99**(10): 6883-8.

Reichel MT, S. (1940). Studies on Animal lipids. *J. Biol. Chem.* **135**: 1-13.

Renart J, Reiser J and Stark GR (1979). Transfer of proteins from gels to diazobenzyloxymethyl-paper and detection with antisera: a method for studying antibody specificity and antigen structure. *Proc Natl Acad Sci U S A* **76**(7): 3116-20.

Revie D, Smith DW and Yee TW (1988). Kinetic analysis for optimization of DNA ligation reactions. *Nucleic Acids Res* **16**(21): 10301-21.

Riethmuller J, Anthonysamy J, Serra E, Schwab M, Doring G and Gulbins E (2009). Therapeutic efficacy and safety of amitriptyline in patients with cystic fibrosis. *Cell Physiol Biochem* **24**(1-2): 65-72.

Rolig RL, Layher SK, Santi B, Adair GM, Gu F, Rainbow AJ and Nairn RS (1997). Survival, mutagenesis, and host cell reactivation in a Chinese hamster ovary cell ERCC1 knock-out mutant. *Mutagenesis* **12**(4): 277-83.

Romiti E, Meacci E, Tani M, Nuti F, Farnararo M, Ito M and Bruni P (2000). Neutral/alkaline and acid ceramidase activities are actively released by murine endothelial cells. *Biochem Biophys Res Commun* **275**(3): 746-51.

Rotolo JA, Zhang J, Donepudi M, Lee H, Fuks Z and Kolesnick R (2005). Caspase-dependent and -independent activation of acid sphingomyelinase signaling. *J Biol Chem* **280**(28): 26425-34.

Rouet P, Smih F and Jasin M (1994). Expression of a site-specific endonuclease stimulates homologous recombination in mammalian cells. *Proc Natl Acad Sci U S A* **91**(13): 6064-8.

Ruiz-Arguello MB, Basanez G, Goni FM and Alonso A (1996). Different effects of enzyme-generated ceramides and diacylglycerols in phospholipid membrane fusion and leakage. *J Biol Chem* **271**(43): 26616-21.

Saad AF, Meacham WD, Bai A, Anelli V, Elojeimy S, Mahdy AE, Turner LS, Cheng J, Bielawska A, Bielawski J, Keane TE, Obeid LM, Hannun YA, Norris JS and Liu X (2007). The functional effects of acid ceramidase overexpression in prostate cancer progression and resistance to chemotherapy. *Cancer Biol Ther* **6**(9): 1455-60.

Scheel-Toellner D, Wang K, Craddock R, Webb PR, McGettrick HM, Assi LK, Parkes N, Clough LE, Gulbins E, Salmon M and Lord JM (2004). Reactive oxygen species limit neutrophil life span by activating death receptor signaling. *Blood* **104**(8): 2557-64.

Schissel SL, Keesler GA, Schuchman EH, Williams KJ and Tabas I (1998). The cellular trafficking and zinc dependence of secretory and lysosomal sphingomyelinase, two products of the acid sphingomyelinase gene. *J Biol Chem* **273**(29): 18250-9.

Schneider CA, Rasband WS and Eliceiri KW (2012). NIH Image to ImageJ: 25 years of image analysis. *Nat Methods* **9**(7): 671-5.

Schuchman EH (2007). The pathogenesis and treatment of acid sphingomyelinase-deficient Niemann-Pick disease. *J Inherit Metab Dis* **30**(5): 654-63.

Schuchman EH, Levran O, Pereira LV and Desnick RJ (1992). Structural organization and complete nucleotide sequence of the gene encoding human acid sphingomyelinase (SMPD1). *Genomics* **12**(2): 197-205.

Schuchman EH and Miranda SR (1997). Niemann-Pick disease: mutation update, genotype/phenotype correlations, and prospects for genetic testing. *Genet Test* **1**(1): 13-9.

Scrable H and Stambrook PJ (1999). A genetic program for deletion of foreign DNA from the mammalian genome. *Mutat Res* **429**(2): 225-37.

Seelan RS, Qian C, Yokomizo A, Bostwick DG, Smith DI and Liu W (2000). Human acid ceramidase is overexpressed but not mutated in prostate cancer. *Genes Chromosomes Cancer* **29**(2): 137-46.

Seino K, Kayagaki N, Takeda K, Fukao K, Okumura K and Yagita H (1997). Contribution of Fas ligand to T cell-mediated hepatic injury in mice. *Gastroenterology* **113**(4): 1315-22.

Shah J, Atienza JM, Rawlings AV and Shipley GG (1995). Physical properties of ceramides: effect of fatty acid hydroxylation. *J Lipid Res* **36**(9): 1945-55.

Shtraizent N, Eliyahu E, Park JH, He X, Shalgi R and Schuchman EH (2008). Autoproteolytic cleavage and activation of human acid ceramidase. *J Biol Chem* **283**(17): 11253-9.

Shulman MJ, Nissen L and Collins C (1990). Homologous recombination in hybridoma cells: dependence on time and fragment length. *Mol Cell Biol* **10**(9): 4466-72.

Simonaro CM, Desnick RJ, McGovern MM, Wasserstein MP and Schuchman EH (2002). The demographics and distribution of type B Niemann-Pick disease: novel mutations lead to new genotype/phenotype correlations. *Am J Hum Genet* **71**(6): 1413-9.

Simons K and Ikonen E (1997). Functional rafts in cell membranes. *Nature* **387**(6633): 569-72.

Singer SJ and Nicolson GL (1972). The fluid mosaic model of the structure of cell membranes. *Science* **175**(4023): 720-31.

Siskind LJ and Colombini M (2000). The lipids C2- and C16-ceramide form large stable channels. Implications for apoptosis. *J Biol Chem* **275**(49): 38640-4.

Skarnes WC, Rosen B, West AP, Koutsourakis M, Bushell W, Iyer V, Mujica AO, Thomas M, Harrow J, Cox T, Jackson D, Severin J, Biggs P, Fu J, Nefedov M, de Jong PJ, Stewart AF and Bradley A (2011). A conditional knockout resource for the genome-wide study of mouse gene function. *Nature* **474**(7351): 337-42.

Southern EM (1975). Detection of specific sequences among DNA fragments separated by gel electrophoresis. *J Mol Biol* **98**(3): 503-17.

Strausberg RL, Feingold EA, Klausner RD and Collins FS (1999). The mammalian gene collection. *Science* **286**(5439): 455-7.

Sugita M, Dulaney JT and Moser HW (1972). Ceramidase deficiency in Farber's disease (lipogranulomatosis). *Science* **178**(4065): 1100-2.

Sun FL and Elgin SC (1999). Putting boundaries on silence. *Cell* **99**(5): 459-62.

Swift GH, Hammer RE, MacDonald RJ and Brinster RL (1984). Tissue-specific expression of the rat pancreatic elastase I gene in transgenic mice. *Cell* **38**(3): 639-46.

Szabo I, Adams C and Gulbins E (2004). Ion channels and membrane rafts in apoptosis. *Pflugers Arch* **448**(3): 304-12.

Szatmari T, Lumniczky K, Desaknai S, Trajcevski S, Hidvegi EJ, Hamada H and Safrany G (2006). Detailed characterization of the mouse glioma 261 tumor model for experimental glioblastoma therapy. *Cancer Sci* **97**(6): 546-53.

Tani M, Kita K, Komori H, Nakagawa T and Ito M (1998). Enzymatic synthesis of omega-amino-ceramide: preparation of a sensitive fluorescent substrate for ceramidase. *Anal Biochem* **263**(2): 183-8.

te Riele H, Maandag ER and Berns A (1992). Highly efficient gene targeting in embryonic stem cells through homologous recombination with isogenic DNA constructs. *Proc Natl Acad Sci U S A* **89**(11): 5128-32.

Teboul L (2009). Transgene design and delivery into the mouse genome: keys to success. *Methods Mol Biol* **561**: 105-10.

Teichgraber V, Ulrich M, Endlich N, Riethmuller J, Wilker B, De Oliveira-Munding CC, van Heeckeren AM, Barr ML, von Kurthy G, Schmid KW, Weller M, Tummler B, Lang F, Grassmé H, Doring G and Gulbins E (2008). Ceramide accumulation mediates inflammation, cell death and infection susceptibility in cystic fibrosis. *Nat Med* **14**(4): 382-91.

Tesson L, Heslan JM, Menoret S and Anegon I (2002). Rapid and accurate determination of zygosity in transgenic animals by real-time quantitative PCR. *Transgenic Res* **11**(1): 43-8.

Thomas KR and Capecchi MR (1987). Site-directed mutagenesis by gene targeting in mouse embryo-derived stem cells. *Cell* **51**(3): 503-12.

Thompson TE, Sankaram MB, Biltonen RL, Marsh D and Vaz WL (1995). Effects of domain structure on in-plane reactions and interactions. *Mol Membr Biol* **12**(1): 157-62.

Tompers DM and Labosky PA (2004). Electroporation of murine embryonic stem cells: a step-by-step guide. *Stem Cells* **22**(3): 243-9.

Truman JP, Garcia-Barros M, Kaag M, Hambardzumyan D, Stancevic B, Chan M, Fuks Z, Kolesnick R and Haimovitz-Friedman A (2010). Endothelial membrane remodeling is obligate for anti-angiogenic radiosensitization during tumor radiosurgery. *PLoS One* **5**(8): e12310.

Urnov FD, Miller JC, Lee YL, Beausejour CM, Rock JM, Augustus S, Jamieson AC, Porteus MH, Gregory PD and Holmes MC (2005). Highly efficient endogenous human gene correction using designed zinc-finger nucleases. *Nature* **435**(7042): 646-51.

Vasquez KM, Marburger K, Intody Z and Wilson JH (2001). Manipulating the mammalian genome by homologous recombination. *Proc Natl Acad Sci U S A* **98**(15): 8403-10.

Veiga MP, Arrondo JL, Goni FM and Alonso A (1999). Ceramides in phospholipid membranes: effects on bilayer stability and transition to nonlamellar phases. *Biophys J* **76**(1 Pt 1): 342-50.

Venter JC, Adams MD, Myers EW, Li PW, Mural RJ, Sutton GG, Smith HO, Yandell M, Evans CA, Holt RA, Gocayne JD, Amanatides P, Ballew RM, Huson DH, Wortman JR, Zhang Q, Kodira CD, Zheng XH, Chen L, Skupski M, Subramanian G, Thomas PD, Zhang J, Gabor Miklos GL, Nelson C, Broder S, Clark AG, Nadeau J, McKusick VA, Zinder N, Levine AJ, Roberts RJ, Simon M, Slayman C, Hunkapiller M, Bolanos R, Delcher A, Dew I, Fasulo D, Flanigan M, Florea L, Halpern A, Hannenhalli S, Kravitz S, Levy S, Mobarry C, Reinert K, Remington K, Abu-Threideh J, Beasley E, Biddick K, Bonazzi V, Brandon R, Cargill M, Chandramouliswaran I, Charlab R, Chaturvedi K, Deng Z, Di Francesco V, Dunn P, Eilbeck K, Evangelista C, Gabrielian AE, Gan W, Ge W, Gong F, Gu Z, Guan P, Heiman TJ, Higgins ME, Ji RR, Ke Z, Ketchum KA, Lai Z, Lei Y, Li Z, Li J, Liang Y, Lin X, Lu F, Merkulov GV, Milshina N, Moore HM, Naik AK, Narayan VA, Neelam B, Nusskern D, Rusch DB, Salzberg S, Shao W, Shue B, Sun J, Wang Z, Wang A, Wang X, Wang J, Wei M, Wides R, Xiao C, Yan C, Yao A, Ye J, Zhan M, Zhang W, Zhang H, Zhao Q, Zheng L, Zhong F, Zhong W, Zhu S, Zhao S, Gilbert D, Baumhueter S, Spier G, Carter C, Cravchik A, Woodage T, Ali F, An H, Awe A, Baldwin D, Baden H, Barnstead M, Barrow I, Beeson K, Busam D, Carver A, Center A, Cheng ML, Curry L, Danaher S, Davenport L, Desilets R, Dietz S, Dodson K, Doup L, Ferriera S, Garg N, Gluecksmann A, Hart B,

Haynes J, Haynes C, Heiner C, Hladun S, Hostin D, Houck J, Howland T, Ibegwam C, Johnson J, Kalush F, Kline L, Koduru S, Love A, Mann F, May D, McCawley S, McIntosh T, McMullen I, Moy M, Moy L, Murphy B, Nelson K, Pfannkoch C, Pratts E, Puri V, Qureshi H, Reardon M, Rodriguez R, Rogers YH, Romblad D, Ruhfel B, Scott R, Sitter C, Smallwood M, Stewart E, Strong R, Suh E, Thomas R, Tint NN, Tse S, Vech C, Wang G, Wetter J, Williams S, Williams M, Windsor S, Winn-Deen E, Wolfe K, Zaveri J, Zaveri K, Abril JF, Guigo R, Campbell MJ, Sjolander KV, Karlak B, Kejariwal A, Mi H, Lazareva B, Hatton T, Narechania A, Diemer K, Muruganujan A, Guo N, Sato S, Bafna V, Istrail S, Lippert R, Schwartz R, Walenz B, Yooseph S, Allen D, Basu A, Baxendale J, Blick L, Caminha M, Carnes-Stine J, Caulk P, Chiang YH, Coyne M, Dahlke C, Mays A, Dombroski M, Donnelly M, Ely D, Esparham S, Fosler C, Gire H, Glanowski S, Glasser K, Glodek A, Gorokhov M, Graham K, Gropman B, Harris M, Heil J, Henderson S, Hoover J, Jennings D, Jordan C, Jordan J, Kasha J, Kagan L, Kraft C, Levitsky A, Lewis M, Liu X, Lopez J, Ma D, Majoros W, McDaniel J, Murphy S, Newman M, Nguyen T, Nguyen N, Nodell M, Pan S, Peck J, Peterson M, Rowe W, Sanders R, Scott J, Simpson M, Smith T, Sprague A, Stockwell T, Turner R, Venter E, Wang M, Wen M, Wu D, Wu M, Xia A, Zandieh A and Zhu X (2001). The sequence of the human genome. *Science* **291**(5507): 1304-51.

Vooijs M, van der Valk M, te Riele H and Berns A (1998). Flp-mediated tissue-specific inactivation of the retinoblastoma tumor suppressor gene in the mouse. *Oncogene* **17**(1): 1-12.

Wagner EF, Covarrubias L, Stewart TA and Mintz B (1983). Prenatal lethalities in mice homozygous for human growth hormone gene sequences integrated in the germ line. *Cell* **35**(3 Pt 2): 647-55.

Wang X, Ikeguchi Y, McCloskey DE, Nelson P and Pegg AE (2004). Spermine synthesis is required for normal viability, growth, and fertility in the mouse. *J Biol Chem* **279**(49): 51370-5.

Waterston RH, Lindblad-Toh K, Birney E, Rogers J, Abril JF, Agarwal P, Agarwala R, Ainscough R, Alexandersson M, An P, Antonarakis SE, Attwood J, Baertsch R, Bailey J, Barlow K, Beck S, Berry E, Birren B, Bloom T, Bork P, Botcherby M, Bray N, Brent MR, Brown DG, Brown SD, Bult C, Burton J, Butler J, Campbell RD, Carninci P, Cawley S, Chiaromonte F, Chinwalla AT, Church DM, Clamp M, Clee C, Collins FS, Cook LL, Copley RR, Coulson A, Couronne O, Cuff J, Curwen V, Cutts T, Daly M, David R, Davies J, Delehaunty KD, Deri J, Dermitzakis ET, Dewey C, Dickens NJ, Diekhans M, Dodge S, Dubchak I, Dunn DM, Eddy SR, Elnitski L, Emes RD, Eswara P, Eyras E, Felsenfeld A, Fewell GA, Flicek P, Foley K, Frankel WN, Fulton LA, Fulton RS, Furey TS, Gage D, Gibbs RA, Glusman G, Gnerre S, Goldman N, Goodstadt L, Grafham D, Graves TA, Green ED, Gregory S, Guigo R, Guyer M, Hardison RC, Haussler D, Hayashizaki Y, Hillier LW, Hinrichs A, Hlavina W, Holzer T, Hsu F, Hua A, Hubbard T, Hunt A, Jackson I, Jaffe DB, Johnson LS, Jones M, Jones TA, Joy A, Kamal M, Karlsson EK, Karolchik D, Kasprzyk A, Kawai J, Keibler E, Kells C, Kent WJ, Kirby A, Kolbe DL, Korf I, Kucherlapati RS, Kulbokas EJ, Kulp D, Landers T, Leger JP, Leonard S, Letunic I, Levine R, Li J, Li M, Lloyd C, Lucas S, Ma B, Maglott DR, Mardis ER, Matthews L, Mauceli E, Mayer JH, McCarthy M, McCombie WR, McLaren S, McLay K, McPherson JD, Meldrim J, Meredith B, Mesirov JP, Miller W, Miner TL, Mongin E, Montgomery KT, Morgan M, Mott R, Mullikin JC, Muzny DM, Nash WE, Nelson JO, Nhan MN, Nicol R, Ning Z, Nusbaum C, O'Connor MJ, Okazaki Y, Oliver K, Overton-Larty E, Pachter L, Parra G, Pepin KH, Peterson J, Pevzner P, Plumb R, Pohl CS, Poliakov A, Ponce TC, Ponting CP, Potter S, Quail M, Reymond A, Roe BA,

Roskin KM, Rubin EM, Rust AG, Santos R, Sapojnikov V, Schultz B, Schultz J, Schwartz MS, Schwartz S, Scott C, Seaman S, Searle S, Sharpe T, Sheridan A, Shownkeen R, Sims S, Singer JB, Slater G, Smit A, Smith DR, Spencer B, Stabenau A, Stange-Thomann N, Sugnet C, Suyama M, Tesler G, Thompson J, Torrents D, Trevaskis E, Tromp J, Ucla C, Ureta-Vidal A, Vinson JP, Von Niederhausern AC, Wade CM, Wall M, Weber RJ, Weiss RB, Wendl MC, West AP, Wetterstrand K, Wheeler R, Whelan S, Wierzbowski J, Willey D, Williams S, Wilson RK, Winter E, Worley KC, Wyman D, Yang S, Yang SP, Zdobnov EM, Zody MC and Lander ES (2002). Initial sequencing and comparative analysis of the mouse genome. *Nature* **420**(6915): 520-62.

West AG, Gaszner M and Felsenfeld G (2002). Insulators: many functions, many mechanisms. *Genes Dev* **16**(3): 271-88.

Wienholds E, van Eeden F, Kosters M, Mudde J, Plasterk RH and Cuppen E (2003). Efficient target-selected mutagenesis in zebrafish. *Genome Res* **13**(12): 2700-7.

Williams RD, Wang E and Merrill AH, Jr. (1984). Enzymology of long-chain base synthesis by liver: characterization of serine palmitoyltransferase in rat liver microsomes. *Arch Biochem Biophys* **228**(1): 282-91.

Wunderlich F, Kreutz W, Mahler P, Ronai A and Heppeler G (1978). Thermotropic fluid goes to ordered "discontinuous" phase separation in microsomal lipids of Tetrahymena. An X-ray diffraction study. *Biochemistry* **17**(10): 2005-10.

Xu ZL, Mizuguchi H, Ishii-Watabe A, Uchida E, Mayumi T and Hayakawa T (2001). Optimization of transcriptional regulatory elements for constructing plasmid vectors. *Gene* **272**(1-2): 149-56.

Yagi T, Ikawa Y, Yoshida K, Shigetani Y, Takeda N, Mabuchi I, Yamamoto T and Aizawa S (1990). Homologous recombination at c-fyn locus of mouse embryonic stem cells with use of diphtheria toxin A-fragment gene in negative selection. *Proc Natl Acad Sci U S A* **87**(24): 9918-22.

Yanagawa Y, Kobayashi T, Ohnishi M, Tamura S, Tsuzuki T, Sanbo M, Yagi T, Tashiro F and Miyazaki J (1999). Enrichment and efficient screening of ES cells containing a targeted mutation: the use of DT-A gene with the polyadenylation signal as a negative selection maker. *Transgenic Res* **8**(3): 215-21.

Yanez RJ and Porter AC (1999). Influence of DNA delivery method on gene targeting frequencies in human cells. *Somat Cell Mol Genet* **25**(1): 27-31.

Zeidan YH and Hannun YA (2007). Activation of acid sphingomyelinase by protein kinase Cdelta-mediated phosphorylation. *J Biol Chem* **282**(15): 11549-61.

Zhang AY, Yi F, Zhang G, Gulbins E and Li PL (2006). Lipid raft clustering and redox signaling platform formation in coronary arterial endothelial cells. *Hypertension* **47**(1): 74-80.

Zhang Y, Li X, Carpinteiro A and Gulbins E (2008). Acid sphingomyelinase amplifies redox signaling in Pseudomonas aeruginosa-induced macrophage apoptosis. *J Immunol* **181**(6): 4247-54.

Zhang Y, Yao B, Delikat S, Bayoumy S, Lin XH, Basu S, McGinley M, Chan-Hui PY, Lichenstein H and Kolesnick R (1997). Kinase suppressor of Ras is ceramide-activated protein kinase. *Cell* **89**(1): 63-72.

Zhang Z, Mandal AK, Mital A, Popescu N, Zimonjic D, Moser A, Moser H and Mukherjee AB (2000). Human acid ceramidase gene: novel mutations in Farber disease. *Mol Genet Metab* **70**(4): 301-9.

Zhao K, Hart CM and Laemmli UK (1995). Visualization of chromosomal domains with boundary element-associated factor BEAF-32. *Cell* **81**(6): 879-89.

Zon LI, Dorfman DM and Orkin SH (1989). The polymerase chain reaction colony miniprep. *Biotechniques* **7**(7): 696-8.

9. APPENDIX

9.1 Oxidation and β-elimination step of the AC activity assay

Conversion of RBM14-12 by AC was stopped by the addition of methanol. Subsequently, $NaIO_4$ fresh solution in an alkaline buffer, pH 10.6, was added. The enzyme reaction product undergoes oxidation and β-elimination and the fluorophore, umbelliferone, is generated. The umbelliferone production by β-elemination of the oxidized product was investigated. To this end, kidney (high AC activity, (Li *et al.* 1998)), liver (intermediate AC activity, (Li *et al.* 1998)), and testicle (low AC activity, (Li *et al.* 1998)) tissue of wild type animals was lysed. Protein samples (10, 30, and 50 µg protein of each tissue) were incubated with RBM14-12 at pH 4.5 for 2 hours. After the addition of methanol, the samples were immidiately put into the fluorescence microplate reader and fluorescence (excitation 360 nm, emission 446 nm) quantified every 2 minutes for 1 hour (see figure 9.1).

Fluorescence production during the oxidation and β-elimination step reaches a plateau after 1 hour. When performing the AC activity assay, reaction plates were left in the dark for 2 hours to ensure that the total of enzyme reaction product undergoes oxidation and β-elimination.

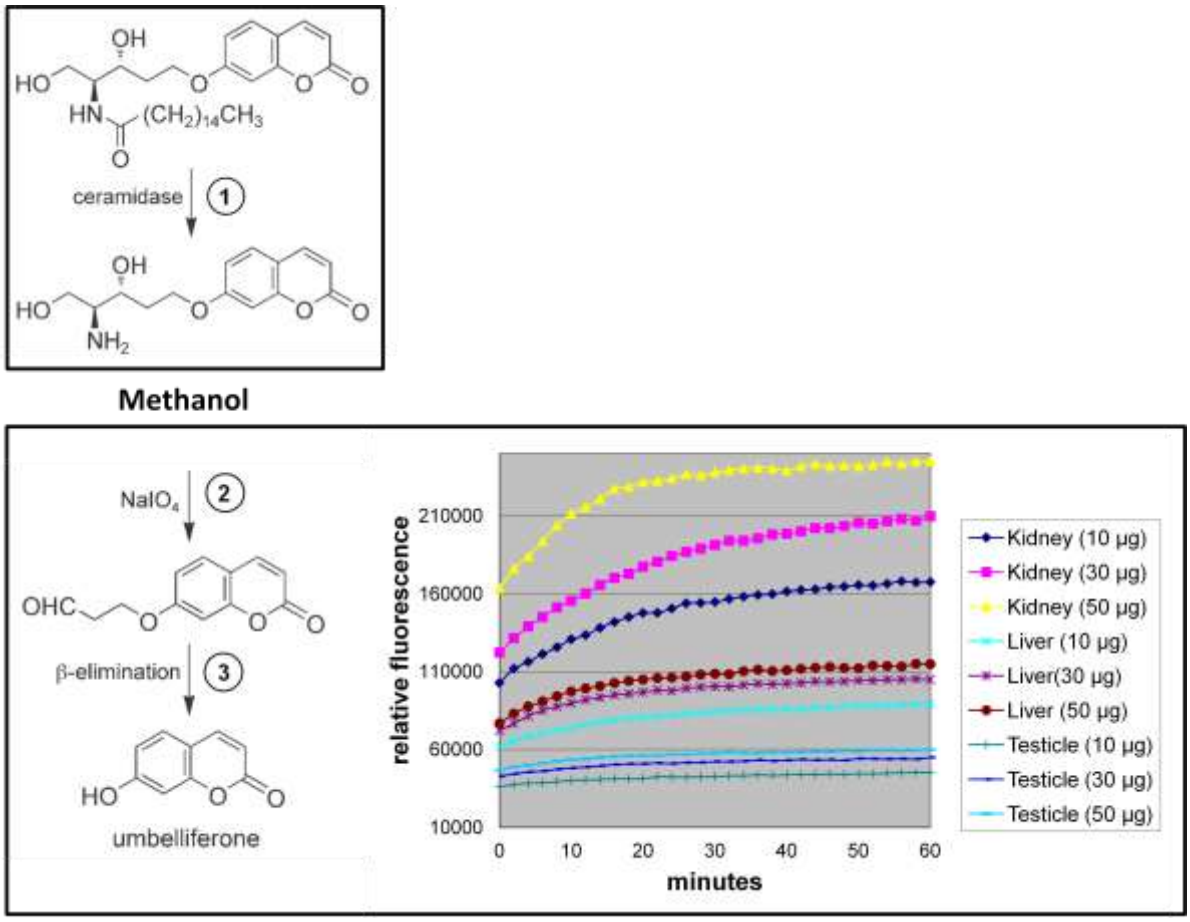

Figure 9.1: Oxidation and β-elimination of RBM14-12. Acid ceramidase cleaves the RBM14-12 substrate. The enzyme reactions were stopped by addition of methanol after 2 hours. The remaining aminodiol of the sphingoid base is oxidized in an alkaline buffer containing $NaIO_4$ and the fluorophore, umbelliferone, is generated by β-elemination of the oxidized product. Protein samples (10, 30, and 50 µg) of kidney, liver and testicle were incubated with RBM14-12 for 2 hours at pH 4.5 and 37°C. After the addition of methanol, the samples were immidiately put into the fluorescence microplate reader and fluorescence (excitation 360 nm, emission 446 nm) quantified every 2 minutes for 1 hour. Fluorescence was quantified with a fluorescence microplate reader using an excitation of 360 nm and an emission of 446 nm. The RBM14-12 conversion scheme was adapted from (Bedia et al. 2007), copyright 2007, with permission from WILEY-VCH Verlag GmbH & Co. KGaA, Weinheim.

9.2 Sequence of the CAG-Asah1 transgene cassette

Legend: The DNA sequence is colored analogous to the following DNA features

bGH-polyA
SCS insulator
CAG-promoter
Asah1 cDNA
hGH-polyA
other

> CAG-Asah1, 281 bp (AscI) – 7554 bp (PmeI), direct, 7274 bp total

cgcgccggatcagcctcgactgtgccttctagttgccagccatctgttgtttgcccctccccgtgccttccttgaccctggaaggtgcc
actcccactgtcctttcctaataaaatgaggaaattgcatcgcattgtctgagtaggtgtcattctattctgggggtggggtggggca
ggacagcaagggggaggattgggaagacaatagcaggcatgctggggatgcggtgggctctatggcttctgaggcggaaagaacc
agctggggctcgactgtttggtcgccatgttgtccagtccatggacgtgggcatgcttgttgtagcccaaatcggcgtttccgtttccac
caggaaacatctctgcttgtagttcgaatatgctctttaaatcccagctgtattcctcagttatcgaggttttcttcacgagtgaaacga
attttcgtcgccttctacgccattttcttgctcagcccgttttgtcattcgcagcgaagcggtaacagcgggtcgctcatatgacggtatt
tttttaatacacttcagctatactgttatttcaaaaacatatttcttttgttacttttttatgcagttcatttgccaccaaaaagtagtctttt
ggattgatttatttctaaaaatggtgtaattcaagaaattcagagggccaagtaatatacttaatgaccgttatttaaaacacactca
aggagatttatttaaacggctacaatggttttccaaataacttatttactgttgacttctataaaacataggtgtatatattattatttctt
attgatttgagataattttaatttccacaatatttttttcttgtgattaacagagaaagtcaaactcataacatttatcgggtaaaagtctc
tatgaagtagcggttaacagtgaagtcacaaaagtgtggccgtacgccaatcgagcgagtatccctaacctgcaatatttttagttgg
ttttttcagcaatagccccacttttctcaaagagtgcaacaagtgattctgtttatgttttcaacaacttctctctgcggaacttgacgtg
agcggacgtatgcggacgcgtcgctgccggaaaaataagttgcgtcggcgttgcggcgttgttgtttacgtgttataataaatttgtgt
gcgtgcgagaagggcgcgctcctgtctgtgttggtgttattgtcggtcgttctcagcgcgagttttgaaataccgcattgtttaattaca
gccgccgcgactaatttcaatacaaacaaaagctggtgtgtgaatgaaattatgctaaaatagataatagttaaaggtaaaagaaa
ttaaaagatgaagaaggagaagaggaagagaagttctgcagcgcagttgcgtcggcgcagcagcgtttctatcggtgtgtgtctga
gtctgtctgtagtggtttgtctagttttttttcgggctgtgtgtgttcgtgtttgccaagcaacaatttaattgctattcaattttaaaagca
gttcaattgcaaaccattacaaatatgtaatttgctgtcgattgcttttgcactggaggactctagagcttaaggtgcacggcccacga
cattgattattgactagttattaatagtaatcaattacggggtcattagttcatagcccatatatggagttccgcgttacataacttacg
gtaaatggcccgcctggctgaccgcccaacgacccccgcccattgacgtcaataatgacgtatgttcccatagtaacgccaatagggg
actttccattgacgtcaatgggtggactatttacggtaaactgcccacttggcagtacatcaagtgtatcatatgccaagtacgccccc
tattgacgtcaatgacggtaaatggcccgcctggcattatgcccagtacatgaccttatgggactttcctacttggcagtacatctacg
tattagtcatcgctattaccatgggtcgaggtgagccccacgttctgcttcactctccccatctccccccccctccccacccccaattttgt
atttatttatttttaattattttgtgcagcgatgggggcgggggggggggggcgcgcgccaggcggggcggggcggggcgagggg
cggggcggggcgaggcggagaggtgcggcggcagccaatcagagcggcgcgctccgaaagtttccttttatggcgaggcggcggc
ggcggcggccctataaaaagcgaagcgcgcggcgggcgggagtcgctgcgttgccttcgccccgtgccccgctccgcgccgcctcg
cgccgcccgccccggctctgactgaccgcgttactcccacaggtgagcgggcgggacggcccttctcctccgggctgtaattagcgct
tggtttaatgacggctcgtttctttttctgtggctgcgtgaaagccttaaagggctccgggagggccctttgtgcgggggggagcggctc
ggggggtgcgtgcgtgtgtgtgtgcgtggggagcgccgcgtgcggcccgcgctgcccggcggctgtgagcgctgcgggcgcggcgc
ggggctttgtgcgctccgcgtgtgcgcgaggggagcgcggccgggggcggtgccccgcggtgcgggggggctgcgaggggaacaa
aggctgcgtgcggggtgtgtgcgtgggggggtgagcaggggggtgtgggcgcggcggtcgggctgtaacccccccctgcaccccccct
ccccgagttgctgagcacggcccggcttcgggtgcggggctccgtgcggggcgtggcgcggggctcgccgtgccgggcgggggggtg

gcggcaggtgggggtgccgggcggggcggggccgcctcgggccggggagggctcgggggaggggcgcggcggccccggagcgc
cggcggctgtcgaggcgcggcgagccgcagccattgccttttatggtaatcgtgcgagagggcgcagggacttcctttgtcccaaatc
tggcggagccgaaatctgggaggcgccgccgcaccccctctagcgggcgcgggcgaagcggtgcggcgccggcaggaaggaaat
gggcggggagggccttcgtgcgtcgccgcgccgccgtcccctttctccatctccagcctcggggctgtccgcgggggacggctgccttc
gggggggacggggcagggcggggttcggcttctggcgtgtgaccggcggctctagagcctctgctaaccatgttcatgccttcttctttt
ttcctacagctcctgggcaacgtgctggttattgtgctgtctcatcattttggcaaagaattagcttggccggccgccaccatgcgggg
ccaaagtcttctcacctgggtcctagccgcggcagtcacctgcgcccaggcacaggatgtgccgccgtggacagaagattgcagaa
aatcaacttatcctccttctggaccaacctatagaggaccagttccgtggcacaccataaatcttgatttaccaccctacaaaagatg
gcatgaattattggctcaaaaggcaccagcgttgaggattttagtgaattccataacgagtttagtgaatacatttgtgccaagtgga
aaactaatgaagatggtggatcaaaagctgcctggtatgattggcagccttcctgacccttttggagaggaaatgaggggaattgca
gatgttactgggattcctctaggagagattatttcattcaacattttctatgaattgtttaccatgtgtacatcaatcataactgaagatg
agaaaggtcatttactacatgggagaaacatggattttggaatatttcttgggtggaatataaataataacacttgggttgtcacaga
agaattaaagcccttaacagtgaatttggacttccaaagaaacaataagactgttttcaaggctacaagttttgttggatatgtgggc
atgttgacaggattcaaaccaggactgttcagtctttcactaaatgaacgtttcagtataaatggtggttatctgggtatcctagaatg
gatgttcggaaggaaagatgcccagtgggtagggtttatcactcgatcagttctggaaaacaccacaagttatgaagaagccaaga
acacactgaccaagaccaagataatggcgccagtatattttatcctgggaggcaagaagtctggagagggttgtgtgatcacacgg
gaaagaaaagagtctttggatgtctatgaacttgatcctaagcatggcagatggtatgtggtacaaaccaattatgacaggtggaaa
aacaccttgtttattgatgaccgcagaacaccggccaagaagtgtctaaatcacaccacacagaagaatctctcctttgctaccatct
atgatgtcctatcaacaaaacctgtcctcaacaagctgactgtattcacaaccttgatggatgttaccaaaggtcaatttgaaagtca
ccttcgagattgcccagacccttgtataggctggtgagcacacgttgggatcccaaggcccaactccccgaaccactcagggtcctgt
ggacagctcacctagcggcaatggctacaggtaagcgcccctaaaatccctttgggcacaatgtgtcctgaggggagaggcagcga
cctgtagatgggacgggggcactaaccctcaggtttggggcttctgaatgtgagtatcgccatgtaagcccagtatttggccaatctc
agaaagctcctggtccctggagggatggagagagaaaaacaaacagctcctggagcagggagagtgctggcctcttgctctccggc
tccctctgttgccctctggtttctccccaggctcccggacgtccctgctcctggcttttggcctgctctgcctgccctggcttcaagaggg
cagtgccttcccaaccattcccttatccaggctttttgacaacgctatgctccgcgcccatcgtctgcaccagctggcctttgacaccta
ccaggagtttgtaagctcttggggaatgggtgcgcatcaggggtggcaggaaggggtgactttcccccgctgggaaataagaggag
gagactaaggagctcagggtttttcccgaagcgaaaatgcaggcagatgagcacacgctgagtgaggttcccagaaaagtaacaa
tgggagctggtctccagcgtagaccttggtgggcggtccttctcctaggaagaagcctatatcccaaaggaacagaagtattcattcc
tgcagaacccccagacctccctctgtttctcagagtctattccgacaccctccaacagggaggaaacacaacagaaatccgtgagtg
gatgccttctccccaggcggggatgggggagacctgtagtcagagcccccgggcagcacagccaatgcccgtccttcccctgcaga
acctagagctgctccgcatctccctgctgctcatccagtcgtggctggagcccgtgcagttcctcaggagtgtcttcgccaacagcctg
gtgtacggcgcctctgacagcaacgtctatgacctcctaaaggacctagaggaaggcatccaaacgctgatgggggtgagggtggc
gccaggggtccccaatcctggagccccactgactttgagagctgtgttagagaaacactgctgccctctttttagcagtcaggccctg
acccaagagaactcaccttattcttcatttcccctcgtgaatcctccaggcctttctctacaccctgaaggggagggaggaaaatgaa
tgaatgagaaagggagggaacagtacccaagcgcttggcctctccttctcttccttcactttgcagaggctggaagatggcagcccc
cggactgggcagatcttcaagcagacctacagcaagttcgacacaaactcacacaacgatgacgcactactcaagaactacgggct
gctctactgcttcaggaaggacatggacaaggtcgagacattcctgcgcatcgtgcagtgccgctctgtggagggcagctgtggcttc
tagctgcccgggtggcatccctgtgacccctccccagtgcctctcctggccctggaagttgccactccagtgcccaccagccttgtcct
aataaaattaagttgcatcattttgtctgactaggtgtccttctataatattatggggtggaggggggtggtatggagcaaggggcaa
gttgggaagacaacctgtagggcctgcggggtctattgggaaccaagctggagtgcagtggcacaatcttggctcactgcaatctcc
gcctcctgggttcaagcgattctcctgcctcagcctcccgagttgttgggattccaggcatgcatgaccaggctcagctaatttttgtttt
tttggtagagacggggtttcaccatattggccaggctggtctccaactcctaatctcaggtgatctacccaccttggcctcccaaattg

ctgggattacaggcgtgaaccactgctcccttccctgtccttctgattttaaaataactataccagcaggaggacgtccagacacagc
ataggctacctggccatgcccaaccggtgggacatttgagttgcttgcttggcactgtcctctcatgcgttgggtccactcagtagatg
cctgttgaattcctcgacctgcagcggccccccctcgacgaagttcctatactttctagagaataggaacttcggccgccaccggccg
ccatatgcatcctaggatcgatcgcgcgcagatcctgtgaaaataaaatgccgttcgtttgaattgtgaagcgggcgtgtgcgtgatg
aggcgaatggcaagtgtgcgatactatcggttggtggaagaatatcgtgactttgtagtgttagaaaatgttatattgtgtattatttc
aatttgaaatcaagagaattattgaatagtgctctaaactttggcatttatgttattttaaccttaatttctatctctatacaaatacatct
atcaaagcgtcttaattttgaaaatatgttaattcgtcgcactttattttgattaaccggacgatagactatcggaagatatttataaat
atcgttaattgtgtacatctcaattccaatatttttttatttctggtgactgtgaaccagaacagctgtgattttatcgggcatctctgaac
atcaggtgttatcaacaagcaaagtttttattgaattcgactgttt

9.3 Sequence of the pPS-Smpd1/KO plasmid in the vicinity of exon 2

Legend: The DNA sequence is colored analogous to the following DNA features

Exons
loxP sites
FRT sites
RNA polymerase II promoter
Neomycin resistance gene
PGK-polyA
other

>pPS-Smpd1/KO, 3008 bp – 7256 bp, direct, 4249 bp total

ataagaggaacaggaaggggaggagctgttttgtggctggctgctgagctatcagtcaaccacaacgaagggtaatcaggtgtctc
cagcgttacccgggccccgagggccagccagggcttcggcctgtggggcctggaggggcaagccagtcctgtctacgagcctggca **Exon 1**
atgccccaccacagagcatcatccggccaggaccacctcagagccggctgggagcagagactggagaggtccttaccggcaccca
gagtgggactcctttggatggggctgggcttggcgctggttctggctctgtttgactccacggttctttgggttcctgccagagcttatcc
tcttccttctgaaggccattctgtcaaattcagtgccatagcgccgccgctccagagtgcctttgggtggcagaacctcacttgccccg
cctgcaaagtcttattcactgctctcaaccatgggctgaaggtgagtgcgtgaagggctgttgtggaatgctgggggcaggatgaag
tgcactggtatgcccgggggagggggcaatatatttctggtagagggtgcttcctatgcagtttgggctgcaggaattctctagaata
acttcgtataatgtatgctatacgaagttataagctctcaccgcggtggcggccgaagttcctattctctagaaagtataggaacttcg
cggccaattctaccgggtaggggaggcgcttttcccaaggcagtctggagcatgcgctttagcagccccgctggcacttggcgctac
acaagtggcctctggcctcgcacacattccacatccaccggtagcgccaaccggctcccttctttggtggccccttcgcgccaccttct
actcctcccctagtcaggaagttcccccccgccccgcagctcgcgtcgtgcaggacgtgacaaatggaagtagcacgtctcactagt
ctcgtgcagatggacagcaccgctgagcaatggaagcgggtaggcctttggggcagcggccaatagcagcttggctccttcgctttc
tgggctcagaggctgggaaggggtgggtccgggggcgggctcaggggcgggctcaggggcggggcgggcgcgaaggtcctccgg
agcccggcattctgcacgcttcaaaagcgcacgtctgccgcgctgttctcctcttcctcatctccgggcctttcgacctgcaggtcataa
tgggatcggccattgaacaagatggattgcacgcaggttctccggccgccttgggagaggctattcggctatgactgggcacaacag
acaatcggctgctctgatgccgccgtgttccggctgtcagcgcaggggcgcccggttctttttgtcaagaccgacctgtccggtgccct
gaatgaactgcaggacgaggcagcgcggctatcgtggctggccacgacgggcgttccttgcgcagctgtgctcgacgttgtcactga
agcgggaagggactggctgctattgggcgaagtgccggggcaggatctcctgtcatctcaccttgctcctgccgagaaagtatccat
catggctgatgcaatgcggcggctgcatacgcttgatccggctacctgcccattcgaccaccaagcgaaacatcgcatcgagcgagc

acgtactcggatggaagccggtcttgtcgatcaggatgatctggacgaagagcatcaggggctcgcgccagccgaactgttcgcca
ggctcaaggcgcgcatgcccgacggcgaggatctcgtcgtgacccatggcgatgcctgcttgccgaatatcatggtggaaaatggcc
gcttttctggattcatcgactgtggccggctgggtgtggcggaccgctatcaggacatagcgttggctacccgtgatattgctgaaga
gcttggcggcgaatgggctgaccgcttcctcgtgctttacggtatcgccgctcccgattcgcagcgcatcgccttctatcgccttcttga
cgagttcttctgaggggatcgatccgctgtaagtctgcagaaattgatgatctattaaacaataaagatgtccactaaaatggaagtt
tttcctgtcatactttgttaagaagggtgagaacagagtacctacattttgaatggaaggattggagctacgggggtgggggtggggt
gggattagataaatgcctgctctttactgaaggctctttactattgctttatgataatgtttcatagttggatatcataatttaaacaagc
aaaaccaaattaagggccagctcattcctcccactcatgatctatagatctatagatctctcgtgggatcattgtttttctcttgattccc
actttgtggttctaagtagcttatcgataccgtcgaggaagttcctattctctagaaagtataggaacttcgtcgagggggggcccggt
acactgcatccatgttaccactaccccactgtgacctttataaagttagggagagtaaagtcagctggctaattgtgggcttgaaatg
gtagcacaccctgagctagagtaggtagctagaggcctggtgctgaactgctgggcagtgtgtgggagatactgatgtctctttatca
tggtgacagagttatcctagctccgatttagacatggaagcctgtggagtggtggccagggttcacttgttctgtctctgacctaacttc
attggttccttccaccacagaaggagcccaatgtggcacgggtaggctctgtggccatcaagatatgcaagatgctgaacatagcac
cactagatgtgtgccagtcagccgtccatctctttgaggacgatgtggtggaggtgtggacacgttcagttctgagcccatcagaggc
ttgtggcttgcttctgggctcctcttgtggacactgggacatcttttcgacttggaacatctctttgccatcagtgccgaagccacccccc **Exon 2**
aaagccaccgagcccaccagcccccggtgcccctgtcagccgtgtcctcttccttactgatctacactgggaccatgagtacctggag
ggcacagacccttactgtgcagatccactttgctgccgccgggggtccggatggccacccaactcccagaaggggctgggttctgg
ggcgagtacagcaagtgtgacctgcccttgcgaacgctagaaagcctgttgaaaggactgggccctgccggccctttttgaaatggtg
tactggacgggagatatccctgcccatgatgtctggcaacagtctcgccaagatcagctgagggccctgaccaccatcacagacctc
gtgaggaagttcttgggcccagtgccagtgtaccctgctgtgggcaaccatgagagcactcctgtcaatggcttccctcctcccttcat
aaagggaaaccaatcttcacaatggctctatgaagccatggccaaggcatgggaaccctggttaccagctgatgcccttcacaccct
aaggtacttactgtcggtggaaacccaggaaggaagaagaaagatggatgagggagaaaggaggagggaactgggtagactact
ccagcaggtgtcctcagcactctctactgccctccctaacctgaccctgccttccctttaattatctccagccaccctcttttcagagcta
gaataacttcgtataatgtatgctatacgaagttataagctctagcagtacatccccactccctagcttgtgtctttgcctacagtagct
ctctttgtaaaatgaattctccctccctctttaatatctcccatttttttctcaacgtggccaggcctataacatctcccgacagaaaggc
ctttgctttctgactcacctcactctttgtcctgaattcatgaagctctcaaccctctgaggcttctttactgtcagaggagccctataatt
actgctgttggtcttcagctagggtgggagctcctgggggtgggagatgacatcatgtgtacctctgcctgatgtgcaggactattgac
atctcggttacttttgtttcagaattgggggcttctatgccctcaccccacgccctggcctccgcctcatctctctcaatatgaatttttgt
tcccgtgagaacttttggctcttgatcaactccacagatcctgctggacaactccagtggctggtggaggagcttcaggctgctgaga **Exon 3**
atcgaggagacaaagt

9.4 Real-time PCR data analysis using the $2^{-\Delta\Delta Ct}$ method

Calculations were done according to Livak et al. (Livak and Schmittgen 2001).

Table 9.1: nAsah1 determination by $2^{-\Delta\Delta Ct}$ calculation

		Primer pair										
		Asah1.3 + Asah1.4		Ragf + Ragr								
Mouse	Founder	Ct	Mean Ct	Ct	Mean Ct	ΔCt	Calibrator	ΔΔCt	$2^{-\Delta\Delta Ct}$	n*Asah1*	Mean n*Asah1*	SD
1	wild type	17.36	17.24	18.32	18.45	-1.21	-1.24	0.00	1.00	2.00	2.00	
1	wild type	17.27		18.43								
1	wild type	17.09		18.61								
2	wild type	17.04	17.13	18.91	18.39	-1.26						
2	wild type	17.16		17.95								
2	wild type	17.18		18.31								
3	Founder 1	15.46	15.30	19.56	19.94	-4.64		-3.40	10.54	21.09	22.09	1.22
3	Founder 1	15.14		19.94								
3	Founder 1	15.30		20.31								
4	Founder 1	15.04	15.10	20.76	19.89	-4.79		-3.55	11.73	23.45		
4	Founder 1	15.19		19.65								
4	Founder 1	15.07		19.26								
5	Founder 1	15.65	15.83	20.84	20.51	-4.68		-3.44	10.87	21.73		
5	Founder 1	15.93		21.04								
5	Founder 1	15.90		19.64								
6	founder 2	12.14	12.36	18.26	18.01	-5.65		-4.41	21.28	42.57	46.09	5.18
6	founder 2	12.41		17.83								
6	founder 2	12.54		17.95								
7	founder 2	11.74	11.58	17.69	17.52	-5.94		-4.70	26.02	52.04		
7	founder 2	11.51		17.54								
7	founder 2	11.48		17.32								
8	founder 2	12.23	12.25	18.74	17.94	-5.69		-4.45	21.83	43.66		
8	founder 2	12.32		17.33								
8	founder 2	12.21		17.75								
9	founder 3	16.07	16.14	20.28	20.59	-4.45		-3.21	9.23	18.46	16.72	1.98
9	founder 3	16.24		20.89								
9	founder 3	16.11		30.33								
10	founder 3	14.66	14.97	19.67	19.08	-4.10		-2.87	7.29	14.57		
10	founder 3	15.19		19.10								
10	founder 3	15.07		18.46								
11	founder 3	14.82	15.01	19.04	19.34	-4.34		-3.10	8.56	17.13		
11	founder 3	15.42		19.43								
11	founder 3	14.78		19.56								
	Wasser P1	24.07		29.65								

Acknowledgements

In der Online-Version nicht enthalten.

Curriculum vitae

In der Online-Version nicht enthalten.

Erklärungen

Hiermit erkläre ich, gem. § 6 Abs. 2, f der Promotionsordnung der Math.-Nat. Fakultäten zur Erlangung der Dr. rer. nat., dass ich das Arbeitsgebiet, dem das Thema „Generation of transgenic mice for the investigation of ceramide metabolism“ zuzuordnen ist, in Forschung und Lehre vertrete und den Antrag von Martin Knüwer befürworte.

Essen, den _____ _____

Prof. Dr. Erich Gulbins

Erklärung:
Hiermit erkläre ich, gem. § 7 Abs. 2, c und e der Promotionsordnung der Math.-Nat. Fakultäten zur Erlangung des Dr. rer. nat., dass ich die vorliegende Dissertation selbständig verfasst und mich keiner anderen als der angegebenen Hilfsmittel bedient habe und alle wörtlich oder inhaltlich übernommenen Stellen als solche gekennzeichnet habe.

Essen, den _____ _____

Martin Knüwer

Erklärung:
Hiermit erkläre ich, gem. § 7 Abs. 2, d und f der Promotionsordnung der Math.-Nat. Fakultäten zur Erlangung des Dr. rer. nat., dass ich keine anderen Promotionen bzw. Promotionsversuche in der Vergangenheit durchgeführt habe, dass diese Arbeit von keiner anderen Fakultät abgelehnt worden ist, und dass ich die Dissertation nur in diesem Verfahren einreiche.

Essen, den _____ _____

Martin Knüwer